



**Gesellschaft für Anlagen-  
und Reaktorsicherheit  
(GRS) mbH**

**CROP**

**Cluster Repository  
Project**

German Country Annexes



**Gesellschaft für Anlagen-  
und Reaktorsicherheit  
(GRS) mbH**

## **CROP**

### **Cluster Repository Project**

**A Basis for Evaluation and  
Developing Concepts of  
Final Repositories for  
High-Level Radioactive Waste**

**German Country Annexes**

Tilman Rothfuchs  
Johannes Droste  
Horst-Jürgen Herbert  
Klaus-Peter Kröhn  
Klaus Wiczorek  
Chunlinag Zhang

With contributions of  
Wilhelm Bollingerfehr  
(DBE-TEC, Peine)

June 2004

#### **Remark:**

This report was prepared under contract No. FIRI-CT-2000-20023 with the European Commission within the framework of the Cluster Repository Project (CROP).

The work was conducted by the Gesellschaft für Anlagen- und Reaktorsicherheit (GRS) mbH.

The authors are responsible for the content of this report.

**GRS - 201  
ISBN 3-931995-68-2**

**Deskriptoren:**

Aktiver Abfall, Design, Endlagerung, EU, Felsformation, Forschungsprojekt, Geosphäre, Internationale Zusammenarbeit, Langzeitsicherheit, Salz, Technische Barriere

## Preface

Several underground research and development projects, which deal with disposal of radioactive waste in crystalline rock, salt and clay formations, have been supported by the European Commission. By constituting a forum (the Cluster Repository Project (CROP) for synthesising construction experience and results from testing engineered barrier systems (EBS) in underground laboratories, and correlation of theoretical predictions with the outcome of performed experiments) a basis was to be worked out for the assessment of the status achieved in Underground Research Laboratories (URL) with regard to future design and construction as well as technical/economical improvement of concepts of future European repositories for highly radioactive waste. The focus of the CROP project was on the behaviour of and processes in EBS, primarily buffer and backfill materials used for embedding waste containers and on backfill materials in boreholes, tunnels and shafts for sealing the repository from the biosphere.

The work was conducted in the form of desk studies under four headings representing the work packages of CROP:

1. Design and construction of engineered barriers
2. Instruments and experimental procedures
3. Assessment of the function of EBS and the understanding of and capability to model the important processes
4. Application of conceptual & mathematical models for predicting THMBC performance

The outcome of the project are country annexes provided by the individual project partners and a general part synthesising the collected information and recommendations for design and construction of future safe repositories. This report entitled „Comparison of URLs, Repository Concepts and Recommendations for Design and Construction of future safe Repositories” will be published separately by the European Commission (EC).

This report presents the Country Annexes on salt (sections 2 through 5) which were provided by GRS, the German project partner. GRS was supported by DBE-TEC, which entered the project at a later stage as observer.

During the course of the CROP project, each country annex was written as a stand-alone paper. This fact might lead to repetitions of text paragraphs, figures, and tables in this report.

## Table von Contents

	<b>Preface .....</b>	<b>I</b>
<b>1</b>	<b>Introduction .....</b>	<b>1</b>
<b>2</b>	<b>Work Package 1: Design and construction of engineered barriers .....</b>	<b>3</b>
2.1	Description of the system for high-level waste .....	3
2.1.1	Waste types and amounts .....	3
2.1.2	Principles of waste isolation .....	4
2.1.3	Host medium .....	7
2.1.3.1	Geology .....	7
2.1.3.2	Seismicity .....	9
2.1.3.3	Rock mechanics .....	9
2.1.3.4	Hydrology .....	11
2.1.3.5	Chemical aspects of the mobilisation and retention of radionuclides .....	11
2.1.3.6	Thermal loading .....	14
2.2	Principles for repository design with special respect to EBS performance .....	15
2.2.1	Design criteria .....	15
2.2.2	Geometry .....	16
2.2.3	Backfilling and sealing .....	18
2.2.4	Petrology .....	18
2.2.5	Rock structure characterization .....	19
2.2.6	Rock stability and deformation in a short and long perspective .....	19
2.2.7	Heat evolution .....	20
2.2.8	Boundary conditions .....	20
2.3	Positioning, construction and manufacturing of holes, tunnels, plugs, heaters and EBS. Stabilization of host medium .....	20
2.3.1	Host formation .....	20
2.3.1.1	Positioning of shafts and disposal areas .....	21
2.3.1.2	Excavation of shafts and tunnels .....	21

2.3.1.3	Boring of deposition holes .....	22
2.3.1.4	Boring and sealing of holes for characterization .....	22
2.3.1.5	Stabilization of host formation, temporary and permanent.....	23
2.3.2	EBS concept .....	23
<b>3</b>	<b>Work Package 2: Instruments and experimental procedures.....</b>	<b>27</b>
3.1	Description of test of the repository concept .....	27
3.2	Experimental procedures .....	29
3.2.1	Heater tests .....	29
3.2.2	Brine migration tests .....	30
3.2.3	Backfilling and sealing tests .....	34
3.2.3.1	The DEBORA experiments .....	34
3.2.3.2	The TSDE experiment.....	36
3.3	Selection and application of instruments for recording of major processes in field tests and repositories .....	44
3.3.1	Measuring principles and devices .....	44
3.3.1.1	Temperature.....	45
3.3.1.2	Deformation.....	46
3.3.1.3	Stress .....	46
3.3.1.4	Gas and water release .....	49
3.3.1.5	Geoelectric monitoring .....	50
3.3.1.6	Fibre optic monitoring systems .....	50
3.3.1.7	Supporting investigations .....	51
3.3.2	Post-test analysis of instruments used in the TSDE experiment.....	52
3.3.2.1	Temperature.....	52
3.3.2.2	Deformation.....	53
3.3.2.3	Stress .....	54
3.3.2.4	Gas and water release .....	56
3.4	Conclusions and recommendations .....	56
3.4.1	Experimental procedures .....	56
3.4.2	Instruments .....	58

<b>4</b>	<b>Work Package 3.1: Assessment of the function of EBS and the understanding of and capability to model the important processes .....</b>	<b>69</b>
4.1	Features and Processes .....	70
4.1.1	Backfilling of disposal drifts and boreholes with crushed salt.....	70
4.1.2	Moisture release from the host rock.....	72
4.1.3	Sealing of drifts with special salt mixtures.....	73
4.1.4	Sealing of drifts and shafts with bentonite.....	74
4.2	Models and EBS Data used for Modelling .....	75
4.2.1	Heat distribution .....	76
4.2.2	Mechanical behaviour of rock salt and crushed salt backfill.....	77
4.2.3	Fluid flow in rock salt.....	78
4.2.4	Fluid flow in crushed salt backfill .....	81
4.2.5	Swelling pressure of bentonite in contact with saline solutions.....	85
4.3	Data used for modelling .....	86
4.3.1	Rock salt .....	86
4.3.2	Crushed salt backfill .....	87
4.3.3	Cogéma canister containing reprocessed and vitrified HLW.....	88
4.3.4	Pollux disposal cask containing spent fuel.....	89
4.3.5	Bentonite as drift and shaft sealing material .....	89
4.4	Description of interaction of EBS and surrounding rock.....	90
4.4.1	Geological and mineralogical data from the host rock at Asse research mine .....	90
4.4.2	Rock properties .....	91
4.4.3	Experiments at Asse that provide information on the interaction of EBS and the host rock .....	92
4.4.3.1	DEBORA experiments .....	92
4.4.3.2	TSDE experiment.....	93
4.5	Codes for describing and evaluation of EBS performance.....	93
4.5.1	Structure code SUPERMAUS .....	94
4.5.2	Two-Phase Flow code MUFTE .....	96
4.5.3	Code TRAVAL.....	98

4.5.4	Two Phase Flow code TOUGH2.....	99
4.5.5	Thermo-hydro-mechanical simulation code FLAC.....	102
4.5.6	Code EQ3/6.....	104
4.5.7	Code CemApp.....	105
4.5.8	Code LINSOURPREPOST.....	106
4.6	Modelling of chemical processes in the EBS.....	108
<b>5</b>	<b>Work Package 3.2: Application of conceptual &amp; mathematical models for predicting THMBC performance.....</b>	<b>111</b>
5.1	Backfill compaction in HLW disposal drifts.....	112
5.1.1	Models and data used for modelling.....	112
5.1.1.1	Conceptual model.....	112
5.1.1.2	Theoretical models.....	113
5.1.2	Modelling.....	114
5.1.2.1	Codes used.....	114
5.1.2.2	Features of analysis.....	116
5.1.2.3	Comparison of predicted and measured results and conclusions.....	117
5.2	Backfill compaction in disposal boreholes.....	118
5.2.1	Models and data used for modelling.....	119
5.2.1.1	Conceptual model.....	119
5.2.1.2	Theoretical models.....	119
5.2.2	Modelling.....	124
5.2.2.1	Codes used.....	124
5.2.2.2	Features of analysis.....	124
5.2.2.3	Comparison of predicted and measured results and conclusions.....	125
5.3	Two-phase flow in the backfill of HLW disposal boreholes.....	127
5.3.1	Models and data used for modelling.....	127
5.3.1.1	Conceptual model.....	127
5.3.1.2	Theoretical model.....	128
5.3.1.3	Processes studied.....	128
5.3.1.4	Data used.....	128
5.3.2	Modelling.....	129

5.3.2.1	Codes used .....	129
5.3.2.2	Features of analysis .....	130
5.3.2.3	Model results .....	130
5.3.2.4	Conclusions.....	133
5.4	Brine migration in the host rock.....	134
5.4.1	Models and data used for modelling .....	135
5.4.1.1	Conceptual model .....	135
5.4.2	Theoretical model.....	136
5.4.2.1	Processes studied and data used .....	136
5.4.3	Modelling.....	137
5.4.3.1	Code used and features of analysis .....	137
5.4.3.2	Comparison of predicted and measured results and conclusions.....	137
5.5	Volume changes due to dissolution-precipitation reactions in a flooded repository in salt formations .....	138
5.6	Discussion and conclusions .....	142
<b>6</b>	<b>Lessons Learned and potential areas for improvements.....</b>	<b>145</b>
6.1	Disposal concepts .....	145
6.2	Design and construction of URLs.....	145
6.3	Instruments and experimental procedures .....	147
6.4	EBS testing and process understanding .....	148
6.4.1	EBS testing .....	148
6.4.2	Process understanding .....	149
6.4.3	Future research needs .....	151
<b>7</b>	<b>Summary and conclusions .....</b>	<b>153</b>
	<b>Acknowledgements.....</b>	<b>157</b>
	<b>References .....</b>	<b>159</b>
	<b>List of Tables.....</b>	<b>173</b>
	<b>List of Figures .....</b>	<b>175</b>

# 1 Introduction

The overall objective of an underground nuclear repository is to protect man and his environment against ionizing radiation from radioactive waste emplaced in the repository. According to paragraph 45 of the German Radiation Protection Ordinance, the individual dose to man, possibly caused by radionuclides released from the repository, must remain below a limit of 0.3 mSv/year (BMI 1983). In order to achieve this objective, a multiple barrier system including backfill and special seals (engineered barrier systems (EBS)) is to be implemented.

The best way of developing suitable disposal concepts is first to conduct system analyses on basis of existing knowledge (e. g., types and amounts of waste to be disposed of, processes influencing the repository performance significantly) and to decide preliminarily on basis of the analyses results on the most suited concepts.

In order to prove the preliminarily selected concepts, full-scale testing of the concepts in underground research laboratories (URL) is considered appropriate in many countries (IAEA 1987). Such tests enable the application and validation of models needed for long-term performance assessments and they are therefore indispensable. Confirmation of the models by increasing the predictive capabilities of numerical simulations increases the confidence in the models and thus increases the public acceptance of the proposed disposal concepts.

However, in-situ testing undertaken for model validation requires the application of high precision instruments and verification of their long-term behaviour and applicability. This requirement brings along the need for careful post-test analyses and QA-based instrument recalibration at termination of URL experiments.

The current status of the achievements of URL research on the German HLW disposal concepts are summarized and appraised in the following sections.

## **2 Work Package 1: Design and construction of engineered barriers**

According to the German radioactive waste management concept the „Gorleben” salt dome has been investigated since 1979 in order to prove its suitability to host a final repository for all types of radioactive waste. In view of the change in the Federal Energy Policy, specially in regard to the use of nuclear power, in 1998 the German government expressed certain doubts with respect to the suitability of salt as host rock in general and of the Gorleben site in particular. All exploration activities were halted by the end of 2000 and a moratorium was imposed for three to ten years. During this time all pending issues shall be looked into, and new formation-independent site selection criteria will be developed in order to identify alternative sites with favourable geological settings. Thus, different host rocks like clay/claystone and granite will be considered. The entire procedure provides for the investigation of several sites and, at the end, the evaluation of these sites, including „Gorleben”, and a final site selection. So far, in Germany, no definitive decision on the host rock has been made yet. However, there is a strong tendency towards rock formations with high geological barrier potential. In the following, rock salt is dealt with as host rock medium because of the extensive laboratory, field and PA work done in the last 30 years and in view of the practical experiences gained with low-level waste and intermediate-level waste test disposal in salt formations as well as the commercial disposal of chemic-toxic waste in underground mines. Despite of this rock salt provides under favourable conditions a disposal formation with an isolation potential for several million of years.

### **2.1 Description of the system for high-level waste**

#### **2.1.1 Waste types and amounts**

Two types of heat generating high-level radioactive waste (HLW) will have to be deposited in a German repository for high-level waste, namely: (a) steel canisters containing vitrified fission products remaining from spent fuel reprocessing and (b) Pollux steel casks containing non-reprocessed spent-fuel assemblies.

##### **a) Specification of the vitrified waste canisters (HLW-canisters)**

The dimensions of canisters containing vitrified HLW are given by the French Cogéma and the British BNFL, respectively, as these companies are reprocessing the spent-fuel from German nuclear power plants. The data of the HLW-canisters are summarized in Table 2.1.

A short time after vitrification, the gamma dose rate as estimated by GSF-ECN (1992) amounts to about 0.8 kGy/h and the corresponding thermal power to 1.9 kW. The development of the HLW-canisters decay heat with time is shown in Table 2.3 (see below).

#### b) Specification of Pollux casks

Besides the HLW-canisters from spent fuel reprocessing, also Pollux casks containing non-reprocessed spent-fuel are considered for direct disposal. According to the reference concept for spent fuel direct disposal, a Pollux has a capacity of up to eight, in a further developed variant up to ten LWR fuel assemblies (Spilker 1998). The total cask mass amounts to 65 tons. The cask has a diameter of 1.6 m and a length of 5.9 m. Its surface dose rate amounts to <0.2 mSv/h (Knapp and Closs 1990) in compliance with Type B(U) transport cask requirements. The heat power of a Pollux cask is shown in Table 2.4 below (DBE 1998).

Table 2.2 shows the number of waste canisters/casks expected until the year 2040. Besides the HLW-canisters and the Pollux casks, some more HLW-forms are to be disposed of in a German repository. These include about 9000 Cogéma- CSDC-canisters containing fuel rod hulls, end caps, and other so-called technological waste remaining from reprocessing. Their decay heat power is rather low with about 20 Watts per container. Additionally, about 618,000 THTR-fuel elements and about 290,000 AVR-fuel elements are to be disposed of. However, since the heat generation of all these waste types is very limited, they will not be considered in the following.

### **2.1.2 Principles of waste isolation**

Rock salt is an elasto-viscoplastic material that creeps under the influence of high stresses without significant fracturing. Because of this material behaviour it encapsulates any waste type with time. Especially at higher temperatures caused by heat generating high-level waste, the creep capability increases and leads to a quick encapsulation of the waste containers and hence to an isolation of the waste from the biosphere.

According to the concepts considered in the past thirty years, high-level waste remaining from reprocessing of spent fuel will be vitrified in steel canisters (Table 2.1). The steel canisters will be disposed of in about 300- to 600-m-deep and 0.6-m-wide boreholes (BfS 1990) reaching vertically down from a disposal level at a depth of some 880 meters below ground (Figure 2.1). About 200 canisters will be lowered into a borehole.

**Table 2.1** Specification of the HLW-canister Cogéma 7/86 (see GNS 1991)

Glass Product		SON 68
Burnup of Fuel	[Gwd/t]	33,000
Cooling Time of Fuel Before Reprocessing	[a]	4
Volume (Total/Glass)	[l]	180/150
Mass (Total/Glass)	[kg]	475/400
Canister Diameter	[m]	0.43
Overall Canister Height	[m]	1.34
Canister Stacking Height	[m]	1.27
Canister Material (stainless steel)	Material No. 1.4833	
Activity	[Bq/Can]	
Beta, Gamma		2.8 E16
Alpha		1.4 E14
Cs 137		6.7 E15
Sr 90		4.6 E15
<u>Surface Dose Rate</u>	[Gy/h]	
Short Time after Vitrification		
Neutron	[1/s]	6.1 E-03
Gamma		800*
After 40 Years		
Gamma		300*
<u>Thermal Power</u>	[kW/Can]	
Short Time after Vitrification		1.9
After 40 Years		0.585
*estimated under consideration of the Cs 137 content only		

**Table 2.2** Expected number of HLW-Containers until year 2040

Disposal Container	No. of Containers
<i>From Reprocessing</i>	
Cogema Canisters and BNFL Canisters	4648
<i>Direct Disposal</i>	
Pollux-8-DWR casks	4449

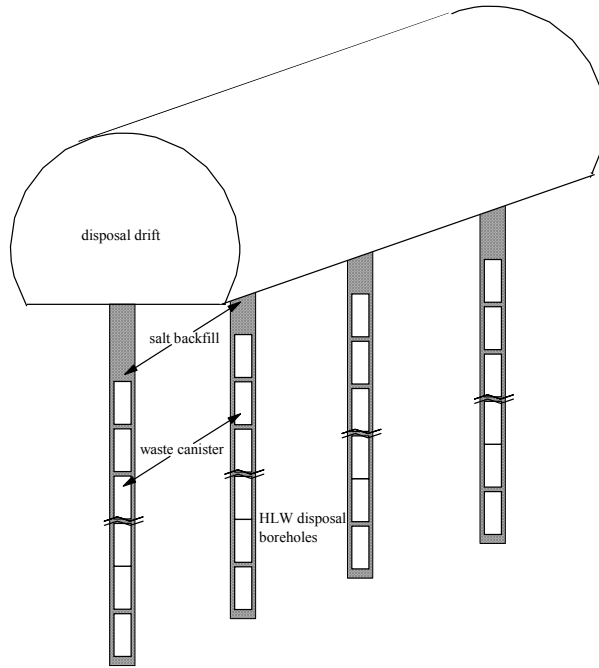


**Figure 2.1** Disposal drift with HLW boreholes

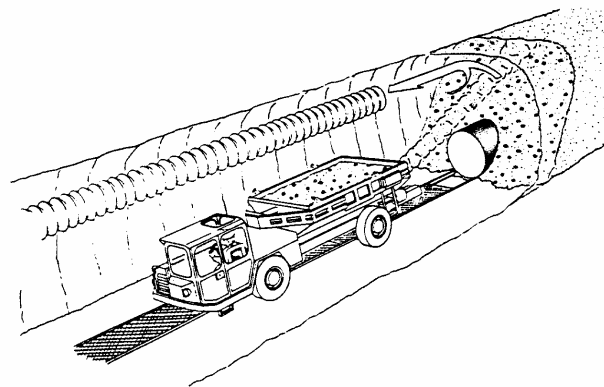


**Figure 2.2** Drift disposal of Pollux casks (source DBE)

To transfer the weight load of the canister stack to the surrounding rock mass, the annulus between the canisters and the borehole wall is to be backfilled with crushed salt. The canisters are completely encapsulated by the creeping salt. At top of the borehole, a seal consisting of crushed salt will be placed.

In addition, a concept has been developed in Germany for the direct disposal of spent fuel (Hartje et al. 1989). Large self-shielding Pollux casks will be emplaced in drifts about 200 m long, 4.5 m wide, and 3.5 m high. Following the emplacement of a Pollux cask, the remaining voids in the drift will be backfilled with crushed salt (Figure 2.2). Similar as in the case of the vitrified HLW-canisters, the creeping of the surrounding rock will lead to compaction of the initially loose material thereby sealing the waste from the biosphere. Also in this case an additional sealing of the waste by buffer materials is not considered necessary.

Several disposal concepts have been developed in Germany as a combination of technical variants and waste types ratios, with the technical variants being:

- pure borehole emplacement of vitrified HLW,
- pure drift emplacement of spent fuel in Pollux casks, and
- combined drift and borehole emplacement of both waste types. These concepts have been analysed by different research teams and the results were reported in (SAM 1989). The most promising concept appeared to be the combined drift and borehole emplacement of both HLW-canisters and Pollux casks.

### **2.1.3 Host medium**

#### **2.1.3.1 Geology**

In the northern part of Germany, marine Zechstein deposits are widely distributed. While thick series of Zechstein carbonates and evaporites were deposited in Northern Germany, only thin layers of continental sediments are found in its southern part (Brinkmann 1977).

The Zechstein Sea was initially formed by the flooding of the Rotliegend peneplain at the beginning of the Upper Permian. The Zechstein transgression came from the Scandic Sea between Greenland and Norway creating an inland sea that reached from Great Britain to the East of Poland (Richter-Bernburg 1987). The North German Basin was situated at the southern margin of the Zechstein Basin.

The development of the Zechstein Basin depended directly on the contact with the open Scandic Sea. With only a narrow channel to the open ocean, sea level changes caused four major transgressions and regressions across the basin. Accordingly, the Zechstein Series was divided into four main sedimentary cycles. Each cycle started with shale deposits followed by the deposition of carbonates. With increasing evaporation, salinity in the basin increased progressively leading to salt deposition from concentrating brines. First, sulphates were formed followed by chlorides and potassium salts. With continuing subsidence, the basin was gradually filled by successive cycles of thick carbonates and evaporites.

In the following, the general evolution of the Zechstein series in Northern Germany will be summarized. At the base of the Zechstein transgression, the detrital Zechstein Conglomerate was deposited. The first cycle, the Werra Series (z1), then continued with a marl shale, the so-called Kupferschiefer, with a high content of sulphides and pyrite. Subsequently, the Zechstein Limestone and the Werra Anhydrite were formed in most parts of the Zechstein Basin. Rock salt and potassium salts were only generated in the central parts of the Hessien Zechstein basin including the potash seams „Hesse” and „Thuringia”.

The following Staßfurt Series (z2) started with shales (Stinkschiefer) and carbonates (Staßfurt Carbonate), followed by the thin Basal Anhydrite. Above it, strong evaporation led to a basin-wide deposition of halite up to several 100 m thick (Staßfurt Halite). During ongoing evaporite deposition, the potash seam Staßfurt was formed which was then overlain by a thin top of rock salt and anhydrite.

At the beginning of the third cycle (Leine Series, z3), again thin shale beds (Grey Salt Clay) and carbonates (Leine Limestone) were deposited. Evaporite sedimentation started with the Main Anhydrite (40 – 100 m) which was followed by up to 200 – 300 m Leine Halite with intercalated anhydrite and clay layers and the potash seams „Riedel” and „Ronnenberg”.

The final Aller Series (z4) was initiated by the Red Salt Clay and the thin Pegmatite Anhydrite. Then, a few 100 m of Aller Halite were deposited characterized by increasing intercalations of clay layers towards the top.

As a result both of the increasing overburden during Mesozoic and Cenozoic time and of the regional stress regime, the viscous Zechstein salt was mobilized. Early salt mobilization started in Triassic time and was intensified during Cretaceous to Cenozoic leading to the development of the present salt domes and diapirs with complicated internal structures.

### 2.1.3.2 Seismicity

In Germany, all sites considered suitable for the construction of deep geological repositories in rock salt are located in the northern part of the country, which is a region of very low seismicity. According to Leydecker et al. (1999), the probabilistic quantification of earthquakes is considered necessary to confirm the deterministic assessments required by KTA 2201.1 (1990).

All current candidate repository sites in Germany are located in three seismotectonic provinces classified in accordance with the IAEA Earthquake Safety Guide (1991). In these provinces, very few isolated earthquakes with a maximum intensity of VI MSK (Macroseismic Scale after Medvedev-Sponheuer-Karnik (Sponheuer 1965)) have been observed in the past 1,200 years.

As a reference case, the results published by Leydecker et al. (1999) for the Konrad mine located about 35 km away from the Asse are taken. An exceeding probability of  $<10^{-5}$ /year for an earthquake with the intensity of VI ½ MSK was determined by the agreeing results of deterministic and probabilistic risk assessments.

### 2.1.3.3 Rock mechanics

Rock salt exhibits relatively high ductility and tightness. The basic characteristics of the Asse salt, referred to as referential material, are summarised in the following: the density  $\rho = 2.16 - 2.19 \text{ g/cm}^3$ ; the dynamic Young's modulus = 33 – 35 GPa, the static Young's modulus = 20 – 0 GPa; the Poisson's ratio  $\nu = 0.23 - 0.28$ ; the uniaxial compressive strength  $\sigma_c = 20 - 35 \text{ MPa}$ ; the tensile strength  $\sigma_t = 0.5 - 2.3 \text{ MPa}$ ; the permeability of host rock  $k < 1\text{E-}21 \text{ m}^2$ .

Creep of the rock salt is very dependent on stress and temperature. The steady state creep rate is an exponential function of effective stress with an exponent of 5, without lower stress limit. An increase of temperature of 10 K causes an increase of strain rate by a factor of about two due to thermally activated micromechanical mechanisms. The widely used creep law according to Hunsche and Hampel (1999) is:

$$\dot{\epsilon}_s = A \cdot \exp\left(\frac{-Q}{RT}\right) \cdot \left(\frac{\sigma}{\sigma^*}\right)^n \quad (2.1)$$

with  $A = 0,18 \text{ d-1}$ ;  $n = 5$ ;  $Q = 54 \text{ kJ / mole}$ ;  $\sigma^* = 1 \text{ MPa}$ ;  $R = 8.31441 \text{ kJ/ (mole K)}$ .

The creep rate is also dependent on air humidity, but only under low mean stresses where an increase of the rate by a factor of 50 (Hunsche and Schulze 1996) can occur. Different types of rock salt exhibit rather different creep behaviour due to a different distribution of microscopic impurities within the grains. In fact, different types can show differences in steady state creep rate by a factor of more than 100.

Deformation, damage (dilatancy) and failure of the rock salt are essentially dependent on the mean stress, stress geometry, loading rate and temperature. The ductile deformation increases with increasing mean stress and increasing temperature as well as with decreasing deformation rate. At sufficiently low deformation rates, rock salt deforms essentially by creep, without short-term failure. Dilatancy increases with creep deformation. When damage reaches a certain value of about  $0.6 \text{ MJ/m}^3$ , creep rupture can occur under dilatant conditions. In the compressive domain, dilatancy is decreasing with time. The failure strength increases with increasing hydrostatic pressure, but with decreasing temperature. At high temperatures, the rock becomes more ductile and deforms by creep. In addition, the strength is always lower in extension compared with compression. The rock salt has a pronounced strength anisotropy, which decreases with increasing isotropic pressure. The dilatancy boundary and short-term failure for the Gorleben and also for the Asse salt are summarised by Hunsche (1993):

Conservative failure strength:

$$\tau_B = f(\sigma) \cdot g(m) \cdot h(T) \text{ with}$$

$$f(\sigma) = b (\sigma / \sigma^*)^p$$

$$g(m) = 2k / [(1+k) + (1-k)J_m]$$

$$J_m = m (9 - m^2) / (3 + m^2)^{3/2}$$

$$h(T) = 1 \text{ for } 20^\circ\text{C} < T < 100^\circ\text{C}$$

$$h(T) = 1 - c(T - 100^\circ\text{C}) \text{ for } 100^\circ\text{C} < T < 260^\circ\text{C}$$

$$b = 2.7 \text{ MPa}, p = 0.65, c = 0.002 \text{ K}^{-1}, k = 0.74, \sigma^* = 1 \text{ MPa}$$

Conservative residual strength:  $\tau_R = \tau_B$

Dilatancy boundary (only  $m = -1$ ):  $\tau_D = 0.86\sigma - 0.0168\sigma^2$

#### **2.1.3.4 Hydrology**

Inflow of brine or water into underground storage rooms is a major point of concern in a salt repository. Such a scenario may take place if brine/water enters the repository mine via rock parts with permeabilities higher than the intact rock mass or via the shaft. The latter scenario will not be considered here because such an event will be prevented by installing a shaft seal (see section 2.3.2).

Although a salt repository will be located in a very homogeneous part of a salt dome, anhydrite ( $\text{CaSO}_4$ ) layers above the rock salt seam or excavation disturbed zones (EDZ) around drifts and storage rooms may represent rock zones of higher permeability.

Investigations in the Main Anhydrite A3 at a depth of 400 m below ground in the Bernburg salt mine performed by Kamlot et al. (1999), however, did not indicate higher permeabilities in the anhydrite in comparison to data obtained in rock salt. Even in the case of carnallite filled fractures in the test intervals no higher permeabilities were found. In the undisturbed anhydrite at a borehole depth of 9 m, typical values were in the range of  $1\text{E-}21 \text{ m}^2$ . Close to the drift wall, the permeability values increased to  $1\text{E-}17 \text{ m}^2$  indicating the existence of an EDZ.

Investigations by Wieczorek and Zimmer (1999) on the permeability of the EDZ in rock salt around drifts in the Asse mine rendered permeabilities of the intact rock salt of  $<1\text{E-}20 \text{ m}^2$  and maximum permeabilities in the EDZ of about  $1\text{E-}16 \text{ m}^2$ .

Healing of the EDZ was also investigated at a more than 80 years old bulkhead in the Asse mine. Typical values measured around the bulkhead were in the order of  $1\text{E-}18 \text{ m}^2$ .

In summary it is concluded that homogeneous rock salt formations typically show very low permeabilities, which are less than  $1\text{E-}20 \text{ m}^2$ . These values may increase in the EDZ around drifts and storage rooms to about  $1\text{E-}15$  to  $1\text{E-}16 \text{ m}^2$ , but the EDZ heals with time. Models to describe EDZ healing in dependence of the stress field are currently developed at different institutions.

#### **2.1.3.5 Chemical aspects of the mobilisation and retention of radionuclides**

For repositories in salt formations one of the key safety features is the quality of the host rock itself. Apart from the necessary geochemical characterization of the host rock, geochemical

questions are mainly directed towards processes that occur in case of water intrusions from the overburden. However, in salt rock formations such processes have to be considered only in accident scenarios, quite in contrast to hardrock as host medium. A basic geochemical question which has to be answered whenever brine inflow occurs is whether the brines are connate waters (i.e. limited in volume, without connecting pathways with the overburden and hence harmless) or if the water comes from outside of the salt formation, which may lead to a complete flooding of the repository and, thus, to a mobilisation and transport of radionuclides.

Mobile species can be generated by dissolution of waste. Solubility and mobility may be further increased via complexation with chloride ions. Colloids are not expected to play a significant role owing to the limited stability of colloids in high saline solutions. Immobilisation and retardation can occur due to precipitation and sorption, respectively. The extent of mobilisation and immobilisation governs the transport velocity of the respective species relative to the flow rate of the liquid phase. All these processes depend on the geochemical near field conditions and the oxidation states of elements in question (Papp 1997).

Due to the high salinity of brines the chemical boundary conditions in the near field are very special and depend on the following effects:

1. mobilisation of radionuclides from the waste matrix (glas, cement, bitumen, spent fuel)
2. retention of radionuclides
3. chemical boundary conditions pH and Eh in the near field
4. sorption on buffer materials and on corrosion products
5. dissolution of salt formations, volume changes, changes of porosity
6. radiation effects in salt formations
7. production and fate of gases in the repository

Reducing conditions prevail in the repository near field due to the presence of high amounts of canister iron. Under these conditions the relevant actinides and technetium occur in the III and IV valent form. The time span for the failure of the canisters and the subsequent mobilisation of radionuclides seems not to be of major importance. However, a more detailed knowledge of the mobilisation from vitrified and cemented waste forms is needed. A very important aspect is the volume ratio between waste and liquid. The better knowledge of this ratio can lead to a significant reduction of conservativities in safety analysis. This is

especially the case for cemented waste forms. After mobilisation many nuclides can be partially immobilised in different parts of the repository via precipitation and sorption processes. The latter are especially important for elements which have not yet reached their solubility limits. Whereas sorption on salt minerals is negligible it is important on corrosion products of cements and container materials. Other processes which influence the transport of radionuclides indirectly are dissolution precipitation reactions in the salt formation itself due to water intrusion. These reactions influence the total amount of resulting solutions, their chemistry and their transport. Inflow of fluids and gases into the repository as well as radiation effects on the salt minerals must be taken into account as these processes can accelerate corrosion and influence the transport of contaminated brines. These processes so far have not been taken into account in safety analyses. Therefore their quantitative impact on the results can not be stated.

Several safety analyses have already been performed for a repository in salt formations for all kinds of radioactive wastes except for the direct disposal of fuel rods (PSE (Brüggemann et al. 1985), PAGIS (EUR 11778, 1988), SAM (1989), PACOMA (Hirse Korn et al. 1991)). These calculations rendered the following radionuclides as being especially relevant for the resulting radiation exposure: Tc-99, Np-237, U-234, Ra-226, Pb-210, I-129, Se-79, C-14, Cs-135, U-236, U-238, U-235, Ac-227, U-233, Ni-59, Mo-93, Nb-94, Pd-107, Cl-36 and Ca-41.

With the present knowledge the geochemistry of some radionuclides in salt formations can be described for relatively simple and well characterised closed systems only, using appropriate thermodynamical data for the description of the nuclide activity in high saline solutions, i.e. Pitzer coefficients, and a more phenomenological description of the formation of colloids. Several aspects of the complex near field system (like e.g. solubilities, speciation, formation of secondary mineral phases, sorption processes) can be described by laboratory experiments and geochemical modelling. Such geochemical processes and relations have been implemented, often in a simplified manner, in the long-term safety analysis models available today. For realistic and comparative long-term safety analysis, however, a more detailed quantitative understanding of all relevant processes is required. Also, a sufficient and consistent thermodynamical database for actinides and long-lived fission products including respective solubility limits and sorption parameters is still missing. A well founded quantitative source term, i.e. the integration of the reactions of the host rock salt with the waste, containers, gases, radionuclides, buffer materials, radiolyses effects is still needed. Furthermore the geochemical description of the sorption processes and the colloid transport still must be quantified for the geochemical description of the radionuclide migration. Maybe

even the hitherto mostly unknown processes of formation and remobilisation of secondary accumulations of sorbed and precipitated radionuclides must be taken into consideration.

### 2.1.3.6 Thermal loading

When defining the maximum permitted thermal loading of a salt formation hosting a HLW-repository, the following two criteria are to be considered:

- a) tensile stresses are to be avoided in the near- and in the far-field (for instance at the interface to the overburden strata or in mechanically sensitive rocks like anhydrite) in order to avoid the generation of pathways for intruding liquid solutions or the migration of radionuclides from the repository.
- b) thermal decomposition of salt minerals is to be avoided as far as possible to avoid disintegration of the host rock and thus the generation of pathways for migration of radionuclides.

The temperature field development in the host formation, which gives rise to thermally induced stresses, depends upon the waste package spatial arrangement and upon the waste decay heat. The decay heat, in turn, follows from the radionuclide content and the interim storage time. For the waste forms considered the decay heat is shown in Table 2.3 and 2.4.

**Table 2.3** Heat power of Cogéma HLW-canisters calculated with data presented by Scheibel et al. (1990)

Time/years	0*)	2	4	5	10	20	40	60	80	100	200	400	500	700	1000
Heat Power/w	1,902	1,521	1,377	1,332	1,172	927	585	375	244	163	38.4	18.7	15.8	11.5	7.1

\*) short time after vitrification

**Table 2.4** Heat power of a Pollux-8-DWR cask (Source: DBE 1998)

Time/years	*)	1	2	5	10	20	40	70	100	500	103	104	105	106
Heat Power/kw	8,165	56.59	31.58	12.53	8.08	6.18	4.32	2.81	2.02	0.62	0.35	0.08	0.01	0.00

\*) time of discharge

The thermomechanical consequences of HLW disposal were analysed in several projects (SAM 1989 and SEK 1993). Considering interim storage periods of 30 and 40 years for HLW

and spent fuel, respectively, Wallner et al. (1989) calculated maximum temperatures between 134 and 150 °C in the disposal fields. In conjunction with this, the probability of tensile stresses exceeding the tensile strength of rock salt (+ 1 MPa) at the salt top was assessed to be rather low.

The second criterion for designing a HLW repository in rock salt is given by the maximum acceptable temperature with regard to the thermal stability of salt minerals. Jockwer (1981) investigated the thermal stability of minerals like polyhalite ( $K_2MgCa_2(SO_4)_4 \cdot 2H_2O$ ) and kieserite ( $MgSO_4 \cdot H_2O$ ) which commonly occur as accessory hydrated minerals in natural rock salt. Polyhalite shows a distinct thermal decomposition starting at a temperature of 235 °C whereas kieserite starts to decompose significantly only at a temperature above 280 °C. Considering a certain safety margin, a maximum temperature of 200 °C was thus proposed for a HLW repository in rock salt.

The decomposition temperature, however, depends on the water vapour partial pressure as it was shown earlier by Jockwer (1980) for carnallite. As a consequence of this, Kern and Franke (1980) investigated the thermal release of water from carnallite as a function of the pore pressure. They showed that the decomposition temperature of carnallite increases from 100 °C to about 135 °C if the pore pressure increases from atmospheric pressure to about 4 MPa. On basis of these findings, a safety distance between the HLW disposal field and possible carnallite seams of 40 m was proposed in EUR 8179 (1982).

## **2.2 Principles for repository design with special respect to EBS performance**

### **2.2.1 Design criteria**

Criteria used in the mentioned conceptual studies for designing a HLW repository in a salt dome in Germany were reported by Storck et al. (1988). They include:

- retrievability is not to be considered
- two shafts should be sufficient for driving the mine and for all kinds of transport and the ventilation system
- different waste forms with respect to waste type and container shall be stored in different disposal areas

- the mine works shall have a lateral safety distance to the flanks of 200 m and a vertical safety zone beneath salt level and cap rock of 300 m. Additionally, a safety area (pillar) of 300 m will remain around each shaft which should not be used for disposal purposes
- all disposal areas shall be on one level
- salt and waste shall be transported in different drifts, preferably in a one-way system. However, the mining of drifts and other excavations should be kept as low as possible in order to minimize the required number of drift seals (dams).

## 2.2.2 Geometry

The typical layout of a HLW repository is shown in Figure 2.3. The underground mine with its disposal boreholes and drifts keeps a safety distance of 200 m from the edges of the salt dome. Shaft 1 will be used as air intake shaft and shaft 2 as exhaust shaft and for transportation of waste packages. The layout of disposal fields and drifts is mainly determined by the actual geology at the disposal level, i.e., the distance of the disposal areas to the carnallite or anhydrite seams and the maximum allowable temperature of 200 °C at the interface waste canisters- host rock. Table 2.5 summarizes possible geometrical data of a site-specific repository concept for Gorleben (DBE 1998) under consideration of the aforementioned criteria.

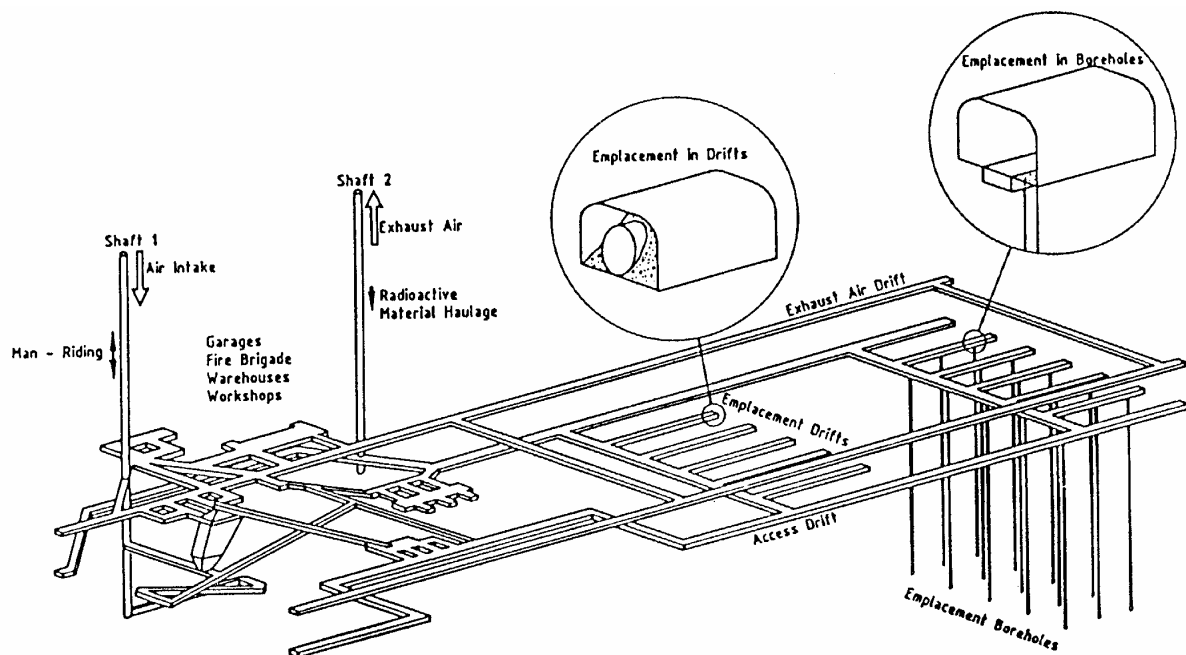


**Figure 2.3** Typical layout of a high-level waste repository in a salt formation in Germany (source DBE)

**Table 2.5** Possible geometrical data of the Gorleben repository concept (DBE 1998)

	<b>Interim storage period (years)</b>	<b>Cask spacing (m)</b>	<b>Drift spacing (m)</b>
<b>Drift disposal of Pollux-casks</b>	15	6	28
	30	1	36
<b>Borehole disposal of HLW-canisters</b>	<b>Interim storage period (years)</b>	<b>Borehole spacing (m)</b>	<b>Drift spacing (m)</b>
	10	24.50	21.22
	15	21.00	20.00
	30	17.25	14.94

In case of borehole disposal, a drift cross-section of about 5 x 6 m is required for placing the disposal machine. The borehole diameter will be about 0.6 m. The remaining annulus of 8.5 cm around the canister is to be backfilled with crushed salt (compare section 2.2). In case of drift disposal, a drift cross-section of about 4.5 x 4 m is to be considered to enable the emplacement of the 1.6-m-wide Pollux cask. The remaining voids around the cask will be backfilled with crushed salt (see Figure 2.2).

The SAM-project (SAM 1989) showed that a radionuclide release into the overburden rock strata and the biosphere is not to be expected if the HLW disposal fields are located closer to the central shaft than the non heat producing disposal fields. The main reason for this is that the heat producing waste causes a significant temperature increase in the disposal fields and the adjacent rock mass, thus leading to high convergence rates and to a comparably quick compaction of the salt backfill in borehole seals and drifts. The convergence-induced transport of contaminated brine from the disposal drifts or boreholes to the shafts is prevented because the backfill porosity in the drifts connecting the disposal areas with the central field will reach its end-value in a relatively short period of time. In the SAM-example, the flank drift connecting the central field and the HLW-field will be closed after 155 years whereas the brine coming from the shaft will reach this drift only after 233 years. The drifts above the HLW-disposal boreholes, into which a limited amount of brine from undetected brine inclusions is released, will be closed after 70 to 80 years so that a contact with the brine coming from the shaft is here prevented, too.

### **2.2.3 Backfilling and sealing**

The overall objective of an underground nuclear repository is to protect man and his environment against ionizing radiation from radioactive waste emplaced in the repository. According to paragraph 45 of the German Radiation Protection Ordinance, the individual dose to man, possibly caused by radionuclides released from the repository, must remain below a limit of 0.3 mSv/year (BMI 1983). In order to achieve this objective a multiple barrier system including backfill and special seals (engineered barrier systems (EBS)) is to be implemented.

Backfilling and sealing of a salt repository have the following objectives:

#### a) Backfilling

- mechanical stabilisation of the natural barrier system (host rock and overburden)
- dissipation of heat from HLW disposal areas
- reduction of voids for potential fluid storage
- minimisation of radiation dose to personnel in the operation phase

#### b) Sealing

- mechanical stabilisation of disposal rooms and areas
- sealing against brine intrusion from undetected brine reservoirs or from the overburden
- avoidance of radionuclide release from the disposal rooms and areas into the biosphere

Backfilling of underground openings will take place immediately after the operational phase of individual repository areas. Sealing systems are to be installed at specific locations or disposal rooms. Typical seal systems are borehole seals, drift seals (dams) and shaft seals. Further details with regard to the design of the EBS concept are described in section 2.3.2.

### **2.2.4 Petrology**

Petrology does not play a major role in a salt repository with regard to rock variations in the near-field around disposal drifts and boreholes. Normally, salt formations are thick and homogeneous to enable the selection of suitable disposal fields in a geological salt formation. However, considering far-field effects, namely the creation of tensile stresses in

rock seams around the rock salt formation, as well as the shaft intersecting overburden strata, the detailed knowledge of the overall petrology is necessary for assessing the petrophysical and hydrogeological situation at the repository site. Initial site investigations from the surface by drilling and later underground investigations are obligatory.

### **2.2.5 Rock structure characterization**

As outlined in section 2.1.3.1, salt domes and salt diapirs show rather complex structures of various salt seams. Numerical simulations of the thermomechanical consequences of HLW disposal require representative models of the geological formation and thus a good knowledge of the rock structure. This includes the boundaries of the salt formation at different depths as well as the distribution of potential disposal volumes in lateral and vertical direction. Knowledge of most important petrophysical properties is also required because different salt types may differ significantly. The Staßfurt Halite Na<sub>2</sub> for instance, exhibits up to ten times the mobility of the Leine Halite Na<sub>3</sub>.

### **2.2.6 Rock stability and deformation in a short and long perspective**

Comprehensive experience gained from the construction of underground storage caverns for oil and gas in salt domes and from the mining of salt is available to design and construct a repository in salt. Owing to the creep capability of rock salt, very large deformations of the rock with or without fracturing, depending on local conditions, are to be expected. In the operation phase, increase in temperature generated by HLW will induce thermal expansion of the surrounding rock and accelerate closing of boreholes and drifts. Thermally induced stresses in the near-field are limited by the repository design to keep adequate safety margins against significant fracturing. The rock creep reduces in the course of time any remaining deviatoric stresses and leads to a re-consolidation of the rock and the backfill. High density of crushed salt backfill is to be expected after long-term consolidation (Bechthold et al. 1999). Notwithstanding, thermally induced fractures could occur in anhydrite layers even in the far-field. Therefore, the integrity of the salt dome in case of an unfavourable distribution of anhydrite layers must be examined (compare section 2.2.7).

### **2.2.7 Heat evolution**

The thermo-mechanical consequences of various disposal concepts were analysed by Wallner and Stührenberg (1989) in the framework of the project „Systemanalyse Mischkonzept“ (SAM 1989) for a simplified model of the Gorleben salt dome. Assuming an amount of 700 t of spent fuel being discharged from LWRs annually and a ratio of 500:200 for non-reprocessed and reprocessed HLW as well as interim storage times for both types of waste of 30 and 40 years, respectively, maximum temperatures between 134 °C and 150 °C were calculated in the emplacement zones. 1000 years after emplacement, the temperature increase in the salt top does not exceed 5 °C and also the stresses in the salt top are similar for all concepts. Tensile stresses exceeding the tensile strength of rock salt (1 MPa) only occurs if low creep capacity and a large panel width of 300 m are assumed. In all other cases they remain below the „1 MPa-limit“ (Bechthold et al. 1993).

### **2.2.8 Boundary conditions**

Thermomechanical modelling of near-field effects has been successfully performed in various projects using different finite element codes (Prij et al. 1995). In general, a homogeneous stress state at sufficient distance (50 - 100 m) from the modelled structure was adequate for modelling. The boundary stress value, however, has to be based on measurement data, since a value derived from the overburden mass is usually too high for salt domes, especially when there are many openings in the salt structure.

In far-field models it is meaningful to also consider the overlaying and surrounding strata, since the more or less stiff overburden will absorb part of the stress resulting from excavation of openings.

## **2.3 Positioning, construction and manufacturing of holes, tunnels, plugs, heaters and EBS. Stabilization of host medium**

### **2.3.1 Host formation**

As described in section 2.1.3.1 the Permian salt formations in northern Germany are formed by the four Zechstein evaporation cycles z1 - z4. The central parts of the salt domes and diapirs are mainly composed of the Zechstein series z2 (Staßfurt Halite Na<sub>2</sub>) and z3 (Leine Halite Na<sub>3</sub>). Disposal rooms in a repository will therefore be located in the Na<sub>2</sub>-Staßfurt

Halite about 800 m below ground. Exemplarily, the situation at the Asse research mine is shown in Figure 2.4.

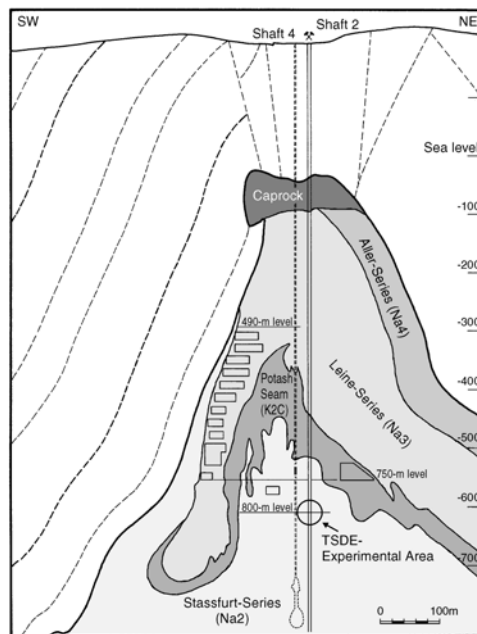


**Figure 2.4** Cross section of the Asse research mine

### 2.3.1.1 Positioning of shafts and disposal areas

Positioning of shafts, disposal areas and transport drifts has been briefly reported in section 2.2.1. As outlined in section 2.2.5, the creep of the Staßfurt Halite Na2 is much higher than that of the Leine Halite Na3. It is therefore considered reasonable to locate the disposal areas for heat producing HLW in the Staßfurt Halite Na2 and the shafts in the more stable Leine Halite Na3.

### 2.3.1.2 Excavation of shafts and tunnels

In the Gorleben Rock Characterisation Facility two vertical shafts with a diameter of 7.5 m were sunk in the central part of the salt dome. One of them used for air intake, man ride and materials hoisting the other one for air exhaust and as emergency exit. In order to support the unstable, water bearing overlaying strata (unconsolidated quaternary and tertiary sediments and cap rock) with about 250 m thickness the freezing method was applied for shaft sinking through the overburden. Shaft excavation was first performed by drilling and

blasting and later in the vicinity of the salt dome by means of a special machine (shaft short helix).

A watertight shaft lining was installed in both shafts down to approx. 100 m below the salt dome top.

At a depth of 840 m an exploration level with horizontal drifts was excavated for geoscientific investigations by drilling and blasting. At a later stage road headers were also used for further drifting. Site survey is to be carried out in spatially limited sections called exploration areas. The first one located to the north east of the shafts was almost completely surveyed until end of 2000.

### **2.3.1.3 Boring of deposition holes**

As outlined in section 21.2, canisters containing vitrified HLW will be disposed of in 300- to 600-m-deep vertical boreholes. In order to avoid any intrusion of water or brine into the disposal boreholes, which would lead to undesired corrosion of the waste canisters, dry air will be used as flushing medium during drilling.

The feasibility of drilling such deep boreholes without brine was demonstrated within a special project at the Asse mine (Kolditz 1993). The salt cuttings produced by drilling are transported out of the borehole inside the drill rods by compressed air. The procedure was successfully demonstrated in a 500-m-deep borehole drilled at the 750-m level in the Asse mine.

### **2.3.1.4 Boring and sealing of holes for characterization**

At the exploration level drilling niches for horizontal, vertical and inclined boreholes were arranged at special positions in the excavated drifts. Drilling site preparation and borehole drilling were performed concurrent to the drift excavation work. In order to gain a maximum of information about the structure of the salt dome all boreholes were core drillings. Special attention was paid to cores orientation. Drill cuttings were discharged by air flushing with respect to a good core quality. The boreholes itself were used for geoscientific investigations in order to determine strike and dip of the borehole as well as permeability and temperature of the surrounding host rock.

Further vertical boreholes starting from the exploration level will be performed in order to explore the geological structure of the deep parts of the salt dome. Finally, all boreholes will be filled with cement beginning at the borehole bottom in order to ensure a bubble free and stable sealing.

#### **2.3.1.5 Stabilization of host formation, temporary and permanent**

Because of the excellent creep properties of rock salt, underground voids in a salt formation do not need to be supported during the operational phase. This is valid for salt mines as well as for underground research laboratories and repositories. In special cases, where high stress concentrations might occur due to unfavourable room geometry, rock bolting is a common measure against roof spalling.

With regard to the long-term stability of the host formation after operation of the repository or parts of the underground excavations, backfilling with inert crushed salt backfill is considered as the most suited measure (compare also the following section 2.3.2). Backfilling should take place as soon as possible after waste emplacement if it is not done simultaneously with waste emplacement as in the direct disposal procedure (compare section 2.1.2). The interaction of crushed salt backfill and the host rock formation under repository relevant conditions has been studied in the BAMBUS-project at the Asse mine (Bechthold et al. 1999). In addition, backfilling of about 130 old excavations with a total volume of 3,400,000 m<sup>3</sup> remaining from rock salt mining at the Asse mine takes place since 1995 (GSF 1997). An extensive observation programme has been set up to monitor backfill consolidation and stabilisation of convergence processes in the mine.

#### **2.3.2 EBS concept**

According to the preliminary salt repository concept in Germany (DBE 1998), the EBS of a salt repository will mostly consist of borehole seals, drift seals (dams), and shaft seals. In addition to the seals, access and transport drifts will be backfilled with crushed salt to minimize remaining voids in the repository and to assure rock stability as soon as possible after filling the disposal areas. The principles of the EBS are shown in Figure 2.5.

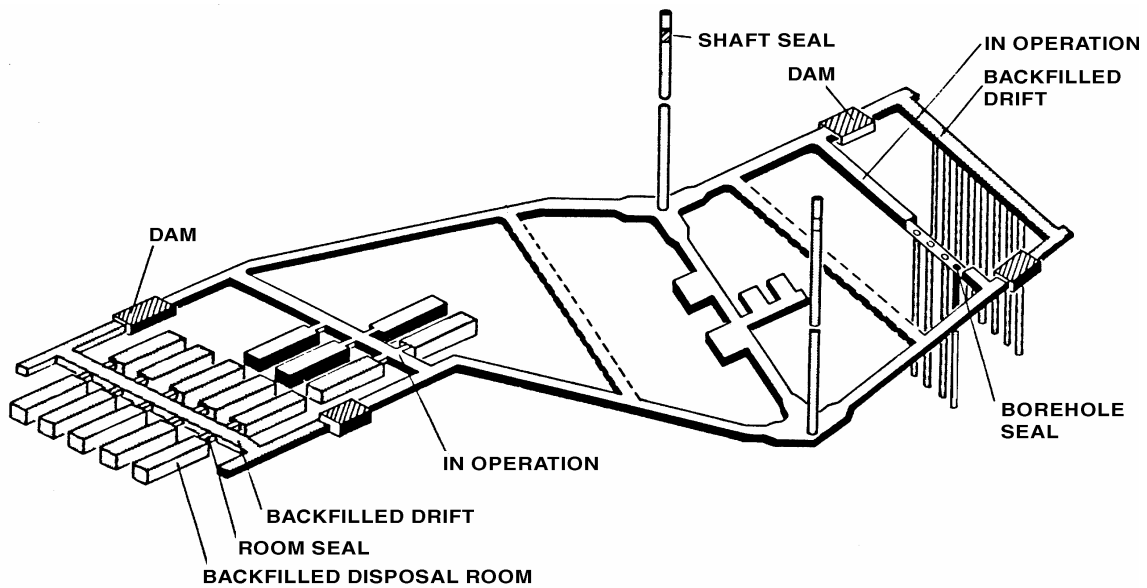


**Figure 2.5** Principle seals in a salt repository

At top of each HLW disposal borehole, a 30-m-long seal consisting of crushed salt will be placed. The crushed salt will be compacted by the creeping host rock and will reach similar sealing properties as the surrounding rock within about 10 years (Prij and van den Horn, 1993). No additional sealing of the waste emplaced in the borehole is required. As mentioned above, the backfill in the drifts above HLW boreholes will be compacted to very low porosities and permeabilities within about 150 years, so that thereafter any brine entering the repository will not reach the waste canisters.

The drifts for direct disposal of spent fuel in Pollux casks will be backfilled with crushed salt simultaneously to cask emplacement (Figure 2.2). As mentioned, the compaction and the sealing behaviour of salt backfill has been investigated in detail within the BAMBUSII-project (Bechthold et al. 1999).

Drift seals (dams) between the shaft area and the disposal fields will be installed after the repository operational period. A preliminary drift seal design was developed by Stockmann et al. (1994). The proposed design (Figure 2.6) includes a short-term seal of sand-asphalt which is required in the early stage after installation to prevent an inflow of solutions, a long-term seal consisting of pre-compacted salt bricks and an abutment of salt concrete needed to guarantee stability against brine pressure in case of complete flooding of the mine. The sealing function of the long-term seal is generated with time by further compaction due to drift convergence.

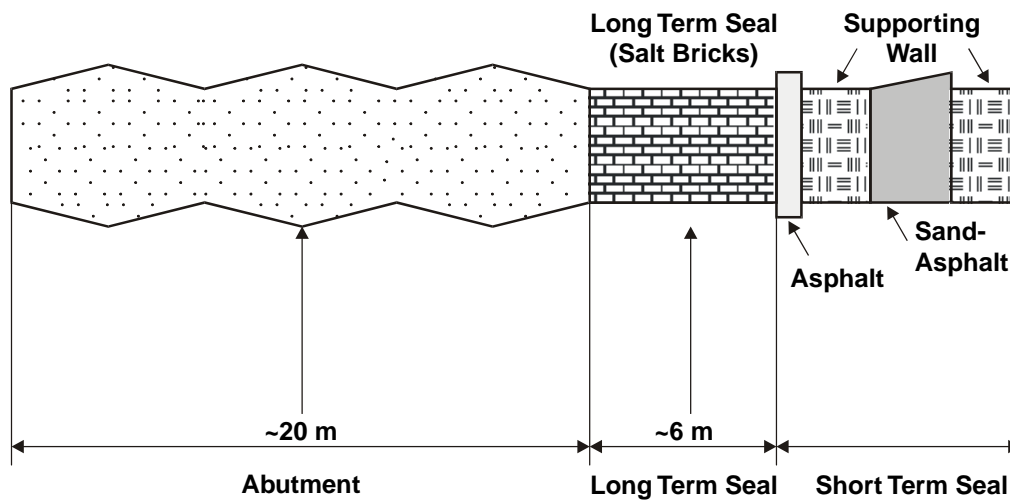


**Figure 2.6** Principle design of a drift seal (dam)

After the operation period, the infrastructure in the repository will be dismantled and shaft seals will be installed to close the mine definitely. A concept for a shaft seal (Figure 2.7) was developed by Schmidt et al. (1995). An in-situ experiment on the effectiveness and stability of a shaft seal consisting of bentonite pellets has been successfully tested at the Salzdetfurth mine in Germany (Bredung 2001).

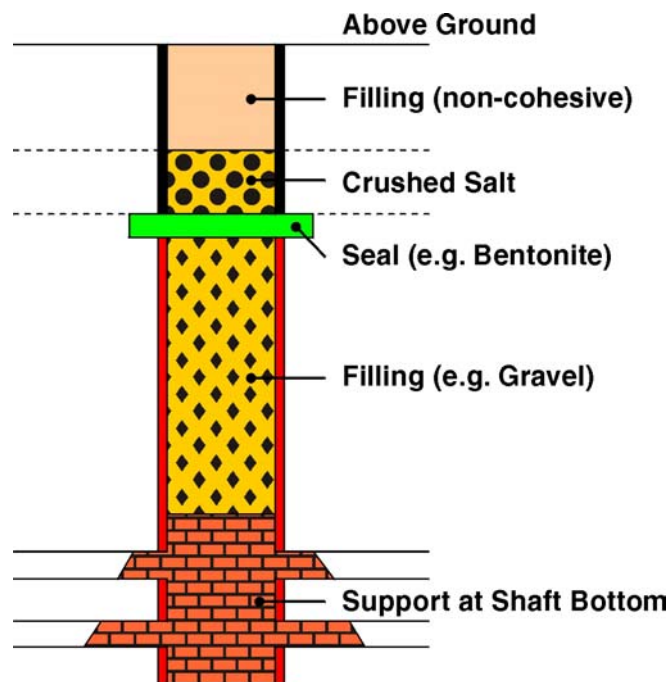


**Figure 2.7** Principle design of a shaft seal

### **3 Work Package 2: Instruments and experimental procedures**

#### **3.1 Description of test of the repository concept**

In Germany, research for the final disposal of radioactive waste in deep geological formations is performed on basis of two major research programmes which are

(1) (FZK-PTE 1998) „Programme for Promotion of Research for the Disposal of hazardous waste in deep geological formations (1997 - 2001)”

and

(2) (GSF 1990) „Repository Safety in the Post-Operation Phase”.

The research programme described in (FZK-PTE 1998) is divided into the following chapters:

- A1 Waste characterization
- A2 Safety requirements
- A3 Improvement of disposal and monitoring techniques
- A4 Geotechnical barriers
- B1 Development of scenarios
- B2 Behaviour of host rocks
- B3 Chemical and physical effects in the nearfield
- B4 Behaviour of geotechnical barriers
- B5 Behaviour of geological barriers
- B6 Computer codes for safety analyses
- B7 Model validation

The second programme (GSF 1990) includes the following chapters:

- 1. Scenarios and computer codes
- 2. Chemical effects in the nearfield
- 3. Geotechnical and physical effects in the nearfield
- 4. Transport processes in the geosphere

While (FZK-PTE 1998) represents more a programmatic overview of envisaged R&D, (GSF 1990) represents more an analysis of R&D needs still to be carried out for the improvement of repository concepts.

The in-situ experiments on high-level waste (HLW)/Spent Fuel disposal in a salt repository focused on investigating the effects mentioned above under items A3, A4, B2, B3 and B4.

In 1965, the Asse mine (Figure 3.1) was owned by the German government in order to perform in-situ testing of repository concepts. In the framework of the research activities, about 130,000 drums of 200 l volume containing low-level radioactive waste from research and industry and about 1,300 drums of 200 l volume containing non-heat producing medium-level waste were disposed of in the Asse mine. Main objective of this test disposal was the development of optimized transport, unloading, emplacement and backfilling techniques.

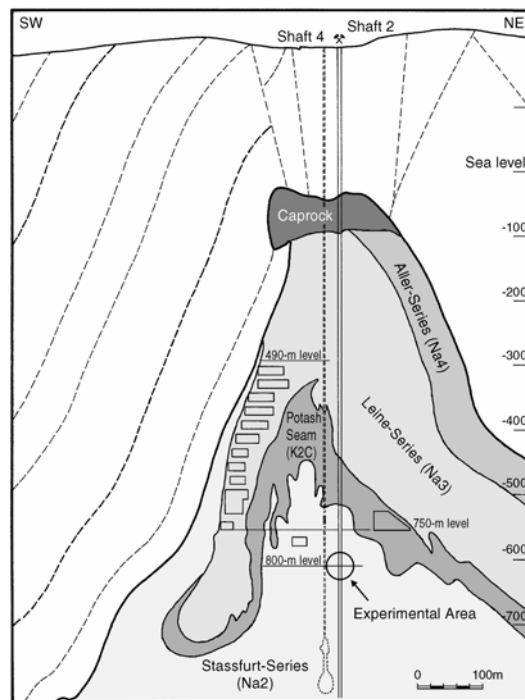


**Figure 3.1** Cross section of Asse salt mine

Research for the disposal of heat-producing HLW from reprocessing of Spent Fuel was already started in the mid sixties and concentrated in the first stage until the mid-eighties on the investigation of thermal and coupled thermo-mechanical as well as hydraulic and radiolytic effects in the nearfield of disposed vitrified HLW. Later on, several full-scale

simulation tests were performed focussing on development, testing and improvement of disposal techniques and on backfilling and sealing of HLW repositories.

Table 3.1 gives an overview of the individual tests related on HLW/Spent Fuel disposal that were performed at the Asse mine from 1967 until today.

**Table 3.1** Overview of in-situ tests at Asse mine on HLW disposal

<b>Test/Experiment</b>	<b>Period</b>
Temperature Test 1-3	1967 - 1976
Temperature Test 4	1978 - 1979
Temperature Test 5	1982 - 1983
Temperature Test 6	1985
Brine Migration Test	1983 - 1985
Test Disposal of Highly Radioactive Radiation Sources (abandoned)	1988 – 1993
DEBORA-Project (Development of Seals for HLW disposal boreholes)	1991 – 1995 (Phase I) 1996 – 1999 (Phase II)
Thermal Simulation of Drift Emplacement (TSDE)	1990 – 2000
Post Test Analysis of the TSDE experiment	2000 - 2004

## **3.2 Experimental procedures**

### **3.2.1 Heater tests**

The stability of salt formations has been proven for the past million years and it can thus be regarded as a natural guarantee for their stability for some thousands of years in the future. It must be realized, however, that the necessary mining activities for the repository as well as the decay heat especially of HLW/Spent Fuel can disturb the stability and the isolation capability of the salt formation during this period.

In order to make a good design and a reliable safety analysis of a radioactive waste repository, a reliable prediction of the thermo-mechanical behaviour (spatial and temporal distribution of the temperatures, deformations and stresses) is necessary. The thermo-mechanical behaviour of the host rock has to be known to assess the stability of the openings during the mining and operation phase of the repository, and that of the formation as a whole during the post-closure period.

Experimental determination of the long-term thermo-mechanical behaviour of a repository, however, is impossible due to the fact that the period in which the phenomena are working is in general much longer than it can be reached in an experiment. Therefore, numerical simulation of the thermo-mechanical behaviour has to be applied. The thermo-mechanical behaviour is described by fundamental equations of solid mechanics such as equilibrium equations, compatibility equations, constitutive relations and the corresponding boundary and initial conditions. Numerical methods as the finite-element method are capable to solve these equations. When performing the analyses, problems to deal with are the description of the geometry, the definition of the boundary and loading conditions, the constitutive relations and the numerical schematization.

The fact that a model is the only way to determine the long-term thermo-mechanical behaviour of a repository does not imply that experiments are not necessary. Experiments are needed to derive the material properties and to build confidence in the numerical models. This can be achieved by performing experiments under many different loading and geometrical conditions from simple samples to complex full-scale in-situ demonstrations. Since the mid-sixties, about ten heater tests on thermo-mechanical behaviour have been performed in the Asse salt mine. In these experiments, the temperature, stress, and deformation fields around single boreholes and around arrangements of several boreholes were measured. For most of the experiments, predictive calculations were made and the models used were continuously improved on basis of findings from comparisons of experimental and calculation results.

### **3.2.2 Brine migration tests**

Rock salt contains small amounts of water and gases (Jockwer 1981) which tend to move toward a heat source or disposed heat-producing HLW. The water contained in rock salt consists of different forms like crystalline water of the hydrated minerals polyhalite ( $K_2MgCa_2(SO_4)_4 \cdot 2H_2O$ ) and kieserite ( $MgSO_4 \cdot H_2O$ ), adsorbed water on grain boundaries, or small liquid inclusions. The analyses of 1000 rock salt samples taken from different geological salt formations at the Asse mine show an average integral water content of 0.04 wt %. If the water is released into the disposal borehole, it may accelerate corrosion of the waste canisters, thus leaching radionuclides from the waste matrix. It can also increase the borehole gas pressure, in case of completely sealed boreholes possibly up to the frac-strength of the salt formation. For the design and selection of waste overpack materials and

borehole plugs, it is therefore necessary to estimate the time-dependent release of water as accurately as possible. During early modelling of brine migration, the migration of both water vapour generated by the evaporation of water contained in the salt porosity or from hydrated minerals and the migration of liquid inclusions were considered.

The design of in-situ simulation experiments should represent the expected repository conditions as far as possible. With regard to the investigation of brine migration it is necessary to differentiate between short-term and long-term effects. It is possible to design the experiments to produce maximum amounts of released water by enforcing both migration mechanisms. These experiments may be called „Accelerated Brine Migration Tests” (ABM). It is also possible to design experiments to produce reduced amounts of water by restraining one of the above mentioned mechanisms. These experiments may be called „Restrained Brine Migration Tests” (RBM). Both types of experiments have advantages and disadvantages.

*ABM-Test:* This type of experiment has the advantage to simulate the short-term phase immediately after waste emplacement into the borehole which is of interest with regard to safety considerations during the operational phase of the repository. This experiment is designed to have

- high thermal gradients (representing a single borehole - enforcing liquid inclusion migration)
- low water vapour pressure in the borehole (representing an open borehole - enforcing vapour migration)
- reduced radial stress at the borehole wall (representing an annulus between waste canister and the borehole wall)

A disadvantage is, that it is impossible to differentiate between the migration mechanisms because of composed effects.

*RBM-Test:* This type of experiment has the advantage to simulate the long-term phase after waste emplacement which is of interest with regard to long-term safety analysis. This experiment is designed to have

- reduced thermal gradients (representing overlapping temperature fields of several boreholes - restraining liquid inclusion migration)

- water vapour pressure built-up in the borehole (representing a sealed borehole - restraining vapour migration)
- high radial stress at the borehole wall (representing a closed annulus between waste canister and borehole wall)

A disadvantage is, that only a very small amount of released water is produced, thus increasing the testing period and introducing measuring difficulties. However, by combining different design parameters of ABM and RBM-tests it is also possible to investigate the contribution or the importance of the different migration mechanisms.

Typical examples of the layout of both types of experiments are shown in Figures 3.2 and 3.3.

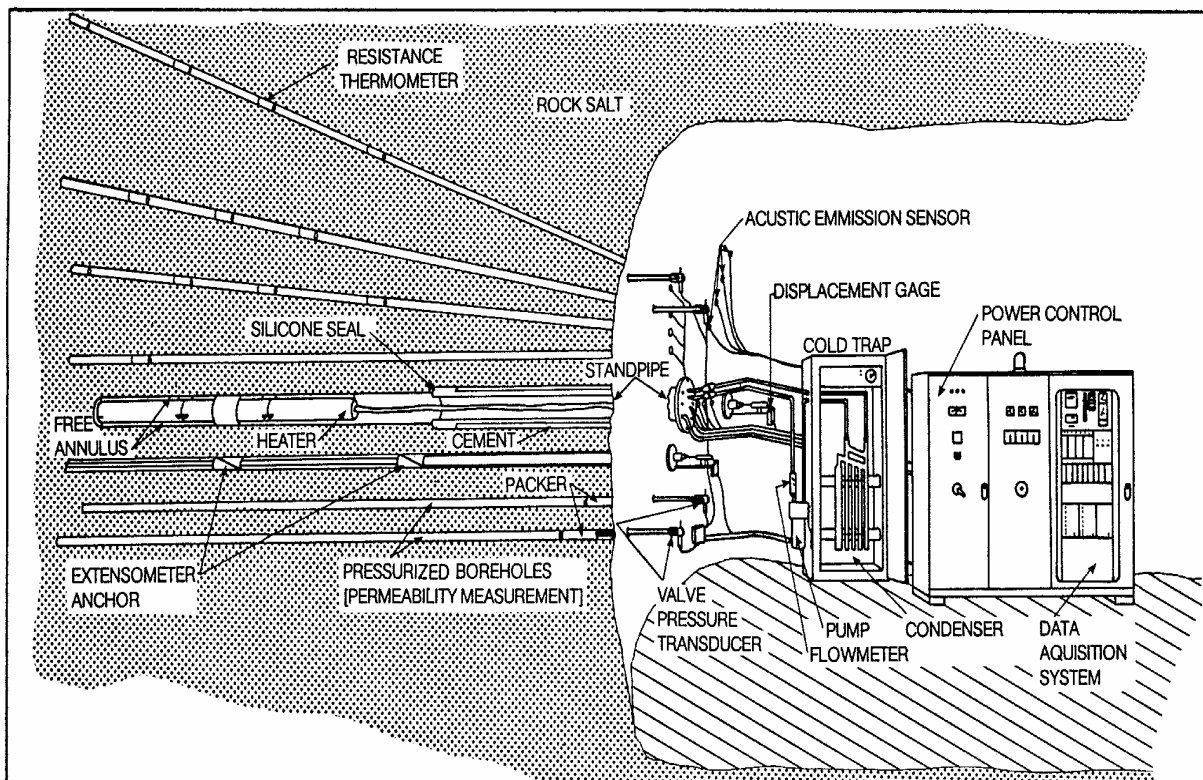


**Figure 3.2** Temperature Test 5

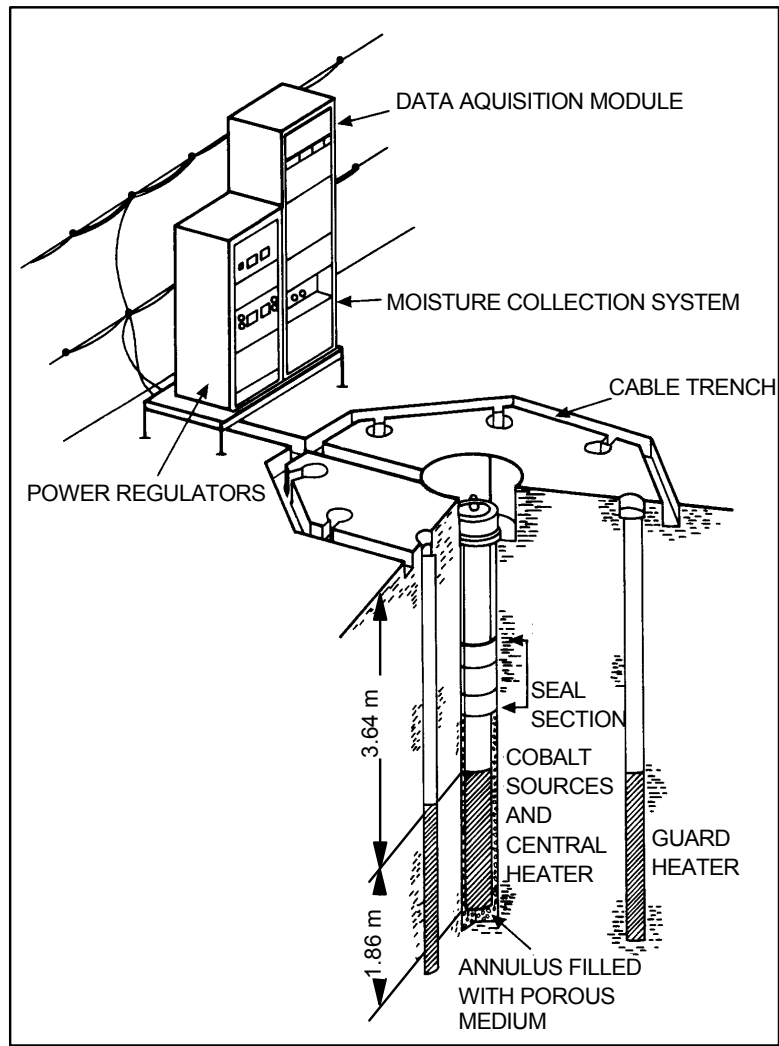


**Figure 3.3** Brine Migration Test

Figure 3.2 shows the test set-up of the Temperature Test 5 which was performed in an unlined horizontal borehole at the 775-m level of the Asse mine (Rothfuchs 1986). This heating test represents a single borehole ABM-test having a free initial annulus of 4 cm between the heater and the borehole wall. The water release to the borehole was measured by continuous condensation of the water in a cold trap, thereby keeping the water vapour partial pressure in the borehole at a low level.

Figure 3.3 shows the configuration of one of the four brine migration tests that were conducted on the 800-m level at Asse mine as a joint American-German effort (Rothfuchs et al. 1988). This experimental set-up represents a RBM-test. The overlapping temperature field of several boreholes was simulated by the use of eight „Guard Heaters” surrounding a

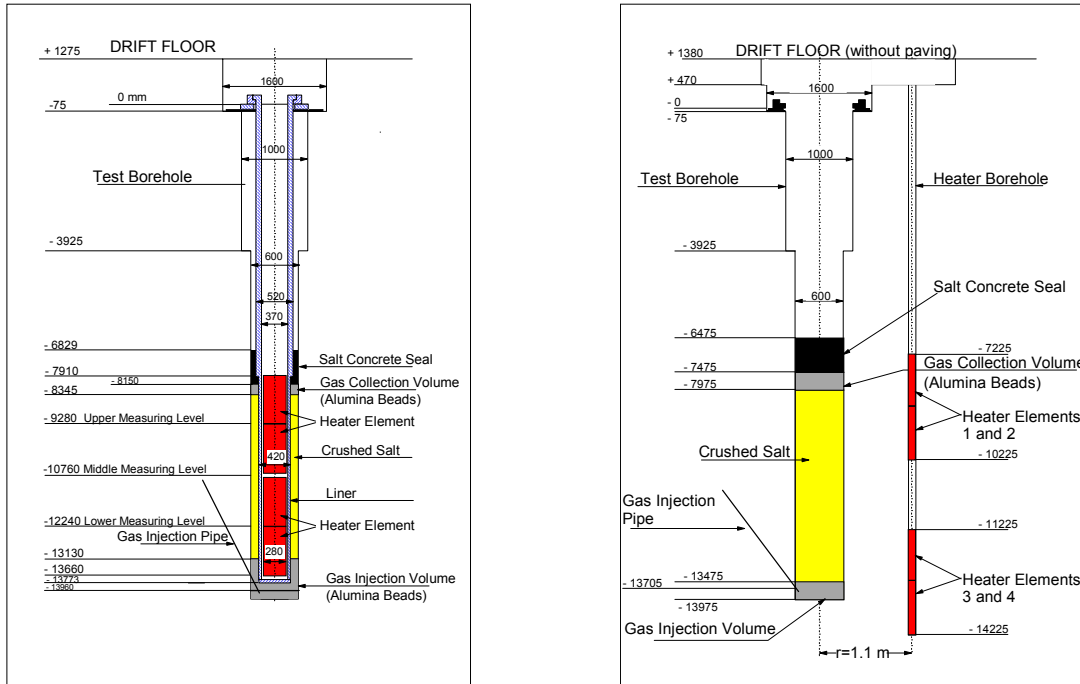
central heater. Hereby, the temperature gradient at the central borehole wall was reduced as desired in a RBM-test. The annulus between the borehole wall and the heater was filled with a porous medium for keeping the annulus open for gas and water collection and for maintaining mechanical stress at the borehole wall. The central borehole was completely sealed and the released gases (e. g., water vapour) were permitted to build up pressure. The water vapour concentration in the borehole atmosphere was determined by periodically performed gas analysis and a final cold trap measurement at the conclusion of the test.

### **3.2.3 Backfilling and sealing tests**

Two important in-situ experiments on backfilling and sealing of HLW repositories were performed in the last ten years at Asse. These experiments were the „Thermal Simulation of Drift Emplacement” (TSDE) experiment and the DEBORA („Development of Borehole Seals for high-level radioactive waste”) experiments. The experiments were comprised in the international BAMBUS (Backfill and Material Behaviour in Underground Salt repositories) project co-funded by the Commission of the European Communities (CEC). Three foreign European countries participated in the phase I of the BAMBUS project. Interim results of project phase I were reported in detail by Bechthold et al. (1999).

#### **3.2.3.1 The DEBORA experiments**

The DEBORA experiments were aimed at the development and investigation of borehole seals consisting of crushed salt backfill in HLW boreholes (Rothfuchs et al. 1999). The DEBORA-1 experiment was focused on investigating the backfill behaviour in the annulus between the waste canisters and the borehole wall. In the DEBORA-2 experiment, the backfill in the seal region between the canister stack in the borehole and the disposal drift was investigated. The measurements were carried out in two separate experiments because the boundary conditions in the two borehole regions are completely different. First, the temperature and thus the rock mass convergence is different in the borehole annulus and in the seal region and second, the grain size of the backfill material is significantly different. Principle studies on the design and the behaviour of crushed salt in HLW boreholes as well as the development of a test plan were performed in the Debora project phase I (Rothfuchs et al. 1996). Figure 3.4 shows the layout of the DEBORA experiments. In order to achieve



- a) Debora-1 experiment for investigation of the crushed salt compaction in the borehole annulus
- b) Debora-2 experiment for the investigation of the crushed salt compaction in the seal area

**Figure 3.4** Layout of the Debora experiments

the necessary degree of compaction within one to two years, the borehole closure was accelerated by heating of the surrounding rock formation.

In both experiments the temperature, the radial stress, and the borehole closure was measured at three different levels and azimuthal directions. The backfill porosity was determined by volumetric evaluation of the convergence measurements. In order to determine the permeability, nitrogen was injected into the deepest part of the boreholes, the gas injection volume, causing an upward gas flow. The gas was collected at the upper end of the backfill column in the gas collection volume. Instruments were installed to measure the inlet and the outlet gas flow and the gas pressure in the gas injection and in the gas collection volumes. When stationary gas flow was achieved, the permeability of the crushed salt was calculated according to Darcy's law for compressible flow media.

### **3.2.3.2 The TSDE experiment**

Today, the TSDE experiment represents the most important in-situ experiment in Germany on direct disposal of Spent Fuel in a salt repository because, after revision of the Atomic Act in the early nineties, the direct disposal of Spent Fuel became an option with equal rights as reprocessing.

#### ***Outline of the project***

According to the German reference concept for the direct disposal of Light-Water Reactor (LWR) spent-fuel elements, the fuel rods are to be emplaced in self-shielding POLLUX-casks which will be disposed of in underground drifts in a salt repository (Hartje et al. 1989). Simultaneously to cask emplacement, the drifts are backfilled with crushed salt. The drift length is assumed to be some hundred meters and a drift will contain up to thirty casks.

The heat release from the waste induces heat-up of the backfill material and of the surrounding rock salt which leads to increased mechanical stresses and accelerated drift closure rates resulting in the compaction of the backfill material. With regard to an intrusion of salt brines from the overburden or from brine pockets in the rock salt, the permeability of the backfill material is of special interest in view of the long-term safety of a repository. A further safety aspect is the keeping of a maximum salt temperature of 200 °C. In the beginning, the low heat conductivity of the backfill at higher porosities leads to high temperatures at the interface of the cask and the backfill. During compaction, however, the heat conductivity increases with time, thereby reducing the interface temperature.

In order to prove the feasibility of the direct disposal, the full-scale TSDE demonstration test was performed in the Asse mine between September 1990 and February 1999 (Droste et al. 2001). The main objective of the experiment was to investigate the in-situ behaviour of the rock mass and of the crushed salt backfill under repository relevant in-situ conditions and to validate the theoretical models used to predict the compaction and permeability of the crushed salt. In addition to the mechanical parameters, the gas development in the pore space of the backfill was monitored and analyzed. In order to study the corrosion behaviour of potential cask materials, 280 material samples were placed on one heater cask at temperatures between 170°C and 200°C and in the backfill at temperatures of about 100°C.

## Test field

The TSDE test field is located in the Asse mine in the north-eastern part of the anticlinal core of the salt dome (Figure 3.1). On the 800-m level, the test field was excavated inside the Staßfurt Halite ( $\text{Na}_2\text{S}$ ) which is dipping to the north-east in this part of the anticline. The Staßfurt Halite is built by a monotonous series of alternating halite and sulphate layers. The thin sulphate intercalations are mainly composed of anhydrite and polyhalite.

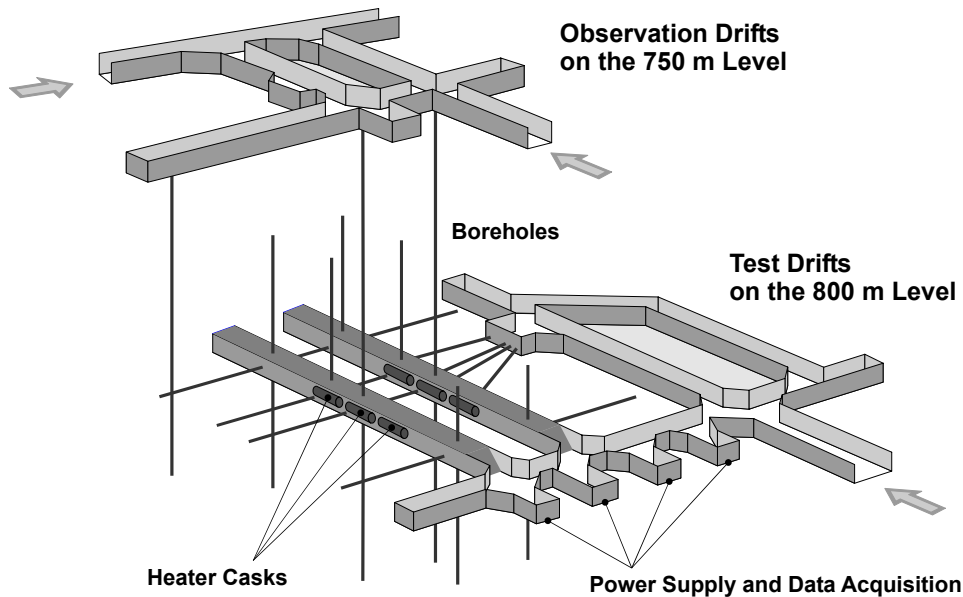


**Figure 3.5** General view of the TSDE test field

The test field was designed to simulate reference repository conditions for Spent Fuel. A general view of the entire test field is given in Figure 3.5. Two parallel test drifts were excavated on the 800-meter level. The drifts were 70 m long, 3.5 m high, and 4.5 m wide, and separated by a 10 m wide pillar. In each drift, three electrically heated casks were deposited. In addition to the two test drifts, the test field included several observation and access drifts on the 800-m level and on the 750-m level. Niches along the observation and access drifts contained the power supply and the data acquisition systems.

After the installation of the heaters and the measuring equipment, the test drifts were backfilled with crushed salt in slinger technique. The crushed salt used for backfilling was obtained from the excavation of the test drifts by means of a continuous miner. The oversized grain fraction was removed by sieving, leaving crushed salt material with a grain

size of less than 45 mm. This backfill material was re-emplaced in the test drifts using a slinger truck. From the total mass of emplaced crushed salt and the total test drift volume, an initial backfill porosity of about 35 % was determined, corresponding to an initial density of 1400 kg/m<sup>3</sup>.

### **Design and manufacturing of heaters**

Each heater cask consisted of seven bolted ring-shaped segments and contained two electric heaters (Figure 3.6). For redundancy reasons, each electric heater contained three heating circuits (4 kW power per heating circuit) with separate conductor to the heater control system. In case of interruption, the heater control system switched over to the next heating circuit. The heater cask layout provided the requested heat power of 6.4 kW per cask with a safety factor of 2.

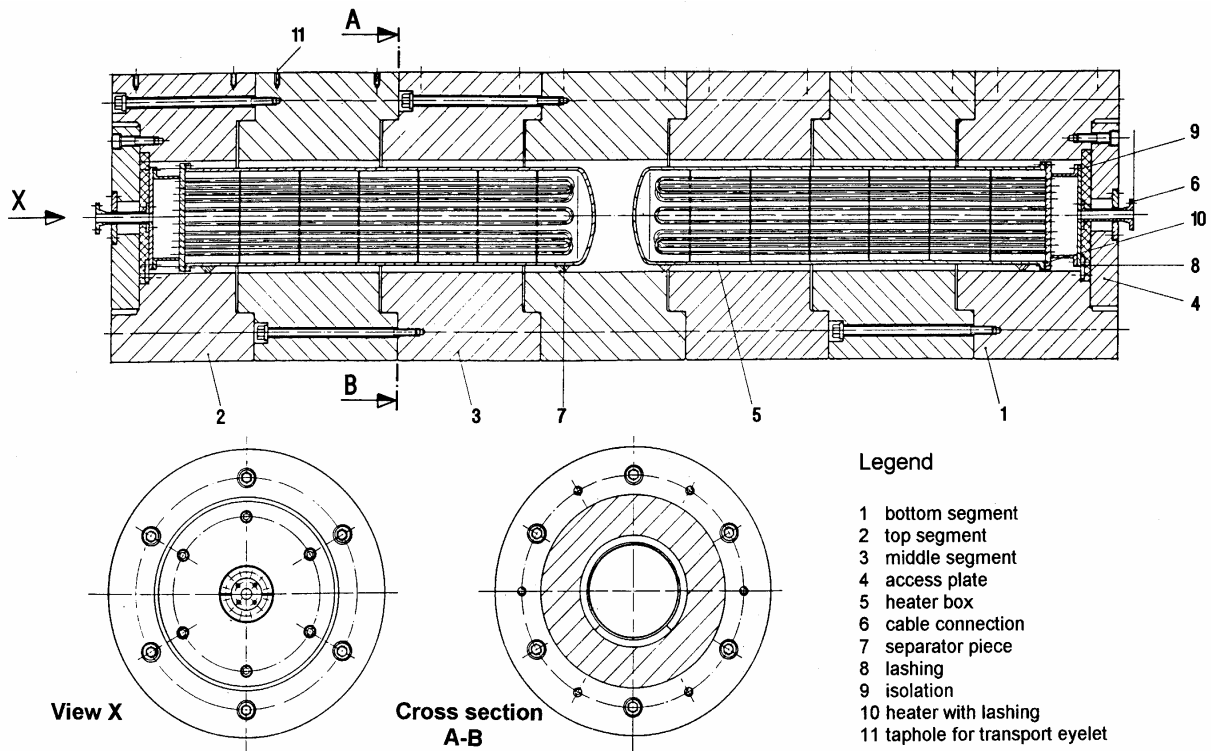


**Figure 3.6** Longitudinal section of a TSDE heater cask

The layout of the heater casks was based on the data of a POLLUX cask for 8 PWR fuel elements and on the test boundary conditions as follows:

Length:	5.50 m
Outside diameter:	1.54 m
Total weight:	65 t
Maximum thermal power per heater:	10 kW
Design service power per heater:	6.4 kW
Heater lifetime:	60,000 h at full load
Redundancy:	in duplicate
Cask and lining strength:	against 18 MPa rock pressure
Distance between the casks:	3 m

### ***Instrumentation***

The investigation programme comprised the measurement of the following parameters:

- temperatures at the cask surface, in the backfill, and in the rock mass
- backfill compaction and backfill pressure
- drift closure (convergence) and rock mass displacements
- initial stress field and stress changes in the rock mass
- permeability of backfill and rock mass
- gas release in consequence of the heat-up of the salt and of material corrosion

Different kinds of measuring methods and measuring devices were used, among them:

- about 750 stationary resistance thermometers of the type PT 100
- 130 glass fibre rod extensometers for measurement of rock displacements
- 22 stationary devices for measurement of drift closure
- 10 stationary devices for measurement of backfill settling

- about 220 hydraulic Glötzl pressure cells and 15 large flat jacks for the determination of rock stresses
- 44 hydraulic Glötzl pressure cells for pressure measurements at the backfill/drift wall interface
- mobile overcoring probes for measurement of the initial stress
- mobile dilatometer probes for measurement of rock stiffness
- a gas sampling system consisting of filter pipes and Teflon tubes

Since the test drifts were no longer accessible after backfilling, special development and fabrication was necessary in many cases to increase the resistance of the measuring equipment against the extreme environmental conditions, as for instance high temperatures and release of corrosive fluids.

### ***Instrumentation plans***

Detailed instrumentation plans were developed for all Asse tests. Exemplarily, Figure 3.7 shows the instrumentation plan of the TSDE experiment. Measuring instruments were installed in the rock around the test drifts from adjacent drifts and in thirteen monitoring cross sections in the test drifts. Most monitoring cross sections were located in the heated area around the casks and between the casks. Further details can be taken from the TSDE test plan (TSS-Testplan, 1993).

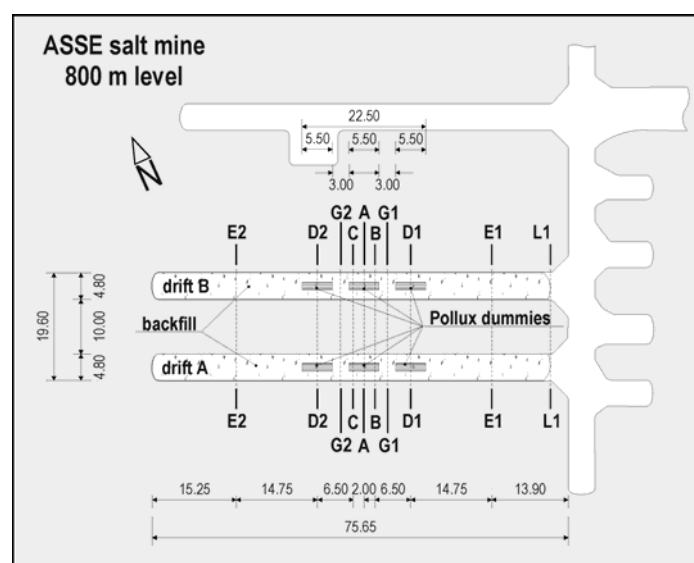


**Figure 3.7** TSDE-test drifts on the 800-m level with monitoring cross sections

### ***Rock instrumentation***

Rock temperatures were recorded by resistance thermometers in boreholes in the surrounding rock salt. Rock deformations around the test drifts were recorded by extensometers and inclinometers in boreholes measuring the axial and radial borehole displacements, respectively. Axial borehole displacements were monitored by multiple point glass fibre rod extensometers which were installed in the sections A and D1 in the heated area and in the non-heated sections E1 and E2 (Figure 3.7). Boreholes in the floor, in the walls, in the pillar, and in the roof of the test drifts were equipped with a set of four extensometers each. From the observation drifts on the 750-m level, further extensometers had been installed in the pillar and above the test drifts. In section A+1, the rock deformations were additionally recorded by inclinometer measurements. From the 750-m level, five boreholes had been equipped with access guide tubes.

To observe long-term stress changes in the host rock induced by drift excavation and by heating, more than fifty stress monitoring probes were installed in a number of boreholes. From the observation drifts on the 750-m level, two boreholes ending above the test drifts and three boreholes extending into the pillar were equipped with monitoring probes. Two additional boreholes were located below each test drift. The probes consisted of seven Glötzl type hydraulic pressure cells which had various orientations for measuring the vertical component, three horizontal components perpendicular, parallel, and at an angle of 45° to the drift axis, and two subvertical components with an incline of 45° perpendicular and parallel to the drift axis.

### ***Backfill instrumentation***

Backfill temperatures were recorded by thermometers at the surface of the heater casks and in the backfill. In order to determine backfill compaction, both drift closure and backfill settling were measured by means of stationary measuring equipments which had been specially designed for the TSDE test. Horizontal and vertical convergence measurements were carried out both in the heated zone and in the non-heated area. Backfill settling was monitored by equipment which was installed in the heated sections and in the non-heated sections E1+1 and E2-1 (Figure 3.7). With each equipment, the settling was measured at three levels. Generally, one gauge was installed at the floor to measure the drift convergence, another one in the middle of the backfill, and the uppermost one on the top of the backfill to monitor the opening and closing of the gap between drift roof and backfill. In the cross sections where separate convergence measurements were carried out, two gauges were installed in

the lower and upper third of the backfill in order to determine the vertical distribution of backfill settling.

Hydraulic Glötzl type pressure cells were used to measure the pressure between backfill and surrounding rock. The pressure cells were installed at the floor, at the roof, and at the walls of the test drifts. Measurements were carried out in the heated sections as well as in the non-heated section E1 (Figure 3.7).

### ***Data collection***

A typical data collection system and procedure was operated in the TSDE experiment. The data collection was carried out by local front end processors which were operating independently. The measurements around the test drifts and from the observation drifts were recorded by two units on each level with one unit recording the electrical readings and the other one the hydraulic measurements. Except for the early heating phase with a higher sampling frequency, the measuring sensors were scanned every twelve hours.

A central PC was installed on the 800-m level which received the data from all front end processors via RS-232C interfaces. The data were converted into a standardized temporary format and stored on hard disk. Once a week, the data on the central PC were transferred via modem to the archiving and evaluation computer in Braunschweig. In Braunschweig, archiving of the data was carried out by a local TCP/IP network on a hard disk of the central file server SUN 1000. The hard disk was saved regularly on DAT-tapes or MO-disks.

Different precautions had been taken against loss of data and unauthorized access. Additionally, an alarm system was recording different fault messages in the test field. The coded fault messages were transmitted above ground to the service facilities where they were shown on a display and recorded as print-out. Further details of the data acquisition system are described in Droste et al. (1996).

### ***Post-test drift excavation and analyses***

Termination of heating in February 1999 led to a rapid temperature decrease in the vicinity of the heater casks. 18 months later in August 2000, the temperature at the top of the central heater had decreased to approximately 50°C (Figure 3.8) and in the area 12 m away from possible, and backfill excavation was started late August 2000 (Rothfuchs et al. 2001).

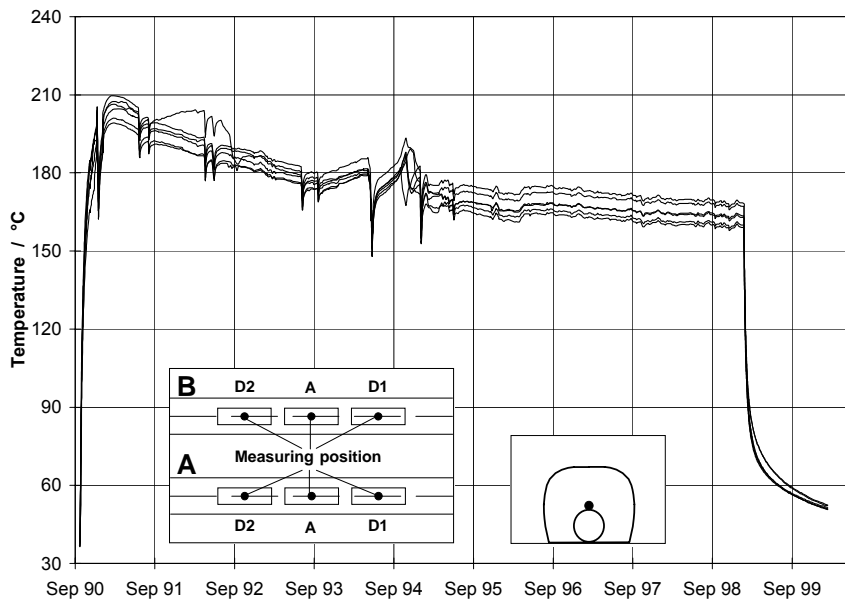


**Figure 3.8** Temperatures at the heater surface in the TSDE experiment

Near to the drift entrance, backfill compaction was low enough to use a shovel loader for drift excavation. With increasing depth, backfill compaction increased. Therefore, a continuous miner was required for removing the backfill. Retrieval of instruments and sampling were performed manually. Since tests to remove the heaters were successful (Figure 3.9), it was decided to remove the heaters as well.

During the TSDE experiment, most data had to be obtained remotely. Originally, the measuring equipment had been designed for a five years testing period, but was operated over more than ten years under repository conditions. As no inspection or maintenance had been possible during the test period, instrument accuracy and reliability could not be checked at site and were to be analysed after termination of the experiment (see section 3.3.2).

During test drift excavation which was finished in May 2001, all instruments which had been located in the backfill and at the surface of the heater casks were therefore retrieved to study their performance regarding sensor drift, measurement errors and failure reasons. The readings from the heating phase were compared with the actual conditions in the test drift in order to verify the data which had been obtained during the in-situ test. Failed gauges were checked carefully with regard to their failure reason. The need to evaluate the conditions and the performance of the long-term monitoring instruments is demonstrated by the convergence measurement device which had been installed near to the central heater. Its horizontal measuring rod had been bent upwards due to floor uplifting (Figure 3.10).



**Figure 3.9** Opening of a heater cask



**Figure 3.10** Bent convergence measuring device

### **3.3 Selection and application of instruments for recording of major processes in field tests and repositories**

#### **3.3.1 Measuring principles and devices**

Underground research laboratories are operated for testing and demonstration of the suitability of repository concepts and for the investigation of combined effects resulting from the disposal of heat generating high-level waste. Well designed in-situ tests are useful for the validation of computer models that are needed for the design of the repository and for long-term safety analyses.

Monitoring of underground laboratories or repositories requires the selection/development and application of a robust measuring instrumentation with adequate resolution under the expected conditions. Calibration of the instruments before and after testing, often over several years in situ, is an indispensable requirement with regard to quality assurance. In many in-situ experiments, the instrumentation is installed in a non-retrievable manner in the host rock. In such cases, post-test uncovering of parts of the test field and representative retrieving of the used measuring equipment is necessary.

In the past years, at the Asse mine, and especially in the TSDE experiment, the following important parameters have been measured which will briefly be described together with the respective measuring sensors/methods.

### **3.3.1.1 Temperature**

The temperature field of a heater test can be measured with various temperature measuring devices with the most adequate being thermocouples and resistance thermometers.

#### ***Thermocouples***

Thermocouples make use of the Seebeck effect: When two conductors consisting of different materials are coupled on one end, a thermal voltage can be measured between the free ends if there is a temperature difference between the coupled ends and the free ends. The value of the voltage depends on the temperature difference and on the materials used. The two conductors are placed in an insulation which is coated (usually by chromel-alumel). The conductors may consist of various materials; for instance nickel-chromium/nickel (NiCr-Ni) or platinum-rhodium/platinum (PtRh-Pt). In Germany, the guaranteed accuracy of thermocouples is determined by the industrial standard DIN 43710. For temperatures up to 400 °C, the permitted deviation is 3 °C. Thermocouples which guarantee an accuracy of 1/2 or 1/4 DIN (e.g., a maximum deviation of 1.5 °C or 0.75 °C) are also commonly used.

#### ***Resistance temperature detectors (RTD)***

The resistance of metallic conductors increases with temperature. This effect is used by resistance temperature detectors (RTD) which consist of an encapsulated metallic wire (usually platinum) with two to four connector wires. The four-wire technique allows for the compensation of the resistance of the connector wires and is therefore the most adequate one.

The platinum wire has a resistance of 100 ohms at 0 °C, increasing by about 0.39 ohms/°C (at 0 °C). The measuring accuracy as regulated by IEC (International Electrotechnical Commission) 751 is 0.3 °C at 0 °C, 0.8 °C at 100 °C, and 1.55 °C at 250 °C. The platinum-type RTD was more accurate than the thermocouple, especially at moderate temperature.

### **3.3.1.2 Deformation**

The most important devices for in-situ displacement measurements are presented in this section. They can be divided into two groups: Devices for measuring displacements in the rock and devices for monitoring the deformation (convergence) of cavities such as drifts or chambers.

#### ***Convergence measurements***

Convergence measurements are performed by determining the relative displacement between two opposite points in an underground opening. This means that they cannot provide any information on absolute movements, which is a restriction of most in-situ displacement measuring techniques. An important advantage of all convergence meters is that they can easily be installed directly after excavation of underground voids. In order to provide data about the initially high deformations caused by primary creep, convergence meters should be installed as soon as possible after excavation (or even during excavation).

#### ***Extensometer measurements***

Borehole extensometers are used to measure movements in the rock mass relative to a reference point (usually located at the borehole collar). Several types of extensometers are applied (Brown 1981 and Paul and Gartung 1991), but most commonly rod extensometers are used. The anchors can be fixed by wedging or by grouting. At the instrument head of the extensometer, the displacement of the anchor points can be registered automatically by displacement transducers.

### **3.3.1.3 Stress**

For the in-situ investigation of the mechanical behaviour of rock salt, stress measurements are very important, too. But while standard methods for displacement measurements are available, rock stress determination is difficult, especially if the rock has a distinct elasto-viscoplastic behaviour like rock salt. In most experiments at the Asse mine, hydraulic pressure cells and AWID cells have been used to monitor stress changes. In addition, the overcoring method is being used to determine absolute stress.

### ***Hydraulic pressure cells***

The hydraulic pressure cell (as produced by GLOETZL) is a flatjack which is filled with mercury or oil. The flatjack is connected to a diaphragm transducer which in turn is connected to a readout unit by flexible tubes. By pumping oil against the diaphragm, the pressure inside the cell is compensated and the compensation pressure is recorded. The pressure inside the cell is determined by the stress acting on it. In the ideal case, the compensation pressure can be interpreted as the stress component normal to the flatjack. For stress measurements in rock salt, the cells are usually emplaced in boreholes and subsequently grouted.

For stress measurements in salt, stress release due to creep is a basic problem. After the installation, the pressure cell takes up stress only gradually. The prevailing stress is approached only after a very long time period in the range of  $10^8$  days (Heusermann 1987), so that the measurement of absolute stress is impossible with this method.

While determination of absolute stress with hydraulic pressure cells is problematic, they are suitable for the measurement of stress changes (for instance, due to temperature changes in the course of a heater test). However, it has to be kept in mind that the measured response, which is due to an increase in compressive stress, is also partly caused by an improvement of the cell's coupling to the rock because of an accelerated creep of the salt.

### ***AWID cells***

The AWID cell (Kessels 1984) is an active pressure cell (in contrast to the hydraulic pressure cell of the GLOETZL type) which also uses the compensation method. It consists of two metal plates (CrNi) which are soldered together at their edges. The space between the plates can be pressurized with oil or air. During the measurement, a constant electric current is injected through the cell, and the voltage over the cell is measured. Then, the cell is pressurized. As long as the inner pressure of the cell is lower than the outer pressure, the current goes over the two plates being in contact with each other; the resistance of the cell and thus the measured voltage is low. As soon as the inner pressure exceeds the outer pressure acting on the cell, the plates will open, and the resistance of the cell will rise sharply, as will the measured voltage. Laboratory tests have shown an accuracy of 0.3 % by determining the pressure from the bend in the voltage-pressure-curve.

Advantages of the AWID cells are their simple construction and their capability of being operated at high temperatures (especially when air instead of oil is used), because the rise in resistance, which is used for the determination of the compensation pressure, is not dependent on material properties of the cell or the surrounding rock (or grout). For installations in a borehole, it is useful to grout the AWID cells in a cylinder and subsequently place this cylinder into the borehole. Thus, a good coupling between the cells and the grout can be assured, and damages of the cells during installation in the borehole are impossible.

### ***Overcoring***

The overcoring method is used for determining absolute stress in a core borehole by measuring the core deformation due to load reduction. The measurement is performed by placing a probe equipped with strain gauges or displacement transducers into a small diameter pilot borehole which is subsequently overcored. The radial deformation of the pilot borehole is measured (Kiehl and Pahl 1990). Assuming an ideal elastic rock, the absolute stress components perpendicular to the borehole axis can be calculated from the change in diameter of the pilot borehole if Young's modulus or the Poisson ratio of the rock are known. The measuring results are then independent of the overcoring diameter and of the time between drilling of the pilot borehole and overcoring.

Numerical studies (Pahl and Heusermann 1989) have shown that this way of evaluation is not appropriate for viscoplastic rocks like salt. The comparison of calculated deformation curves for the ideal elastic case and for the so-called „curve description model” that takes into account a non-linear viscoplastic behaviour of the rock during overcoring has shown that the whole deformation development during overcoring has to be recorded rather than making a diameter measurement before and after overcoring like in case of a rock which is not ideal-elastic. In the curve description model, stress relaxation due to non-linear creep is not taken into account. This requires an additional correction which depends on the overcoring diameter as well as on the time between drilling of the pilot borehole and overcoring.

A realistic estimate of the three-dimensional stress state will only be possible if the measurements are evaluated by numerical modelling of the complete overcoring procedure.

### ***Hydraulic fracturing***

Hydraulic fracturing is a technique for determining both value and direction of the least principle stress component in a homogeneous isotropic rock. It is usually performed by

sealing a part of a borehole and afterwards injecting a fluid into the sealed part. The pressure which is necessary to fracture the rock (recognizable by an increase of fluid flow into the rock) and the so-called shut-in pressure (pressure for which the flow drops to zero again) are recorded. The shut-in pressure is interpreted as the value of the least principle stress (Fischle et al. 1988). The direction of the least principle stress is assumed to be perpendicular to the fracture plane. Reliable methods for determining the fracture plane are acoustic emission monitoring (Manthei et al. 1998) and drilling or mining into the fractured region with surveying of the fracture.

#### **3.3.1.4 Gas and water release**

For determining generated and released volatile components in the rock and in the backfill, two different systems have been developed by GRS (Gies et al. 1989).

Boreholes drilled in solid rock are sealed with a mechanically expandable packer system. It consists of two independent Viton seals which are spanned and pressed against the borehole surface by a nut at the top. All surfaces of the packers and the valves which may have contact with the borehole atmosphere are coated with Teflon. Via Teflon tubes passing through the packer, gas samples can be extracted from the residual borehole for analyses.

In backfill and buffer materials in sealed drifts or disposal fields, permeable filter pipes of ceramic or sintered metal with a diameter up to 10 cm and a length up to several meters are installed. Into the front end plug of each pipe assembly, two holes are drilled in order to insert two Teflon tubes. One of the tubes is led to the back end and the other one to the front end of the ceramic pipe so that the residual volume can be rinsed by inert gas. These Teflon tubes run through the buffer to the open gallery for gas extraction and gas injection. The ceramic pipes have a porosity of 42.5 % and a permeability of  $2 \cdot 10^{-9} \text{ m}^2$  so that they can easily be penetrated both by gases and liquids which allows gas and moisture sampling from the buffer as well as gas injection into the buffer. A similar system had also been installed in the TSDE experiment at the Asse mine.

At the open drift, the Teflon tubes of both systems are closed by valves. For gas sampling and analyses a pump is connected to these valves. Additionally, the humidity of the atmosphere is determined electronically during sampling.

### 3.3.1.5 Geoelectric monitoring

Geoelectric survey combined with laboratory calibration measurements is a non-destructive method for measuring the water content in rock masses as well as in backfilled underground voids. By special electrode arrays and repeated measurements, the resistivity changes in surveyed areas, caused by water accumulations or dryout effects, can be determined. The method can be applied to low-porous and low-permeable rocks, such as rock salt. It has been successfully used for the exploration of excavation disturbed zones (Wieczorek and Zimmer 1999). During application of the method, the direct electric current is introduced into the rock mass by two electrodes. The resulting electric field is observed by two other electrodes and the apparent resistivity is calculated by Ohm's law. Series of readings and inverse modelling are required for converting the apparent resistivities into true resistivities. By means of laboratory calibration measurements, the true resistivity can be related to water content and pore saturation. In recent years, advanced geoelectric measuring systems for the semi-automatic monitoring of large rock masses have been developed (Yaramanci and Flach 1989). Electrode networks of up to 480 electrodes can be operated. The measuring systems are remotely computer-controlled and designed for multipurpose use.

### 3.3.1.6 Fibre optic monitoring systems

Among the different sensing and multiplexing techniques available, the sensor development focuses on the Fibre Bragg Grating technology along with the corresponding multiplexing technique. Fibre Bragg Gratings (FBGs) are diffracting elements printed in the Germanium-doped core of an optical fibre. FBGs consist in a periodical modulation of the core refractive index along a short length. They behave like selective filters which reflect in the fibre core the spectral components  $\lambda$  of a propagating packet according to the Bragg relation  $\lambda = 2 n \cdot \Lambda$ , with  $n$  being the core mean refractive index and  $\Lambda$  the FBG step or the spatial period of the refractive index modulation. If the temperature varies,  $n$  is accordingly modulated through the thermo-optic effect. If the FBG is strained along the fibre axis,  $\Lambda$  is modulated. As a result, the FBG (or Bragg) wavelength is shifted, which is a measure for the parameter under investigation. This working principle enables to measure practically any physical value which yields an elongation of the fibre core (e.g. pressure, stress, strain, convergence).

Since 1995, fibre optic sensors have been developed to measure mechanical displacement and strain as well as temperature, humidity, pH and hydrogen concentration. All sensors

have been successfully tested in the laboratory and except the two last ones the sensors have been validated under in-situ conditions at DBE's Konrad mine in Germany.

Fibre optic cables with opto-mechanical sensing elements built with FBG can be used to monitor the deformation of an underground cavity, e.g., a drift, by installing them along its perimeter. With automatic data acquisition and less maintenance, this kind of configuration provides remote, continuous monitoring at low operational costs. The fibre optic strain cable, based on FBG technology, is an advanced design extensometer. Its advantages are less instrumentation and cabling and the possibility of using smaller boreholes compared to conventional extensometers. A fibre optic temperature cable has been built by printing a couple of FBG's in a fibre to monitor the temperature at selected points on the fibre.

All sensors can be implemented in an all fibre optic network ensuring a secure data transmission and a uniform multiplexing and data acquisition system.

### **3.3.1.7 Supporting investigations**

Further supporting investigations that were conducted at Asse in connection with in-situ experiments were permeability measurements within the ALOHA-project which deals with the development and healing of excavation disturbed zones (EDZ) around underground openings. The effectiveness of borehole and drift seals in repositories for radioactive or toxic waste in salt formation is, among others, dependent on the EDZ of the surrounding rock, which develops as a consequence of displacements and related stress redistribution during and after the excavation. It is assumed that the EDZ is reduced with time when a seal is emplaced and the rock stress increases again. The hydraulic properties of the EDZ and their development during the recovering phase are subject of the investigation in the ALOHA project. As the recovering phase takes too much time for direct measurements, a correlation between permeability and stress state is to be deduced. Therefore, in-situ measurements of permeability and stress have to be performed at various test sites different in stress state and size of the excavation. For stress measurements, the overcoring method is used. Permeability measurements are performed by injecting gas into sealed borehole intervals. From the injection rate and the pressure development during the injection phase and the subsequent shut-in phase, the permeability is derived.

As a result of excavation activities, the initial stress field will change. Further changes must be expected from the effects of heating, i.e., from thermal expansion of rock salt, altered

material properties, enhanced plasticity, creep effects and sudden stress release. Seismic P- and S-wave velocities allow an evaluation of the specific elastic rock parameters, compression modulus, and shear modulus. Especially sudden stress release which may be caused by microfracturing processes can result in locally changed mechanical properties. These effects can be investigated by seismic in-situ measurements as there are a) microseismic (seismological) activity (passive seismic measurements) and b) seismic traveltimes (active seismic measurements). Respective measurements were performed within the HAW-project (Hente 1992) and are currently performed in the BARIAN-project at the Bernburg salt mine (Kamlot and Flach 2001).

### **3.3.2 Post-test analysis of instruments used in the TSDE experiment**

From the recovered measuring equipment in the TSDE experiment, a representative number of gauges was chosen for further investigations and re-calibration. The selected gauges were shipped to their manufacturer. Generally, the re-calibration results revealed the high reliability of the applied sensors. After nearly 12 years of operation at very high temperatures, the linearity of most gauges was still within the manufacturer's respective limit of tolerance. Details for the various instruments analysed will be given in the following.

#### **3.3.2.1 Temperature**

##### ***Resistance temperature detectors (RTD)***

Re-calibration of resistance thermometers, which were retrieved from the TSDE test field, revealed the high reliability of the temperature sensors. After nearly 12 years of operation, the deviations from DIN EN 60751 were very low. Almost all sensor deviations were still within the limits of tolerance for the used class B-sensors ( $\pm 0.3^\circ\text{K}$  at  $0^\circ\text{C}$ ,  $\pm 0.8^\circ\text{K}$  at  $100^\circ\text{C}$ , and  $\pm 1.55^\circ\text{K}$  at  $250^\circ\text{C}$ ). From the comparison of the calibrations in 1990 and in 2002, a low sensor drift can be derived as the re-calibration results at  $0^\circ\text{C}$  and  $100^\circ\text{C}$  were almost identical with the original calibration.

### 3.3.2.2 Deformation

#### ***Convergence measurements***

For the TSDE experiment, convergence measuring devices were designed consisting of a measuring rod and a displacement transducer which are installed between opposite points of a drift. Displacements are measured by an electric transducer which supplies an output voltage proportional to the relative displacement of the drift walls. Both displacement transducer and measuring rod are protected against mechanical impact by telescopic steel tubes. The measuring device is suited for backfilled drifts which are not accessible. The measuring signals can be recorded automatically with maximum measuring ranges up to 400 mm at temperatures up to 180 °C.

During drift excavation, several convergence measuring devices were retrieved. Some had failed during the heating phase because of cable damages. The measuring rods of the horizontal measuring devices, which had been installed directly above the heater casks, were significantly bent due to distinct floor uplifting in the heated area (Figure 3.10). All measuring devices showed significant surface corrosion along the telescopic steel tubes, but the functioning of the measuring systems was not affected by corrosion. For investigation of the electric displacement transducers, the protection tubes were removed at the manufacturer. Subsequently, the sensors were checked and re-calibrated for verification of their accuracy.

The measuring range of the examined displacement transducers was nearly unchanged. But due to temperatures of up to 90 °C which these gauges had been exposed to during operation, the sensors got slightly non-linear though the linearity being still largely within the manufacturer's limit of tolerance of  $\pm 0.2\%$ . Above the heater casks, however, the sensor linearity deviated from the original calibration values what can easily be explained by the mechanical stressing of the displacement transducer due to bending of the measuring rod.

#### ***Extensometer measurements***

In the TSDE experiment, multiple point rod extensometers were used consisting of glass fibre rods which are sliding in protecting PVC tubes. Advantages of this extensometer type are its flexibility allowing it to be installed in one and its low coefficient of linear thermal expansion ( $0.6 \cdot 10^{-6}/^{\circ}\text{C}$  instead of  $13 \cdot 10^{-6}/^{\circ}\text{C}$  for steel) which makes a temperature correction unnecessary.

Usually, the instrument head of an extensometer is installed outside the borehole. Due to high temperatures in the TSDE experiment, however, a special gauge design was chosen with the instrument head being installed in the deepest part of the borehole where temperatures were lower. The accuracy of this measuring system depends on the length of the extensometer ranging between 0.02 mm up to a length of 20 m and 0.3 mm up to a length of 100 m.

After installation of the extensometers, all boreholes had been filled with a supporting cementation. Thus, neither the extensometers nor the displacement transducers, which had been installed in the deepest part of the boreholes, were accessible during drift excavation. But other boreholes had been equipped with extensometers from the observation and the access drifts whose displacement transducers could be retrieved.

A representative number of different transducer types was selected for re-calibration at the manufacturer. The sensors had been in operation between 7 and 14 years at ambient temperatures between 33 °C and 36 °C. The re-calibration results revealed an almost unchanged linearity being still within the manufacturer's respective limit of tolerance. Contrarily to the identical displacement transducers of the convergence measuring devices, original calibration and re-calibration of the extensometer sensors were almost identical. This can be attributed to the lower temperatures which these displacement transducers had been exposed to. The installation of the sensors at a long distance from the heated test drifts can thus be recommended. With their negligible sensor drift, these measuring systems are very suitable for long-term displacement measurements.

### **3.3.2.3 Stress**

#### ***Hydraulic pressure cells***

In the TSDE experiment, hydraulic pressure cells had been installed in different boreholes to observe long-term stress changes in the surrounding rock salt. These pressure gauges had been considerably affected by the accelerated rock deformations after the start of heating leading frequently to damages at the pressure cells. But only a few failures had been caused by damaged hydraulic measuring lines.

Further hydraulic pressure cells of the Glötzl type had been used to determine the pressure between backfill and surrounding rock. The pressure cells had been installed in different

cross sections at the floor, at the roof, and at the walls of the test drifts. Contrarily to the pressure gauges recording rock stress changes in the borehole, most backfill pressure cells had operated over a long time. Almost all failures had occurred in the heated area and could be attributed to damages at the hydraulic measuring lines, particularly inside of cable slots. During drift excavation, a number of these pressure gauges was retrieved for post-test analyses.

The general condition of these pressure gauges was satisfactory. The surface the pressure pads was mostly corroded, but no material break-throughs were detected. All gauges were submitted to functioning tests. For this purpose, the pressurization of the unstressed pressure cell was compared with the initial pressurization. The percentage change of this zero value was between 0.01 % and 0.08 % which is very tolerable after the long operation time. The in-situ measurements are hence assessed as very confidential.

For verification of their accuracy, the backfill pressure gauges were calibrated in an autoclave. The readings were compared with the nominal pressure values, respectively. At a lower pressure level up to 40 bar, which had been the maximum backfill pressure at the end of the in-situ measurements, the deviations from the nominal pressure were below 2 bar. The linearity, which was determined from the nominal pressure deviation, was largely still within the manufacturer's limit of tolerance of  $\pm 0.5$  %.

### ***AWID cells***

In the TSDE experiment, AWID cells (Absolut Widerstandssprung Druckmesskissen (Kessels, 1984)) had been applied for measuring the backfill pressure at the surface of the heater casks. The gauges had been operated electropneumatically. Almost all AWID measuring systems had failed already in the beginning of the heating phase probably due to damaged pneumatic and / or electric measuring lines. Therefore, the whole AWID measuring unit had been shut down early.

During drift excavation, several AWID gauges were recovered from the central heater cask. The retrieved pressure gauges were only slightly corroded. At the manufacturer, the gauges were checked electrically and pneumatically under vacuum. The examination revealed that all AWID cells were tight and functioning completely. Consequently, their failure during the in-situ measurements was definitely caused by damaged measuring lines. But even with a better protection of the measuring lines, the application of the AWID measuring system in a repository is only reasonable for very special cases due to its intricate measuring equipment.

### ***Hydraulic fracturing***

Hydraulic fracturing measurements were performed in the surroundings of the TSDE test field at the Asse mine with a recently developed probe using acoustic emission measurements for the determination of the orientation and extension of the fracture planes (Manthei et al. 1998). The measurements revealed that the stress relief zone extended up to 6 m from the drift surface. Acoustic emission analysis pointed out that clearly discernible fracture planes lay in nearly transverse direction to the borehole axis. At larger borehole depths, in some cases the events were distributed in clouds around the injection interval. These observations are interpreted by larger deviatoric stresses close to the contour of the drift and by increasing isotropic stresses at greater borehole depth.

#### **3.3.2.4 Gas and water release**

For gas sampling from the heated backfill in the TSDE experiment, porous glass filters had been installed at the surface of the central heater casks, at the drift roof, and at the drift floor. Each sampling point had been connected with a Teflon tube leading to the entrance of the test drifts where gas samples had been taken periodically by a membrane pump.

During the heating phase, several gas sampling points had to be shut down as gas sampling had not been possible any more. With the post-test analyses, the failure reasons should be checked which could have been either plugged glass filters or damaged Teflon tubes.

At the manufacturer, the permeability to air of the gas sampling filters was checked by a flowmeter at a flow rate of 0.06 norm litre per minute. All glass filters were permeable and had no loss of flow. Consequently, the failure of some gas sampling points was definitely caused by damaged Teflon tubes. The filters, on the contrary, worked fine throughout the complete testing period and can be recommended for similar applications.

### **3.4 Conclusions and recommendations**

#### **3.4.1 Experimental procedures**

Full-scale in-situ experiments are indispensable to understand the complex processes in a final repository and to provide valuable experience for repository construction and operation.

In various in-situ experiments, the behaviour of backfill and surrounding rock salt was studied in the Asse mine under almost representative repository conditions. However, during the experimental period of the TSDE experiment of up to nine years, differences were observed between the results of numerical simulations and experimental data. Several reasons were determined which led to this behaviour.

For the determination of backfill density, different methods were used. The most reliable results were achieved by drift closure measurements. The obtained porosity values, however, were only mean values over the respective cross sections basing on a limited number of measuring gauges. Non-homogeneous backfill compaction could not be determined with this measuring equipment. Thus, for future experiments, a more extensive instrumentation of the backfill is being recommended to enable measurement of local inhomogeneities in situ and to enable continuous explanation of quantitative differences observed between the results of numerical simulations and experimental data.

Lithostatic rock stress is the most important parameter for the creep behaviour of rock salt and has to be determined precisely in a site characterization programme. In the TSDE test field, the lithostatic rock stress was considerably lower than expected due to the large excavations from former salt mining resulting in lower drift closure and backfill compaction rates. Thus, the backfill compaction had not reached the values expected in a repository, but further decrease in porosity would have required a much longer heating period. A residual porosity down to 1 % cannot be reached in situ within a reasonable time. Thus, the porosity range between the compaction state reached in the TSDE experiment and the remaining porosity in a repository could not be validated by the in-situ test. To confirm extrapolations of model calculations, the final stages of backfill compaction have to be investigated by laboratory tests.

Non-homogeneous backfill compaction was probably also caused by thermal gradients within the backfill leading to deviations between predictions and experimental results.

In order to avoid misinterpretation of numerical and experimental results because of possible malfunctioning of the used measuring instruments and in order to complete the information about the achieved backfill compaction it was decided to re-excavate the test fields after termination of the heating phase. A representative number of measuring instruments was retrieved for post-test re-calibration purposes and samples were taken from the backfill for further laboratory analyses.

The post-test analyses both of the compacted backfill material and the measuring instruments were extremely useful for the confirmation of the applied models. For instance, in the center of the test where data were missed because of early failure of instruments, the achieved backfill compaction was finally found to agree perfectly with the predicted values. Because of these valuable experiences on model confirmation it is recommended for any in-situ demonstration experiment to plan and perform post-test investigations as far as possible and reasonable.

### **3.4.2 Instruments**

Regarding instrument performance, it can be stated that the greatest part of the experimental equipment performed well throughout the duration of the backfill in-situ experiments.

The gauge design of the different measuring equipments proved to be successful as only a limited number of gauges had been damaged during the in-situ test. Most failures of measuring systems had been due to damages at the measuring lines in the center of the test field. Especially, the used multicore cables had been affected revealing a large number of failures. Most cable failures had been caused by squeezing due to convergence of cable slots (Figure 3.11) and boreholes which led to short-circuited or broken cable cores. Further failures had been induced by electrolyte intrusion into the multicores. Cable damages were also located in a cable duct (Figure 3.12) close to the roof.

In conclusion, the multicore cable design cannot be recommended for in-situ measurements in heated areas. A single cable design is more appropriate. The realized cable duct design cannot be recommended neither. The protection of the measuring lines has to be improved. A better protection may be achieved by cable slots along the drift walls or near the roof in regions with low rock deformation.

An overview of various instruments used by German institutions in different experiments is given in Table 3.2.



**Figure 3.11a** Completely closed cable slot in the drift wall at cross section D1 of the TSDE test field



**Figure 3.11b** Squeezed cable in a cable slot in the drift wall at cross section D1 of the TSDE test field



**Figure 3.12** Cable duct (upper left) at cross section D1 in the TSDE test field

**Table 3.2** Instrumentation Used of Asse Underground Research Laboratory

Process/ Parameter	Instrument or Method	Applied in Experiment	Location in Experiment	Operating Range	Accuracy	Datalogging	Performance	References
Thermal Evolution (Temperature)	Thermocouples	DEBORA		To 400°C	Limit of tolerance: 3°C (DIN) or 1.5°C (1/2 DIN) or 0.75°C (1/4 DIN)			DIN 43710, Rothfuchs et al. (1999)
	Resistance temperature detectors of the type PT100	TSDE	Lower temperature locations in rock (boreholes) and backfill	From 0°C to 80°C	±0.01°C at 0°C, ±0.07°C at 100°C Limit of tolerance (Class B-sensors): ±0.3°C at 0°C, ±0.8°C at 100°C	Local front end processor - GSSE logger	164 of 215 sensors operated well until the end of the experiment corresponding to 24 % failures. Most failures were caused by damaged measuring cables.  Re-calibration of retrieved sensors revealed their high reliability. After nearly 12 years of operation, deviations were still within the limit of tolerance. At 0°C and 100°C, re-calibration results in 2002 were almost identical with original calibration in 1990. Cable protection and cable duct design have to be improved.	DIN EN 60751, Droste et al. (2001)
		TSDE	Heater cask surface and high temperature locations in the backfill	From 0°C to 250°C	±0.01°C at 0°C, ±0.07°C at 100°C, ±0.15°C at 250°C Limit of tolerance (Class B-sensors): ±0.3°C at 0°C, ±0.8°C at 100°C, ±1.55°C at 250°C	Local front end processor - GSSE logger	520 of 582 sensors operated well until the end of the experiment corresponding to 10 % failures. Most failures were caused by damaged measuring cables. Re-calibration of sensors revealed their high reliability. After nearly 12 years of operation, deviations were still within the limit of tolerance. Cable protection and cable duct design have to be improved.	DIN EN 60751, Droste et al. (2001)

Process/ Parameter	Instrument or Method	Applied in Experiment	Location in Experiment	Operating Range	Accuracy	Datalogging	Performance	References
Drift Closure	Stationary measuring equipment	TSDE	Backfilled drifts: Measuring rods installed horizontally and vertically between opposite drift surfaces. Perimeter changes measured by Glötzl displacement transducers. Protection against mechanical impact by telescopic steel tubes.	Opening dimensions = 4.5 m. Up to 180°C. Transducer: Measuring range 400 mm, up to 125°C.	Transducer: Linearity $<\pm 0.2\%$ (related to the total measuring range), Resolution 0.01 mm.	Local front end processor - GSSE logger	Gauge design successful and only few transducer failures. Harsh environment application with pressure and moisture impact on cables resulted in failure of 9 of 22 devices during the test. Re-calibration of retrieved transducers revealed their reliability. After nearly 12 years of operation at temperatures of up to 90°C, their linearity was largely within the limit of tolerance. Deviations from the original calibration were only observed for the gauges which had been installed directly above the heater casks. The measuring rods of these devices, however, had been bent significantly. Cable protection and cable duct design have to be improved.	Droste et al. (2001)
Backfill Settling	Stationary measuring equipment	TSDE	Backfilled drifts: With each measuring equipment, 3 measuring rods and 3 anchor plates installed vertically in the drifts for monitoring the distribution of backfill settling at three different levels. Distance changes measured by Glötzl displacement transducers. Protection against mechanical impact by telescopic steel tubes.	Dimensions = 3.5 m. Up to 180°C. Transducer: Measuring ranges 250 mm and 400 mm, up to 125°C.	Transducer: Linearity $<\pm 0.2\%$ (related to the total measuring range), Resolution 0.01 mm.	Local front end processor - GSSE logger	Gauge design successful and only few transducer failures. Harsh environment application with pressure and moisture impact on cables resulted in failure of 11 of 30 devices during the test. Re-calibration of retrieved transducers revealed their reliability. After nearly 12 years of operation at temperatures of up to 90°C, their linearity was largely within the limit of tolerance. Cable protection and cable duct design have to be improved.	Droste et al. (2001)

Process/ Parameter	Instrument or Method	Applied in Experiment	Location in Experiment	Operating Range	Accuracy	Datalogging	Performance	References
Rock Displacement	Multi-point extensometer	TSDE	<p>Boreholes in rock: Anchors fixed by grouting, with glass fibre rods from each anchor to the instrument head at the borehole collar. Rod movement measured with Glötzl displacement transducers at the instrument head.</p> <p>One-dimensional axial displacement of each anchor relative to the instrument head at the borehole collar.</p>	<p>Borehole diameter 131 / 180 mm.</p> <p>Transducer: Measuring range <math>\pm 50</math> mm, up to 70°C.</p>	<p>Extensometer: 0.02 mm up to 20 m length, 0.1 mm up to 50 m length, 0.3 mm up to 100 m length.</p> <p>Transducer: Linearity <math>&lt; \pm 0.5</math> % (related to the total measuring range), Resolution 0.025 mm.</p>	Local front end processor - GSSE logger	<p>Gauge design successful: All 18 extensometers operated well during nearly 12 years of operation. Few transducer failures could be repaired during the experiment.</p> <p>Re-calibration of retrieved transducers, which had been operated at a lower temperature of 33.5°C, revealed their reliability. 14 years after the original calibration, their linearity was almost identical.</p>	Brown (1981), Droste et al. (2001), Paul and Gartung (1991)
	Multi-point extensometer	TSDE	<p>Boreholes in rock: Anchors fixed by wedging, with glass fibre rods from each anchor to the instrument head in the deepest part of the borehole. Rod movement measured with Glötzl displacement transducers at the instrument head. Cables running to the borehole collar.</p> <p>One-dimensional axial displacement of each anchor relative to the instrument head in the deepest part of the borehole.</p>	<p>Borehole diameter 180 mm.</p> <p>Transducer: Measuring range 100 mm, 250 mm, 400 mm, up to 125°C.</p>	<p>Extensometer: 0.02 mm up to 20 m length, 0.1 mm up to 50 m length, 0.3 mm up to 100 m length.</p> <p>Transducer: Linearity <math>&lt; \pm 0.2</math> % (related to the total measuring range), Resolution 0.01 mm.</p>	Local front end processor - GSSE logger	<p>Gauge design successful and only few transducer failures. Harsh environment application with pressure and moisture impact on the used multicore cables resulted in failure of 69 of 112 extensometers during the test.</p> <p>Re-calibration of recovered transducers revealed their reliability. However, sensors could only be retrieved from replaced extensometers, which had been in operation for up to 7 years at an ambient temperature of 36°C. Their linearity was almost identical with the original calibration.</p> <p>Cable protection and cable duct design have to be improved. Multicore cables are not recommendable.</p>	Brown (1981), Droste et al. (2001), Paul and Gartung (1991)

Process/ Parameter	Instrument or Method	Applied in' Experiment	Location in Experiment	Operating Range	Accuracy	Datalogging	Performance	References
Rock Displacement; continued	Inclinometer - mobile probe	TSDE	Boreholes in rock equipped with access guide tubes, measurements with a mobile probe.  Two-dimensional radial displacement perpendicular to borehole axis.	Borehole diameter = 180 mm.  Up to 80°C.	Probe: 0.02 mm per m measuring depth,  Measuring system: 0.1 mm per m measuring depth	Mobile probe readings	Good system performance with no failure of access guide tubes, but measurements very labour intensive.  Several re-calibrations of the mobile probe during the experiment.	Droste et al. (2001)
Backfill Pressure	Glötzl type hydraulic pressure cells	TSDE	Interfaces between backfill and rock, embedded in concrete. Hydraulic lines required to monitor the cells. Oil is pumped into a measuring line and pressure is built up against the diaphragm of the pressure cell until equilibrium with the surrounding backfill pressure is reached. At this pressure, which corresponds to the backfill pressure, the diaphragm opens and the oil turns back via the return line.  Determination of long-term stress changes.	Up to 40 MPa.	±0.02 MPa  Linearity <±0.5 % (related to the total measuring range)	Local front end processor - Glötzl MFA logger	Pressure cells performed well. 14 of 44 gauges failed until the end of the experiment, but most failures could be attributed to damages at the hydraulic measuring lines.  Autoclave re-calibration of retrieved pressure cells revealed their reliability. For the unstressed cells, deviations from initial pressurization were low. After nearly 12 years of operation at temperatures of up to 125°C, their linearity was largely within the limit of tolerance.  Measuring line protection and cable duct design have to be improved.	Droste et al. (2001)

Process/ Parameter	Instrument or Method	Applied in Experiment	Location in Experiment	Operating Range	Accuracy	Datalogging	Performance	References
	AWID type pressure cells	TSDE	<p>Interfaces between backfill and heater cask surface, embedded in concrete. Pneumatic lines and electric cables required to monitor the cells. Air is pumped into the pressure cell until equilibrium with the surrounding backfill pressure is reached. At this pressure, which corresponds to the backfill pressure, the cell opens and its resistance increases distinctly. The resistance is determined during the measurement by injecting a constant electric current and measuring the voltage over the cell.</p> <p>Determination of long-term stress changes.</p>	<p>Up to 60 MPa.</p> <p>Up to 250°C (measurements independent from temperature).</p>	<0.3 % at 15 MPa	Local front end processor - Glötzl MFA logger	<p>No useful results were obtained. Almost all measuring systems failed shortly after the beginning of heating due to damaged pneumatic and/or electric measuring lines. Therefore, the whole measuring unit was shut down early.</p> <p>Post-test investigation of retrieved AWID cells confirmed that the gauges were still tight and functioning completely.</p> <p>Measuring line protection and cable duct design have to be improved.</p> <p>Due to its intricate measuring equipment only recommendable for special application.</p>	Kessels (1984)

Process/ Parameter	Instrument or Method	Applied in Experiment	Location in Experiment	Operating Range	Accuracy	Datalogging	Performance	References
In situ Rock Stress	Stress monitoring probes consisting of several Glötzl type hydraulic pressure cells with various orientation	TSDE	Grouted into boreholes in rock: Hydraulic lines required to monitor the cells. Oil is pumped into a measuring line and pressure is built up against the diaphragm of the pressure cell until equilibrium with the surrounding rock pressure is reached. At this pressure, which corresponds to the rock stress, the diaphragm opens and the oil turns back via the return line.  Hydraulic measuring lines running to the borehole collar.  Determination of long-term stress changes.	Up to 40 MPa.	±0.02 MPa  Linearity <±0.5 % (related to the total measuring range)	Local front end processor - Glötzl MFA logger	47 of 49 gauges failed during the test. 35 gauges were replaced from which 8 failed until the end of the experiment.  Most failures were caused by damages at the pressure cells due to accelerated rock deformation. Only 15 % of the failures could be attributed to the hydraulic measuring lines.  The use of common return lines by several gauges is not recommendable.	Droste et al. (2001), Heusermann (1987)
	Hydraulic fracturing with acoustic emission monitoring - mobile probe	TSDE	Boreholes in rock: By sealing a part of a borehole and injecting a fluid, the rock is fractured. The shut-in pressure is interpreted as the value of the least principle stress.  With a recently developed probe, the orientation and extension of the fracture planes could be determined simultaneously by acoustic emission monitoring. The direction of the least principle stress is assumed to be perpendicular to the fracture plane.  Determination of absolute stress.			Local monitoring with probe and PC logging	Used effectively for determination of the least principle stress and its direction.	Fischle et al. (1988), Manthei et al. (1998)

Process/ Parameter	Instrument or Method	Applied in Experiment	Location in Experiment	Operating Range	Accuracy	Datalogging	Performance	References
In situ Rock Stress; continued	Overcoring - mobile probe	TSDE	Boreholes in rock: Pilot borehole required which is being overcored after the placing of the probe.  Determination of absolute stress.	Triaxial		Local monitoring with probe and PC logging	For viscoplastic rocks like salt, the whole deformation development of the pilot borehole has to be recorded during overcoring (unlike one diameter measurement before and after overcoring in an ideal elastic rock).  Additional correction required for stress relaxation due to non-linear creep taking into account the overcoring diameter and the time between drilling and overcoring of the pilot borehole.  Used effectively for determination of initial stress.	Kiehl and Pahl (1990), Pahl and Heusermann (1989)
Gas Monitoring	Gas sampling for various analyses (gas chromatography , humidity)	HAW	Boreholes in rock: Boreholes sealed with packers consisting of Viton seals. Via Teflon tubes, gas samples were extracted.	Filter porosity: 42.5 % Filter permeability: 2·10 <sup>-9</sup> m <sup>2</sup>  Allowing both gas and moisture sampling.	100 ml Gas required for gas chromatograph y	Sampling of approx. 1 l Gas in Linde gas sampling bags		Gies et al. (1989)

Process/ Parameter	Instrument or Method	Applied in Experiment	Location in Experiment	Operating Range	Accuracy	Datalogging	Performance	References
Gas Monitoring continued	Permeable filters for gas sampling for various analyses (gas chromatography , humidity)	TSDE	Backfilled drifts: Porous glass filters at the heater cask surface as well as at the drift roof and floor. A membrane pump was used to transfer gas from the filters via Teflon tubes to the drift entrance for collection.	Filter porosity: 42.5 % Filter permeability: 2·10 <sup>-9</sup> m <sup>2</sup>  Allowing both gas and moisture sampling.	100 ml Gas required for gas chromatograph y	Sampling of approx. 1 l Gas in Linde gas sampling bags	Satisfactory results were obtained from most sampling points. 17 of 28 sampling points operated well until the end of the experiment.  Post-test investigation of retrieved filters revealed that these filters were not plugged and still permeable. Hence, the failures of sampling points, which had to be shut down during the experiment, were caused by damages at the Teflon tubes.  Tube protection and cable duct design have to be improved.	Droste et al. (2001)

Process/ Parameter	Instrument or Method	Applied in Experiment	Location in Experiment	Operating Range	Accuracy	Datalogging	Performance	References
Permeability	Permeability measurements	ALOHA	Boreholes in rock: Gas is injected into sealed borehole intervals. From injection rate and pressure development during injection and subsequent shut-in phase, permeability is derived by iterative modelling.	10-14 to 10-21 m <sup>2</sup>	Depending on permeability: Low for very low permeability (but better than half order of magnitude).	PC logging with A/D-card	Used successfully for the exploration of excavation disturbed zones in rock salt.	Wieczorek and Zimmer (1999)
Water Content	Geoelectric monitoring	ALOHA, Äspö, Prototype Repository, Mont Terri Heater Test, Mont Terri Ventilation Test, Tournemire	Special electrode arrays installed in boreholes surrounding the volume of rock to be monitored: Determination of resistivity changes.  Inverse modelling and laboratory calibration measurements required.	Low-porous and low-permeable rocks	Depending on water content, water conductivity, rock type, electrode configuration	Automatic datalogger	Used successfully for the exploration of excavation disturbed zones in rock salt.	Wieczorek and Zimmer (1999), Yaramanci and Flach (1989)
Elastic Rock Parameters (Seismic velocities, compression modulus, shear modulus)	Seismic measurements: Microseismic activity (passive measurements), seismic traveltimes (active measurements)	HAW, BARIAN	Acceleration transducers located in boreholes in rock					Hente (1992), Kamlot and Flach (2001)

#### **4 Work Package 3.1: Assessment of the function of EBS and the understanding of and capability to model the important processes**

In a repository in rock salt the host rock is the most important barrier and, therefore, the interactions between host rock and engineered barrier systems (EBS) are of major concern. Due to the plasticity and self-healing properties of rock salt, mined cavities will close by creep deformation. Fracturing of the host rock during this process is avoided by the installation of supporting EBS and potential flow paths for fluids or gases will be sealed under the impact of lithostatic pressure.

If the sealing function is only required at a later stage, seal systems basically consisting of crushed salt are considered suitable. In case of a sudden brine inrush, for instance in the shaft, however, an instantaneous sealing function is required. Sealing systems basically consisting of bentonite or bentonite-sand mixtures with a high swelling potential and significantly reducing permeability are considered suitable in this regard. Sealing systems using asphalt as a short-term sealing component are being considered as well (see section 2.3.2).

Anyway, crushed salt has been selected as the most suitable backfill material in disposal rooms containing heat generating high-level radioactive waste (HLW). According to planning, the material in drifts will consist of crushed salt as received by drift excavation. It is a coarsely grained material with a maximum grain size of 60 mm. For backfilling boreholes finer grained crushed salt with a 10-mm maximum grain size will be used. According to experience from in-situ experiments, the initial porosity of crushed salt backfill will be about 35 %.

In addition to the crushed salt backfill concept for HLW disposal rooms further EBS systems are proposed for isolating repository areas and for definitively closing the repository. Such EBS systems include drift seals like plugs or dams and shaft seals. In Germany, no decision has been made yet regarding the final layout and design of respective seal systems, but concepts have been developed for dams and shaft seals considering differing sealing requirements.

In repository performance assessments the sealing capability of potential EBS has to be predicted by models for which the capability to simulate the relevant processes has

to be demonstrated. Thus, the understanding of the thermomechanical interaction of the EBS and the rock is a precondition for safety assessments for deep geological repositories in rock salt. Key parameters to be studied are the rate of room closure and the changing EBS properties as a function of temperature, rock stress, and time.

## **4.1 Features and Processes**

### **4.1.1 Backfilling of disposal drifts and boreholes with crushed salt**

According to the concepts considered in the past thirty years, high-level waste remaining from reprocessing of spent fuel will be vitrified in steel canisters (see section 2.1.2, Table 2.1). The steel canisters will be disposed of in about 300- to 600-m-deep and 0.6-m-wide boreholes (BfS 1990) reaching vertically down from a disposal level at a depth of about 800 meters below ground (Figures 4.1a and 4.1b). About 200 canisters will be lowered into a borehole. In order to transfer the weight load of the canister stack to the surrounding rock mass, the annulus between the canisters and the borehole wall is to be backfilled with crushed salt. At top of the borehole, a seal consisting of crushed salt will be placed.

In addition, a concept has been developed in Germany for the direct disposal of spent fuel (Hartje et al. 1989). Large self-shielding Pollux casks will be emplaced in drifts about 200 m long, 4.5 m wide and 3.5 m high (Figures 4.1a and 4.1c). Depending on the interim storage time the canister spacing may range between 1 and 6 m. Following the emplacement of a Pollux cask, the remaining voids in the drift will be backfilled with crushed salt.

In both concepts the creeping of the surrounding rock will lead to disposal room closure. In this process grain displacement and finally grain deformation takes place in the crushed salt and it is consolidated to a dense mass. The permeability decreases continuously to very small values almost equal to those of the intact rock. Furthermore, the ongoing material compaction provides a constantly increasing counter-pressure to the rock stress and leads finally to an almost homogeneous stress distribution around drifts and boreholes thereby stabilizing the underground host rock structures.

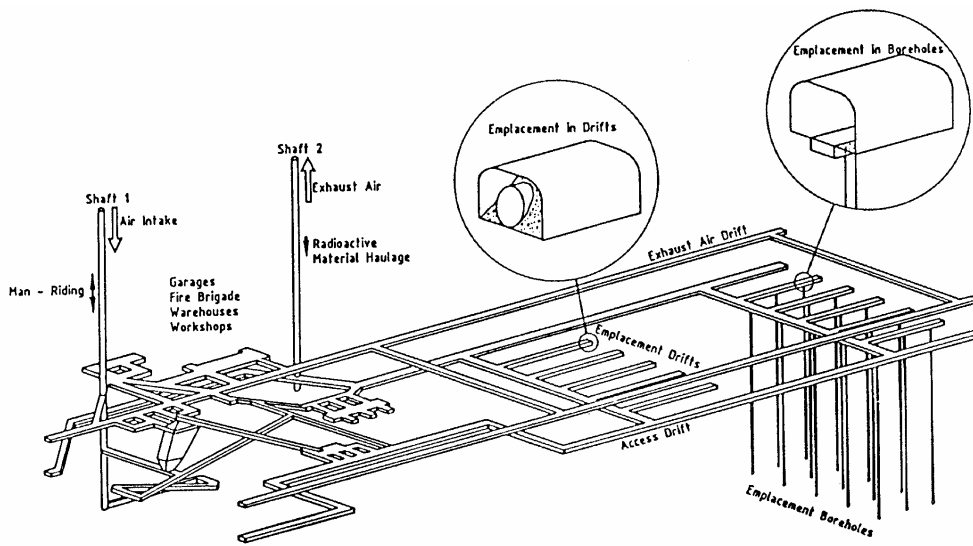


**Figure 4.1a** Typical layout of a high-level waste repository in a salt formation (source DBE)

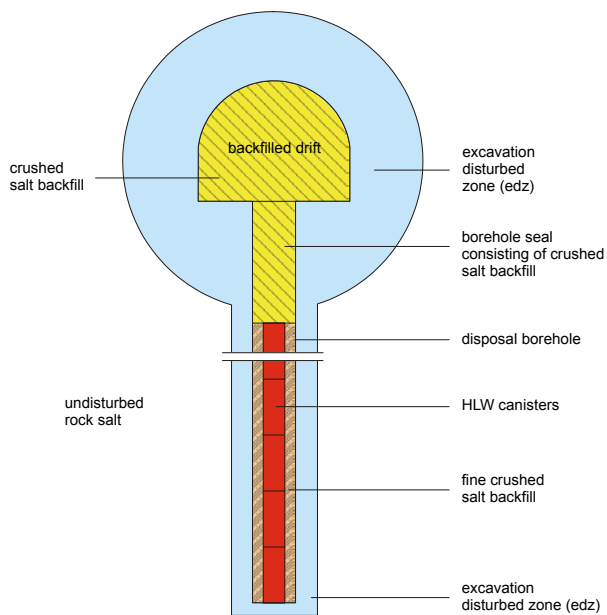


**Figure 4.1b** Borehole disposal concept

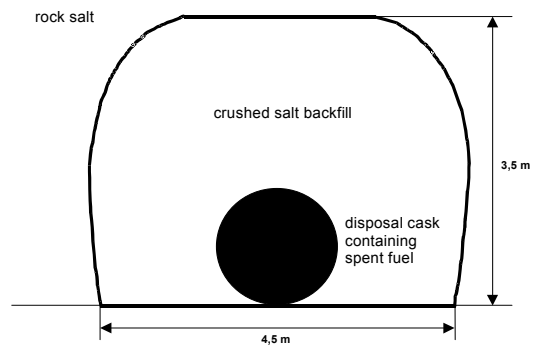


**Figure 4.1c** Drift disposal concept

This process is accelerated at higher temperatures in case of the disposal of high-level waste.

Any additional sealing of the waste by buffer materials is not considered necessary in a salt repository.

#### **4.1.2 Moisture release from the host rock**

It has been observed in both laboratory and field tests that rock salt contains small amounts of water and gases (Jockwer, 1981, Rothfuchs, 1986). These fluids tend to move towards a heat source or heat-producing HLW that is disposed of in rock salt. If the fluids are released into disposal drifts and boreholes or other areas in the repository the following scenarios may occur:

- sealed disposal rooms may be pressurized up to the frac-pressure of the surrounding host rock
- an ignitable atmosphere may be generated in sealed areas
- a corrosive atmosphere may be generated having direct influence on the integrity of the waste containers and the waste solidification matrix
- generated and released gases may influence the transport of radionuclides.

The water contained in rock salt consists of different forms like crystalline water of the hydrated minerals polyhalite ( $K_2MgCa_2(SO_4)_4 \cdot 2H_2O$ ) and kieserite ( $MgSO_4 \cdot H_2O$ ), adsorbed water on grain boundaries, or as small liquid inclusions. The analyses of 1000 rock salt samples taken from different geological salt formations at the Asse mine show that the average integral water content ranges at about 0.04 wt%. The main gases known to occur in rock salt are hydrocarbons like for instance  $CH_4$ , carbon dioxide  $CO_2$  and carbon monoxide  $CO$ .

Besides qualitative and quantitative determination of all fluids generated and released it is of essential importance to know the transport mechanisms in the host rock for the estimation of the consequences of the above mentioned scenarios.

### 4.1.3 Sealing of drifts with special salt mixtures

So far, pure crushed salt has been considered only as suitable backfill material in a salt repository. This material, however, does not act as a barrier against intruding brines in the early compaction stage because the material is chemically inert against intruding saturated brines. The addition of special additives to this backfill, however, renders it into a reactive mixture that upon contact with brine increases its volume thus leading to a substantial reduction of the pore space. The water content of intruding solutions is reduced along their migration pathway through the backfill (Figure 4.2). The water consumption due to the formation of new hydrated minerals leads to a super saturation of the remaining solution and consequently to the precipitation of supersaturated phases. These combined effects eventually lead to a thermodynamically stable new mineralogical composition of the backfill. This altered backfill composition has a dramatically reduced pore volume compared to the initial stage prior to the brine intrusion. The result is an excellent seal. Additives have been identified that render a practically brine tight seal. For the long-term safety of a repository it is essential that the newly formed mineral composition is in equilibrium with the geochemical environment.

So far, only laboratory experiments have been performed to study these reactions (Sander and Herbert, 2000). As the laboratory experiments at different scales proved to be most effective the R&D programme was continued and now large scale experiments in boreholes in the Asse salt mine are in preparation. During these reactions large amounts of hydrated minerals are precipitated. For certain initial compositions the volume increase of the solid phases upon completion of the reaction is almost two-fold. The backfill becomes almost impermeable within 1.5 days after the first contact with brine. A maximum crystallisation pressure of 10 MPa can be reached (Figure 4.3). The resulting permeability is smaller than  $1\text{E-}20\text{ m}^2$ . The resulting crystallisation pressure is dependent on the recipe of the mixture.

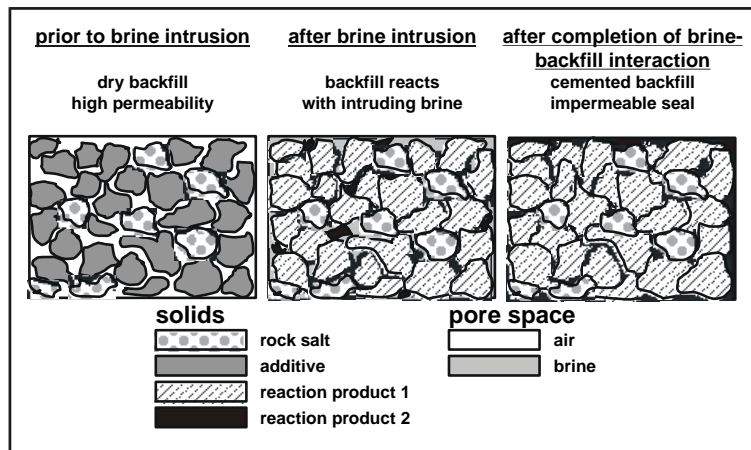


**Figure 4.2** Principle of the self healing process due to the brine-backfill interaction

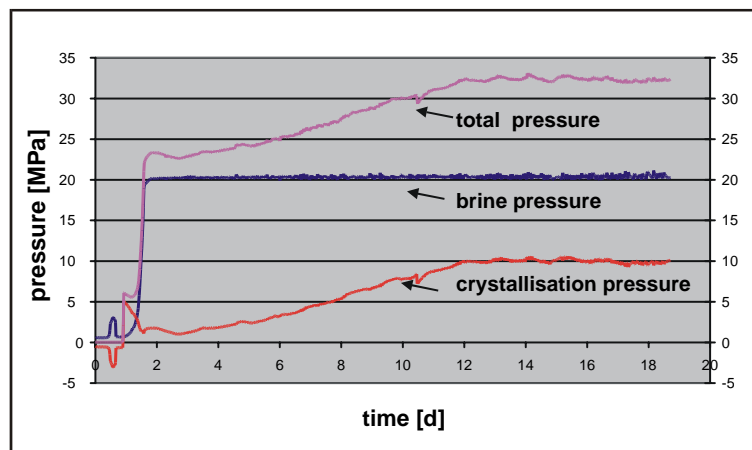


**Figure 4.3** Development of brine and crystallisation pressures during the brine-backfill interaction in the laboratory experiment

From the experiments performed so far, it is concluded that special salt mixtures added to crushed rock salt backfill open new possibilities to prevent brine from intruding into disposal sections of repositories in salt formations.

#### 4.1.4 Sealing of drifts and shafts with bentonite

Bentonites are considered to be ideal sealing and backfilling materials because of their swelling capacity. The swelling develops when bentonites react with aqueous solutions. The swelling pressure is considered to be a key parameter of the technical barrier consisting of compacted bentonite, because it has impact on the time necessary for

any solution to reach the waste canisters, and the migration of radionuclides released from therein.

Concepts for EBS systems isolating repository areas and for sealing repository shafts have been or are currently tested in Germany. A drift sealing system combining bentonite-sand bricks and compacted crushed salt bricks are tested at a potash mine in Sondershausen (Sitz und Koch 1999). A shaft seal combining crushed salt and bentonite (see section 2.3.2) was proposed by Schmidt et al. (1995) and a similar system has recently been tested at the Salzdetfurth mine (Breidung 2001).

Publications describing conceptual models to predict the combined hydro-mechanical behaviour of the seals, however, are actually not yet available and thus cannot be reported here.

However, at the GRS laboratories an approach is currently being made to predict the swelling pressure of bentonites in contact with salt brines (see section 4.2.5).

## **4.2 Models and EBS Data used for Modelling**

For modelling and assessing the performance of HLW repository systems typical conceptual models of the borehole disposal concept and of the drift disposal concept have been used in various projects as for instance „Systemanalyse Mischkonzept“ (SAM, 1989) and the BAMBUS project (Bechthold et al., 1999). The considered conceptual models as well as the data used in the modelling work are compiled in the following sections.

The heat induced convergence of disposal rooms and the resulting compaction and sealing behaviour of crushed salt backfill in disposal drifts and disposal borehole in interaction with the surrounding rock salt was investigated in detail in the Asse mine in the TSDE experiment and the DEBORA experiments. In all experiments the waste containers were simulated by electrically heated dummies. The main objective of the experiments was the validation of computer models by comparing experimental and modelling data. The processes observed and modelled are

- Temperature distribution in the backfill and the rock
- Displacement of host rock and compaction of backfill

- Stress fields in the rock and pressure/stress in the backfill
- Porosity and permeability development in the backfill
- Gas generation due to thermally induced gas and water release from the host rock and due to corrosion of materials

#### 4.2.1 Heat distribution

For calculation of the non-steady state temperature fields the equation of heat conduction under the varying boundary conditions of the actual problem is being solved:

$$\frac{\partial T}{\partial t} = \frac{\lambda}{\rho c_p} \Delta T + \frac{\dot{e}}{\rho c_p} \quad (4.1)$$

$\lambda$  = heat conductivity (W/(m · K))

$\rho c_p$  = heat capacity (J/(m<sup>3</sup> · K))

$\dot{e}$  = heat generation rate (J/(m<sup>3</sup> · s))

t = time (s)

GRS used the fully TM coupled code SUPERMAUS developed at the Technical University of Aachen (Breidenich 1994) for calculating the temperature distribution in the DEBORA experiments (Rothfuchs et al., 1999).

In connection with the BAMBUS project a benchmarking of different codes was performed by modelling the crushed salt behaviour in the TSDE experiment (Bechthold et al, 1999). The numerical simulations yielded the coupled temperature and stress/strain-fields and also the development of crushed salt porosity as a function of time.

In order to calculate the heat transfer in repositories DBE used the computer code LINSOURPEPOST which relies on the analytical solution of the heat transfer differential equation for a finite, line shaped, instationary heat source.

## 4.2.2 Mechanical behaviour of rock salt and crushed salt backfill

### **Rock salt**

Besides its elastic properties, rock salt shows a pronounced visco-plastic behaviour. For modelling this, the widely used creep law according to Wallner (1979) and Hunsche and Hampel (1999) has been used to predict and design most of the in-situ experiments performed at the Asse mine.

Creep of the rock salt is dependent on stress and temperature. The steady state creep rate is

$$\dot{\varepsilon}_s = A \cdot \exp\left(\frac{-Q}{RT}\right) \cdot \left(\frac{\sigma}{\sigma^*}\right)^n \quad (4.2)$$

- $\dot{\varepsilon}_s$  = strain rate (1/s)
- A = constant factor (MPa/s)
- Q = activation energy (J/mol)
- R = universal gas constant: 8.314 (J/(mol · K))
- T = absolute temperature (K)
- $\sigma$  = stress (MPa)
- $\sigma^*$  = 1 (MPa)
- n = stress exponent = 5 (-)

### **Crushed salt backfill**

For predicting the compaction behaviour of the crushed salt in the DEBORA experiments the constitutive law given by Hein (1991) was applied.

$$\dot{\varepsilon}_{ij} = \frac{A}{2} \cdot \left[ \exp\left(-\frac{Q}{RT}\right) \right] \cdot (h_1 \cdot p^2 + h_2 \cdot q^2)^2 \cdot \left( \frac{1}{3} h_1 \cdot p \cdot \delta_{ij} + h_2 \cdot S_{ij} \right) \quad (4.3)$$

- $\dot{\varepsilon}_{ij}$  = strain rate tensor (1/s)
- A = constant factor (MPa/s)
- p = hydrostatic pressure (MPa)
- q = invariant of stress tensor (MPa);  $q = \sqrt{S_{ij} \cdot S_{ji}}$
- $\delta_{ij}$  = Kronecker-Symbol (-);  $\delta_{ij} = 1$  if  $i = j$ , otherwise 0

$S_{ij}$  = deviator of stress tensor (MPa)

$h_1, h_2$  = material parameter (dependent on porosity) ( $1/\text{MPa}^2$ )

The parameters  $h_1$  and  $h_2$  are dependent on the porosity  $\phi$  as follows:

$$h_1(\phi) = \frac{1 - d(\phi) \cdot c_3^2}{\left( \frac{c_4}{c_5} \left( \left( \frac{1 - \phi}{1 - \phi_0} \right)^{c_5} - 1 \right) \right)^2}, \quad h_2(\phi) = c_6 + c_7 \cdot h_1(\phi) \quad (4.4)$$

$d(\phi)$  = porosity dependent material parameter (-);  $d(\phi) = c_1 \cdot \exp(c_2 \cdot \phi)$

$c_i$  = material constants ( $c_3$  = coefficient of internal friction (-);  $c_3 = \tan \varphi$ )

$\varphi$  = angle of internal friction (-)

$\phi_0$  = initial porosity of the crushed salt (-)

#### 4.2.3 Fluid flow in rock salt

Best results in predicting/modelling the migration of water traces in the salt (Jockwer 1981) have been obtained by Schlich (1986) using an evaporation front model (Figure 4.4).

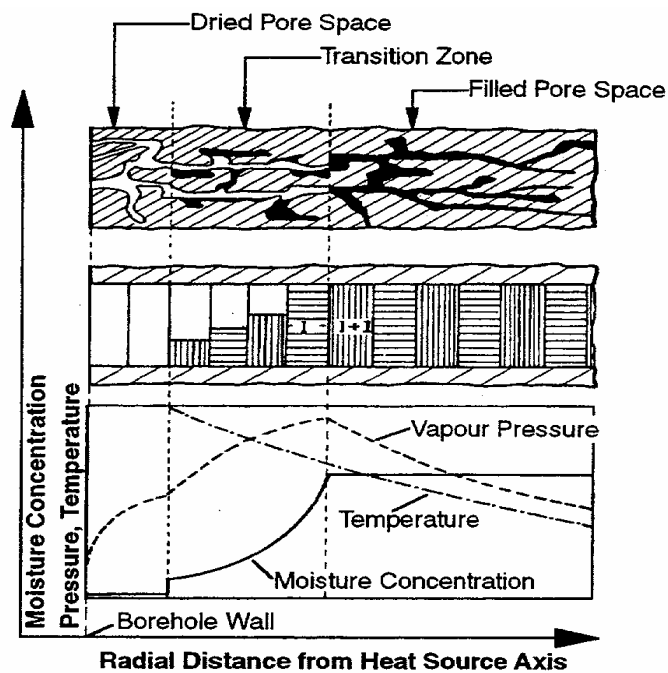


**Figure 4.4** Evaporation front model

In this model it is assumed that the complete intergranular pore space (IP) is filled with brine. In the borehole the concentration and the pressure of water vapour is low in contrast to the area of the IP filled with brine. In the evaporation front model, the brine front moves from the heated borehole into the rock salt and transfers all of the liquid phase into vapour. Behind the front, the released vapour will be transported in the direction of the borehole because of the strong gradient of partial pressure. The velocity of the migrating front  $u$  is given by

$$u = -\frac{\rho_v}{\rho_w \cdot \phi} v \quad (4.5)$$

- $u$  = velocity of the migrating front (m/s)
- $\rho_v$  = vapour density in the IP ( $\text{kg/m}^3$ )
- $\rho_w$  = density of water in the IP ( $\text{kg/m}^3$ )
- $\phi$  = porosity (-)
- $v$  = filter velocity of vapour (m/s); defined as volume flow divided by the area perpendicular to the flow

Using velocity  $u$  the rate of vapour production at the evaporation front can be calculated from a mass balance of evaporated water and released vapour. The balance of mass (continuity equation) for a volume element behind the evaporation front is expressed as

$$\phi \frac{\delta \rho_v}{\delta t} = -\frac{\delta}{\delta r} (r \rho_v v) \quad (4.6)$$

- $r$  = radial distance from the axis of symmetry (m); flow in one dimension.

The relation to partial pressure  $p_v$  of the vapour which is chosen as the variable to be solved for is given by the equation of state

$$p_v = R_w \rho T \quad (4.7)$$

- $p_v$  = partial pressure of the vapour (Pa)
- $R_w$  = special gas constant of water vapour:  $461.7 \text{ (J/(kg} \cdot \text{K))}$
- $T$  = temperature (K).

The equations for the filter velocity  $v$  and the mass flow depend on the mechanism of transport.

According to Engelhardt (1960) the general filter velocity  $v$  is given by:

$$v = \frac{k}{\eta} \text{grad}p + c_K \frac{\sqrt{T}}{p_v} \cdot \phi \text{grad}p_v \quad (4.8)$$

$v$  = filter velocity of the water vapour (m/s)

$k$  = permeability of the salt ( $\text{m}^2$ )

$\eta$  = dynamic viscosity of the water ( $\text{Pa} \cdot \text{s}$ )

$c_K$  = Knudsen factor ( $\text{m}^2/(\text{K}^{0.5} \cdot \text{s})$ )

Whether the first part (Darcy term) or the second part (Knudsen term) governs this equation depends on the relationship of the radius of the salt pores to the average free path length of the water molecules. If the radius of the salt pores is smaller than the average free path length of the water molecules then the Darcy term becomes zero and the Knudsen term becomes dominant.

In case of Knudsen-flow (in very low porous media) it holds (special form of Fick's first law)

$$v = \phi \frac{D_k}{p} \frac{\partial p}{\partial r} \quad (4.9)$$

$$\dot{m} = \rho v = -\phi \frac{D_k}{R_w T} \frac{\partial p}{\partial r} \quad (4.10)$$

$\dot{m}$  = mass flux ( $\text{kg}/(\text{m}^2 \cdot \text{s})$ )

$D_k$  = Knudsen-migration constant ( $\text{m}^2/\text{s}$ ).

According to Schlich the Knudsen-factor  $c_K$  can be defined in  $\text{m}^2/\text{s}/\text{K}^{0.5}$

$$c_K = \phi \frac{D_k}{T^{0.5}} \quad (4.11)$$

As a minor effect on the release of water the thermal expansion of brine in the IP has been included (see Schlich, 1986).

After specification of boundary and initial conditions, the equation of continuity can be solved to obtain the distribution of partial pressure in the IP. The mass flow into the borehole is calculated at the location of the borehole wall to estimate the input rate and the accumulated amount of vapour in the borehole as well as the increase in pressure in case the borehole is considered to be sealed.

The water release from the host rock into a HLW disposal borehole was investigated in the Temperature Test 5 at the Asse mine. In this experiment a 7 m long horizontal borehole was heated by a 3 m long heater of 210 mm diameter. The heat induced water release from the host rock into the test borehole was measured in a cold trap which was part of closed circuit connected to the sealed borehole. The code TRAVAL developed by the Technical University Aachen was used to predict the water release and migration through the pore space of the rock and its release into the borehole.

#### 4.2.4 Fluid flow in crushed salt backfill

In the simplest mathematical form the spreading of gas in a brine saturated backfill is described as a two-phase single-component flow. The concerning balance equations require assumptions for the parameters and for their dependencies. A constant porosity is assumed in all models. The same applies to the liquid density in simplest model mentioned above. Later developments still neglect the influence of pressure on liquids but incorporate a temperature-dependence in the form of:

$$\rho_l = \rho_0 [1 - \beta_T (T - T_0)] \quad (4.12)$$

$\rho_l$  = liquid density (kg/m<sup>3</sup>)

$\rho_0$  = reference density at reference temperature  $T_0$  (kg/m<sup>3</sup>)

$\beta_T$  = thermal expansion coefficient (at constant pressure) (1/K)

In contrast the gas density is always variable and depends on the pressure and the temperature.

The constitutive equation follows the ideal gas law but allows correction for real gases:

$$\rho_g = \frac{p_g}{ZR_gT} \quad (4.13)$$

- $p_g$  = gas pressure (Pa)
- $Z$  = real gas factor (-)
- $R_g$  = individual Gas constant (J/(kg ·K))

The phase velocity is given by the generalized Darcy law:

$$v_\alpha = \frac{k_{r_\alpha}}{\eta_\alpha} k(\text{grad}p_\alpha - \rho_\alpha g) \quad (4.14)$$

- $k_r$  = relative permeability (-)
- $\eta$  = viscosity (Pa·s)
- $g$  = gravitational acceleration (m/s<sup>2</sup>)
- $\alpha$  = index for a specific phase (g for gas, l for liquid)

In the two-phase single-component flow simulator MUFTE (Helmig et al., 1994) the viscosity is assumed to be constant. Later developments apply temperature dependent formulations after IFC (1967) for liquids and gases. If the gas phase consists of two or more components (Index K), the gas viscosity can be approximated after Stephan und Mayinger (1990):

$$\eta_g \approx \sum_K X_g^K \eta_g^K \quad (4.15)$$

- $X_g^K$  = mass fraction of component K in the gas phase (-)
- $\eta_g^K$  = viscosity of component K in the gas phase (Pa·s)
- $K$  = index for a specific component (a for air, w for water)

For the saturation dependent relative permeability several constitutive equations are available, most prominent among them the Brooks-Corey- and the van-Genuchten-relationships. The same applies to the capillary pressure-saturation relationships.

If two-phase two-component flow is considered a binary gas diffusion in the gas phase is taken into account. The mass fraction of dissolved air in water is a function of pressure and temperature and is calculated according to Henry's law. Additionally to pressure and temperature the vapour partial pressure is required in order to calculate the mass fraction of air in the gas phase. The vapour partial pressure is considered to be a function of temperature. Dalton's law concerning the gas phase is applied.

### ***Transport of thermal energy***

In the context of fluid flow there are two relevant transport mechanisms for thermal energy: heat conduction and convective transport by fluid flow. The mathematical description of these processes assumes a local thermal equilibrium. Heat flow due to conduction is then given by Fourier's law

$$J_T = \lambda_m \nabla T \quad (4.16)$$

$J_T$  = heat flux (J/(m<sup>2</sup>·s))

$\lambda_m$  = effective heat conductivity (J/(m·s·K))

The effective heat conductivity is given as the volumetric weighted average of the heat conductivity of liquid, gas and solid phase:

$$\lambda_m = \phi S_l \lambda_l + \phi S_g \lambda_g + (1 - \phi) \lambda_s \quad (4.17)$$

$\lambda_l$  = heat conductivity of the liquid phase (J/(m·s·K))

$\lambda_g$  = heat conductivity of the gas phase (J/(m·s·K))

$\lambda_s$  = heat conductivity of the solid phase (J/(m·s·K))

A constant heat capacity is assumed neglecting the slight temperature dependence:

$c_{v,\alpha}$  = const.

$c_{v,\alpha}$  = heat capacity of the  $\alpha$ -phase (J/(kg·K))

While the specific internal energy of dry air is approximated by

$$u_g^a = c_{v,a} T \quad (4.18)$$

$u_\alpha^K$  = specific internal energy of component K in the  $\alpha$ -phase (J/kg)

the specific internal energy of water  $u_l$  and of steam  $u_g^w$  is calculated after IFC (1967).

A change of internal energy due to vaporization (latent heat of vaporization) is considered.

The specific enthalpy consists of the specific internal energy and the volume changing work:

$$h = u + \frac{p}{\rho} \quad (4.19)$$

$h$  = specific enthalpy (J/kg)

The volume changing work is very small for water which yields

$$h_l \approx u_l \quad (4.20)$$

The specific enthalpy of the gas phase is given as the mass weighted average of the specific enthalpies of the components:

$$h_g = \sum_K X_g^K h_g^K \quad (4.21)$$

The fluid flow in a backfilled HLW disposal borehole was simulated by GRS using the code MUFTE. In the DEBORA experiments, the backfill permeability was determined by inverse modelling of nitrogen flow experiments in the backfill. The results obtained were in quite good agreement with the results obtained by post-test analyses of the in-situ compacted backfill material. In addition, the two phase flow of gas and brine in a backfilled HLW disposal borehole was simulated with the code MUFTE. A comparison between measuring results and numerical results, however, was not possible because brine was not used as fluid in the DEBORA experiments.

DBE has applied the code TOUGH2 to simulate the hydraulic conditions in a shaft seal consisting of bentonite. In particular the results of the precalculations were used to develop an optimum layout of the measurement levels in the seal.

The thermo-hydro-mechanical simulation code FLAC has been applied by DBE to calculate the thermal and mechanical behaviour of engineered barriers in a repository in salt formations as well as to predict the time, temperature and stress dependent behaviour of backfill material and rock salt. At present FLAC is used in the BAMBUS II project to calculate the temperature and stress conditions in a backfilled emplacement drift in a repository.

#### 4.2.5 Swelling pressure of bentonite in contact with saline solutions

A literature review of the existing predictive models for the swelling pressure of bentonites in contact with saline solutions was published by Herbert and Moog (2000). These models may be subdivided into empirical models, double layer models and thermodynamic models. The discussion in that paper gives the reasons why neither one of the existing models can describe the complex processes involved in the actual problem.

Keeping the above given restrictions in mind, we therefore suggest a pragmatic approach to the problem. The following model equation may be set up:

$$\ln p_q = - \frac{A(m_{Na}, m_K, m_{Mg+Ca})}{\rho_{red}} + B(m_{Na}, m_K, m_{Mg+Ca}) \quad (4.22)$$

- $p_q$  = swelling pressure (Pa)
- $\rho_{red}$  = reduced dry density ( $\text{kg/m}^3$ )
- $m_i$  = molality of species  $i$  in solution (-)
- A, B = vectors of adjustable parameters (-)

With this equation the regression formula used by engineers is adopted. Both adjustable parameter vectors A, B are expected to be functions of solution composition. The task is to build up a matrix of experiments with differing values for  $m_{Na}$ ,  $m_K$ ,  $m_{Mg+Ca}$ , and  $\rho_{red}$ . In the experiments a state of equilibrium must be established. Once the experimental data are available and reliable i.e. reproducible, the expressions for A and

B must be found, which match best the observed correlation between swelling pressure and variables. For this approach a large number of swelling pressure experiments is needed. However, with the new and much faster technique developed recently by GRS the needed data should be available in reasonable period of time.

### 4.3 Data used for modelling

#### 4.3.1 Rock salt

Parameter	Value
<ul style="list-style-type: none"> <li>• <i>Rockmechanical properties</i> (Bechthold et al., 1999) <ul style="list-style-type: none"> <li>– Young's modulus E [MPa]</li> <li>– Poisson's ratio <math>\nu</math> [ - ]</li> </ul> </li> <li>• <i>Thermal properties</i> (Bechthold et al., 1999) <ul style="list-style-type: none"> <li>– heat capacity <math>\rho c_p</math> [J/(m<sup>3</sup> · K)]</li> <li>– thermal conductivity <math>\lambda</math> [W/(m · K)]</li> <li>– coefficient of thermal expansion <math>\beta_T</math> [K-1]</li> </ul> </li> </ul>	<p>E = 24000</p> <p><math>\nu = 0.27</math></p> <p><math>\rho c_p(T)</math>:</p> <p>0.607 at 25 °C  0.610 at 50 °C  0.617 at 100 °C  0.642 at 200 °C  0.627 at 180 °C</p> <p><math>\lambda</math> (T):</p> <p>5.51 at 25 °C  5.1 at 50 °C  4.26 at 100 °C  3.33 at 180 °C  2.51 at 200 °C</p> <p><math>\beta_T = 4.2 \cdot 10^{-5}</math></p>
<ul style="list-style-type: none"> <li>• <i>Hydraulic properties</i> <ul style="list-style-type: none"> <li>– Permeability k [m<sup>2</sup>] (Wieczorek 1998)</li> <li>– initial porosity <math>\phi</math> [-] (Jockwer et al., 1995)</li> </ul> </li> <li>• <i>Mineralogy</i></li> </ul>	<p>k = &lt; 10<sup>-20</sup></p> <p><math>\phi = 0.001</math></p> <p>Rock salt consisting of halite (NaCl) and accessory minerals like polyhalite (K<sub>2</sub>MgCa<sub>2</sub>(SO<sub>4</sub>)<sub>4</sub>·2H<sub>2</sub>O and anhydrite (CaSO<sub>4</sub>)</p>

### 4.3.2 Crushed salt backfill

Parameter	Value
<ul style="list-style-type: none"> <li>• <i>Rockmechanical properties (Bechthold et al., 1999)</i></li> <li>– Young's modulus E [MPa]</li> <li>– Poisson's ratio <math>\nu</math> [ - ]</li> </ul>	$E = E_r \exp(-c_k \phi((1 - \phi_0)/(1 - \phi)))$ $c_k = 12.27$ $\phi_0 = 0.35$ $\nu = 0.27$
<ul style="list-style-type: none"> <li>• <i>Thermal properties (Bechthold et al., 1999)</i></li> <li>– heat capacity <math>\rho c_p</math> [J/(m<sup>3</sup> · K)]</li> <li>– thermal conductivity <math>\lambda</math> [W/(m · K)]</li> </ul>	$\rho c_p(T, \phi) = \rho c_p(T) \cdot (1 - \phi)$ $\lambda(T, \phi) = \frac{\lambda(T)(1 - \phi)}{(h_o(1 - (1 - \phi)^b) + (1 - \phi)^b)}$ $h_o = 4.56 \quad b = \ln(2/3) / \ln(-\phi_o)$
<ul style="list-style-type: none"> <li>• <i>Hydraulic properties (Müller-Lyda et al, 1999)</i></li> <li>– Permeability k [m<sup>2</sup>]</li> <li>– initial porosity <math>\phi</math> [-]</li> </ul>	$k = 2.54 \cdot 10^{-10} \cdot \phi^{4.175} \text{ m}^2$ $\phi = 0.35$
<ul style="list-style-type: none"> <li>• <i>Mineralogy</i></li> </ul>	Rock salt consisting of halite (NaCl) and accessory minerals like polyhalite (K <sub>2</sub> MgCa <sub>2</sub> (SO <sub>4</sub> ) <sub>4</sub> ·2H <sub>2</sub> O) and anhydrite (CaSO <sub>4</sub> )

### 4.3.3 Cogéma canister containing reprocessed and vitrified HLW

Parameter	Value
<ul style="list-style-type: none"> <li>• <i>length l [m]</i></li> </ul>	1.34
<ul style="list-style-type: none"> <li>• <i>diameter d [m]</i></li> </ul>	0.43
<ul style="list-style-type: none"> <li>• <i>weight w [kg]</i></li> </ul>	475
<ul style="list-style-type: none"> <li>• <i>thermal properties of stainless steel (1.4833)</i> <ul style="list-style-type: none"> <li>– heat capacity <math>\rho c_p</math> [J/(m<sup>3</sup> · K)]</li> <li>– thermal conductivity <math>\lambda</math> [W/(m · K)]</li> </ul> </li> </ul>	$\rho c_p = 3.65 \cdot 10^6$ $\lambda = 59.0$
<ul style="list-style-type: none"> <li>• <i>thermal properties of borosilicate glass</i> <ul style="list-style-type: none"> <li>– heat capacity <math>\rho c_p</math> [J/(m<sup>3</sup> · K)]</li> <li>– thermal conductivity <math>\lambda</math> [W/(m · K)]</li> </ul> </li> </ul>	$\rho c_p = a_0 + a_1 T$ ; $a_0 = 2.45984 \cdot 10^6$ J/(m <sup>3</sup> K) $a_1 = 1.92924 \cdot 10^3$ J/(m <sup>3</sup> K <sup>2</sup> )  $\lambda = a_0 + a_1 T + a_2 T^2 + a_3 T^3$ $a_0 = 1.0887$ $a_1 = 2.102 \cdot 10^{-3}$ W/(mK) $a_2 = -4.98 \cdot 10^{-6}$ W/(mK <sup>2</sup> ) $a_3 = 7.09 \cdot 10^{-9}$ W/(mK <sup>3</sup> )
<ul style="list-style-type: none"> <li>• <i>heat power [kW]</i></li> </ul>	(see section 2.1.3.6)

#### 4.3.4 Pollux disposal cask containing spent fuel

Parameter	Value
<ul style="list-style-type: none"> <li>• length <math>l</math> [m]</li> <li>• diameter <math>d</math> [m]</li> <li>• weight <math>w</math> [kg]</li> </ul>	5.9 1.6 65000
<ul style="list-style-type: none"> <li>• thermal properties of steel cask</li> <li>  heat capacity <math>\rho c_p</math> [J/(m<sup>3</sup> · K)]</li> <li>– thermal conductivity <math>\lambda</math> [W/(m · K)]</li> </ul>	$\rho c_p = 3.77 \cdot 10^6$ $\lambda(T)$ : 6.11 at 25 °C 5.02 at 50 °C 4.19 at 100 °C 3.57 at 150 °C 3.11 at 200 °C 2.78 at 250 °C
<ul style="list-style-type: none"> <li>• heat power [kW]</li> </ul>	(see section 2.1.3.6)

#### 4.3.5 Bentonite as drift and shaft sealing material

There are mainly two different kinds of bentonite which are currently considered as potential sealing material: Calcium bentonite and Sodium bentonite.

Within the framework of a German research project calcium bentonite has been investigated as shaft sealing material. The values given in the following table should only be seen as reference values due to the fact that the parameters strongly depend on technical boundary conditions like the used dry density during the installation etc.

Parameter	Value
<ul style="list-style-type: none"> <li>• Rockmechanical properties</li> <li>– Young's modulus <math>E</math> [MPa]</li> <li>– Poisson's ratio <math>\nu</math> [-]</li> <li>– swelling pressure <math>p_q</math> [MPa]</li> </ul>	4000  $p_q = c_0 + c_1 S$ ( $c_0 = -0.698$ and $c_1 = 2.053$ ) $S$ = water saturation
<ul style="list-style-type: none"> <li>• Thermal properties</li> <li>– Thermal conductivity <math>\lambda</math> [W m<sup>-1</sup>K<sup>-1</sup>]</li> </ul>	were not considered within the research project

<ul style="list-style-type: none"> <li>– Specific heat capacity</li> <li>– Coefficient of thermal expansion <math>\beta_T</math> [<math>K^{-1}</math>]</li> <li>• Hydraulic properties <ul style="list-style-type: none"> <li>– Permeability <math>k</math> [<math>m^2</math>]</li> <li>– Initial porosity <math>\phi</math> [-]</li> </ul> </li> <li>• Mineralogy</li> </ul>	$k = <10^{-17}$ $\phi = 1 - \rho_d/\rho_0$ ( $\phi = 0.3$ ) ( $\rho_d$ = dry density, $\rho_0$ = grain density)  unprocessed, 70% montmorillonite
---	---

#### 4.4 Description of interaction of EBS and surrounding rock

The most important interaction between the host rock and the backfill in the drifts and boreholes in a salt repository is the stress induced creep of the rock (room convergence) and the resulting backfill compaction with time. The most important barrier function of the backfill is considerably improved with time until a degree of compaction is achieved which is almost equal to that of the undisturbed rock. Thus, modelling of the function of the backfill barrier always requires modelling of the interaction of rock and backfill.

##### 4.4.1 Geological and mineralogical data from the host rock at Asse research mine

The Asse mine is located in a salt anticline the top of which being situated 100 m below sea level and 300 m below ground, respectively (Figure 4.5). The salt formation is composed of three main halite seams: Staßfurt Halite Na2, Leine Halite Na3, and Aller Halite Na4. Between the Na2 and Na3 seam the intermediate potash seam K2C was deposited.

The experimental area is located 800 m below the surface in the Staßfurt Halite Na2. This formation is being considered representative for repository conditions to be expected at any other repository site in northern Germany at similar depth (e.g., Gorleben).

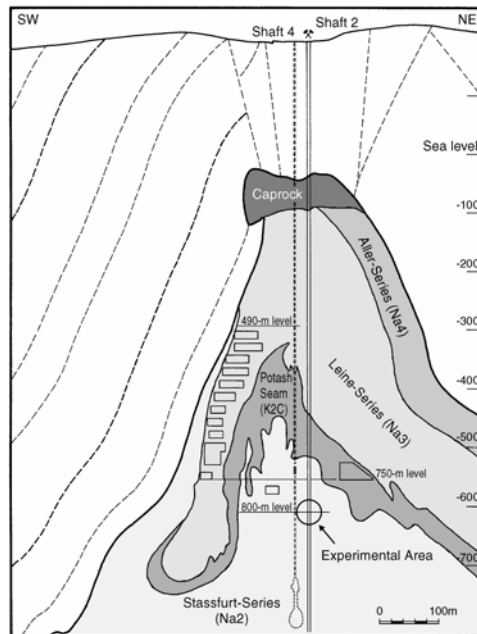


**Figure 4.5** Asse anticline

The Na2 consists of halite (NaCl) and accessory minerals like polyhalite ( $K_2MgCa_2(SO_4)_4 \cdot 2H_2O$ ) and anhydrite ( $CaSO_4$ ). In addition to the hydration water of the accessory minerals, the rock salt at Asse contains about 0.04 wt% of grain boundary water.

Occasionally, limited amounts of high saline brines with high Mg and K-concentrations are found in small pockets in the rock salt.

#### 4.4.2 Rock properties

Absolute stress measurements were carried out in the TSDE test field at the 800-m level to determine the initial state of stress (Heusermann, 1995). From the stress release in slot cutting tests and by means of the overcoring method, an initial stress of approximately 12 MPa was estimated. The obtained lithostatic stress in the test field, however, was considerably lower than the expected lithostatic overburden pressure of about 18 MPa. The reduced rock stress in the test field was caused by far-field creep and stress relaxation around the large excavations in the Asse mine remaining from former salt mining. In the temperature test field 4 at the 750-m level a relation of 0.83 of the horizontal to the vertical stress was determined by Feddersen (1983).

The basic characteristics of the Asse salt, referred to as referential material, are summarised in the following: density  $\rho = 2.16 - 2.19 \text{ g/cm}^3$ ; dynamic Young's modulus  $E_d = 33 - 35 \text{ GPa}$ , static Young's modulus  $E_s = 20 - 30 \text{ GPa}$ ; Poisson's ratio  $\nu = 0.23 - 0.28$ ; uniaxial compressive strength  $\sigma_c = 20 - 35 \text{ MPa}$ ; tensile strength  $\sigma_t = 0.5 - 2.3 \text{ MPa}$ ; permeability of host rock  $k < 10^{-21} \text{ m}^2$ . (compare section 2.1.3.3).

Several underground rooms were excavated in the Asse mine for running different in-situ experiments. Because of the visco-plastic material behaviour creep starts immediately after room opening. For openings at the 800-m level typical isothermal drift convergence rates of 0.25 %/year have been observed (e. g., Droste et al., 2001).

Due to the excavation of underground rooms an excavation disturbed zone of up to 1.5 m develops around the drift contour and an increase of permeability to about  $10^{-16} \text{ m}^2$  was found by Wieczorek and Zimmer (1999).

#### **4.4.3 Experiments at Asse that provide information on the interaction of EBS and the host rock**

##### **4.4.3.1 DEBORA experiments**

This project was performed in two 15 m deep boreholes at the 800 m-level of the Asse mine in order to verify the models used to predict the crushed salt compaction in disposal boreholes containing vitrified high-level waste canisters. The boreholes were equipped with 2 m long electric heaters simulating the waste canisters and measuring sensors to monitor the

- borehole convergence and hence the decrease of backfill porosity
- increase of the backfill pressure
- temperature distribution in and around the heated boreholes
- permeability of the compacting backfill material by performing nitrogen flow measurements periodically.

The results of the coupled THM modelling were compared to the actual measurement results and showed a fairly good agreement.

#### **4.4.3.2 TSDE experiment**

This experiment served for demonstrating the feasibility of direct disposal of spent fuel in self-shielding casks deposited in backfilled disposal drifts. During experiment conduction performed from 1990 to 1999, measurements were performed to monitor

- drift convergence (backfill porosity)
- backfill pressure
- backfill settling
- temperature distribution
- backfill permeability.

The results of 3D temperature calculations show a reasonable agreement with the measuring results. 2D mechanical modelling results show a good agreement with the data obtained at the central measuring cross section where plain-strain conditions prevail. Significant deviations between modelling and measuring data were observed further away from the central cross section where the impact of 3D effects becomes more important.

#### **4.5 Codes for describing and evaluation of EBS performance**

So far, the coupled thermo-hydro-mechanical behaviour of the disposal system has been analyzed by GRS using the MAUS and SUPERMAUS codes. Modelling with these codes revealed the temperature, stress-strain and porosity distribution in the repository system in space and time. The migration of salt brine and gases in the compacted backfill has been modelled using the MUFTE code.

In order to calculate the heat transfer in repositories DBE used the computer code LINSOURPREPOST which relies on the analytical solution of the heat transfer differential equation for a finite, line shaped, instationary heat source.

DBE used the thermo-hydro-mechanical fully coupled code FLAC and FLAC<sup>3D</sup> for analysing the behaviour of repository systems (host rock, backfill, sealings, heat generating waste etc.). For simulating the coupled movement of water, vapour, and gas DBE used the code TOUGH2 in particular with regard to the layout of sealing systems.

In order to model the complex geochemical processes that occur when solutions especially saline water react with rock or sealing material GRS and DBE used the computer code EQ3/6. Investigations on the chemical stability of different sealing materials have successfully be done. Recently, GRS uses also the code ChemApp. It is easier to integrate ChemApp into fluid transport codes than EQ3/6. GRS has developed an interface between ChemApp and the performance assessment code EMOS.

#### 4.5.1 Structure code SUPERMAUS

The code SUPERMAUS was developed at the Technical University of Aachen (Breidenich, 1994). It is a two-dimensional finite element code based on the modules TAUS (for thermal analysis) and MAUS (for mechanical analysis). It provides coupling between thermal and mechanical calculation in the sense that not only the thermal influence on the mechanical parameters and quantities, but also the influence of mechanics on the thermal behaviour is taken into account. This is of special importance for the „soft” backfill which undergoes great changes in its thermal parameters during mechanical compaction.

Besides the standard constitutive laws for heat transfer and elastic deformation behaviour, SUPERMAUS implements the creep law for rock salt and the thermal and mechanical material behaviour of crushed salt presented in section 3.2.1.

The differential equations solved by the code for every volume element  $\Omega$  are the balance equations for mass, momentum, energy, and entropy:

$$\dot{m} = \int_{\Omega} \left( \frac{\partial \rho}{\partial t} + \nabla_i (\rho \cdot v_i) \right) d\Omega = 0 \quad (4.24)$$

$$I_j = \int_{\Omega} \left( \frac{\partial (\rho \cdot v_j)}{\partial t} + \nabla_i (\rho \cdot v_j \cdot v_i) \right) d\Omega = \int_{\Gamma} \sigma_{ij} \cdot n_i d\Gamma + \int_{\Omega} \rho \cdot f_j d\Omega \quad (4.25)$$

$$\dot{U} = \int_{\Omega} \left( \frac{\partial (\rho \cdot u)}{\partial t} + \nabla_i (\rho \cdot u \cdot v_i) \right) d\Omega = - \int_{\Gamma} J_{Ti} \cdot n_i d\Gamma + \int_{\Omega} \sigma_{ij} \cdot \nabla_j (v_i) d\Omega + \int_{\Omega} \rho \cdot \dot{e} d\Omega \quad (4.26)$$

$$\dot{S} = \int_{\Omega} \left( \frac{\partial(\rho \cdot s)}{\partial t} + \nabla_i(\rho \cdot s \cdot v_i) \right) d\Omega = - \int_{\Gamma} J_{T_i} / T \cdot n_i d\Gamma + \int_{\Omega} \rho \cdot \dot{s} d\Omega + \int_{\Omega} \rho \cdot \dot{\bar{e}} / T d\Omega \quad (4.27)$$

$\Omega$	=	volume element (m <sup>3</sup> )
$\Gamma$	=	surface of volume element (m <sup>2</sup> )
$m$	=	mass (kg)
$\rho$	=	density (kg/m <sup>3</sup> )
$v_i$	=	velocity vector (m/s)
$l_i$	=	momentum vector (N·s)
$\sigma_{ij}$	=	Cauchy's stress tensor (Pa)
$f_i$	=	specific force (N/kg)
$U$	=	internal energy (J)
$u$	=	specific internal energy (J/kg)
$J_{T_i}$	=	heat flow vector (W/m <sup>2</sup> )
$\dot{\bar{e}}$	=	specific heat generation rate (W/kg)
$S$	=	entropy (J/K)
$s$	=	specific entropy (J/(kg·K))
$T$	=	Temperature (K)
$\dot{s}$	=	specific entropy production (W/(kg · K))
$t$	=	time [s]

The balance equation of moment of momentum is not mentioned, as it only yields the symmetry of the stress tensor (Breidenich, 1994).

The above equations are solved to give the temperature and the displacement fields. The displacements are calculated as sum of the results of elastic, visco-plastic, and thermal strains.

Instead of calculating the thermal and mechanical quantities with their mutual interaction simultaneously, the relatively slow processes investigated make a stepwise solution possible. The method applied is to

- calculate the temperature field of a time step with the mechanical conditions at the beginning of the time step kept constant through this step, and then

- perform the mechanical calculation for this time step with the temperature change during this time step taken into account.

This is iterated until the calculation is completed.

The coupling method is a mixed form of an explicit method (which would mean that both the temperature and the displacement fields are held constant during a time step) and an implicit method (which would incorporate iterative solving of both temperature and displacements during a time step). Since the mechanical influence on the temperature field during a single time step is sufficiently small, this method is a good compromise between accuracy and performance.

#### 4.5.2 Two-Phase Flow code MUFTE

The code MUFTE (MULTiphase Flow, Transport, and Energy) is a development of the University of Stuttgart and aims at the simulation of groundwater flow of two immiscible fluids in porous, fractured and fractured-porous media. It exists in different versions which allow to tackle different problems and which represent different stages of development as well.

The code employs one-, two- and three-dimensional elements to solve the two-phase flow equations. An arbitrary orientation of the one- and two-dimensional elements in space is allowed to describe discrete fracture networks. The problem of fractures plays of course no relevant role in rock salt. Nevertheless, this option allows simple modelling of two-phase flow for a large variety of geometrically complex domains.

MUFTE exists in an isothermal version which offers the possibility to model a liquid as well as a gas as the non-wetting phase. Mass storage, advection, gravitation, capillary forces are considered in this version. The two-phase single-component flow of a gas (index g) and a liquid (index l) is described by a balance equation - approximated with the finite element method - for the each phase:

$$\frac{\partial(\phi S_{\alpha} \rho_{\alpha})}{\partial t} + \text{div}(\rho_{\alpha} \mathbf{v}_{\alpha}) = \dot{m}_{\alpha} \quad (4.28)$$

$\phi$  = porosity (-)

S = saturation (-)

- $\rho$  = density (kg/m<sup>3</sup>)  
 $t$  = time (s)  
 $v$  = filter velocity (m/s)  
 $\dot{m}$  = mass source/sink (kg/(m<sup>3</sup> · s))  
 $\alpha$  = index for a specific phase (g for gas, l for liquid)

The non-isothermal version is developed as a two-phase two-component flow simulator for air and water. Therefore, it considers in addition to the isothermal version condensation, evaporation and solution. Optional is the simultaneous regard to binary gas diffusion and transport of thermal energy.

The underlying differential equations for the two-phase two-component flow are formulated in terms of mass conservation of the components rather than mass conservation of the phases:

$$\frac{\partial(\phi S_{\alpha} X_{\alpha}^K \rho_{\alpha})}{\partial t} + \text{div}(X_{\alpha}^K \rho_{\alpha} v_{\alpha}) - \text{div}(D \rho_g \text{grad } X_g^K) = r_{\alpha}^K \quad (4.29)$$

- $X_g^K$  = mass fraction of component K in the gas phase (-)  
 $D$  = coefficient for binary gas diffusion (m<sup>2</sup>/s)  
 $K$  = index for a specific component (a for air, w for water)

Note, that special modifications or changes in the equations are required if the flow changes from a two-phase two-component flow to a two-phase single-component flow. One of the most obvious changes is the switch in the primary variables from saturation to mass fraction. For further discussion see (Helmig et al., 1994). The equations are solved with a controlled finite element method.

The transport of thermal energy is calculated by an additional differential equation:

$$\frac{\partial(u\rho)}{\partial t} + \text{div}(\rho v_{\alpha} h) - \text{div}(\lambda_m \text{grad } T) = \dot{e} \quad (4.30)$$

- $u$  = specific internal energy (J/kg)  
 $h$  = specific enthalpy (J/kg)  
 $\lambda_m$  = effective heat conductivity (J/(m·s·K))  
 $T$  = Temperature (K)  
 $\dot{e}$  = heat generation rate (J/(m<sup>3</sup> · s))

The latest development is that of MUFTE-UG (Helmig et al., 1998) which combines the conceptual approach for the physical processes of the earlier MUFTE versions with the advanced numerical methods like multigrid solver and adaptive grid methods of the UG toolbox (Bastian et al., 1996).

#### 4.5.3 Code TRAVAL

In the 1D-code TRAVAL the finite difference method has been used for numerical solution of the problem described in section 4.2.3. Because of the 1D limitation, fluid flow values are only calculated for the length unit used. In order to determine total inflow values, the length unit values are multiplied with the „effective length” of the disposal room (disposal borehole) which is 2/3 of the true length.

The temperature distribution  $T(r)$  in TRAVAL is being approximated by a parabola which is determined by the three temperature values at the borehole wall, the location of the evaporation front and the middle between these both points, respectively.

The displacement increment  $\Delta r$  of the evaporation front between the points of time  $t_n$  and  $t_{n+1}$  is being calculated explicitly. That means, the evaporation front velocity  $u$  between these points of time has the value according to time  $t_n$ . However, this can only be done if the time increment  $\Delta t$  is kept relatively small. Test calculations resulted that the acceptable time step should be smaller than 0.5 days. Since the used temperature calculation programmes normally use also greater time steps a subdivision of these time steps is being performed and for each subdivided time step a linear interpolation in time is being performed.

The calculation of the pressure distribution in the intergranular pore space is being done on basis of the equation of continuity

$$\frac{\partial}{\partial r}(r\rho_v v_v) = 0 \quad (4.31)$$

$\rho_v$  = water vapour density (kg/m<sup>3</sup>)

$v_v$  = filter velocity of water vapour (m/s)

Using the equation of state for water vapour (see page 78) and equations on page 79 the following equation for the pressure  $p_v$  of the water vapour in the intergranular pores is obtained:

$$p_v = C \frac{\phi(r_B) R_w}{c_k(r_B)} \int_{r_B}^r \frac{(T(r))^{0.5}}{\phi(r)r} dr + p_i \quad (4.32)$$

$p_v$  = pressure of the water vapour (Pa)

$r_B$  = borehole radius (m)

$R_w$  = special gas constant of water vapour: 461.7 (J/(kg · K))

The dependence of the Knudsen factor  $c_k$  on the porosity  $\phi$  is considered as

$$c_k(r) = c_k(r_B) \cdot \phi(r) / \phi(r_B) . \quad (4.33)$$

The integral in equation 4.32 is being solved numerically by using the Simpson rule under consideration of the temperature approximation described above. C in equation 4.32 is being determined by the condition that the vapour pressure in the IP at the location of the evaporation front is equal to the saturation pressure  $p_s$ .

The local pressure gradient is obtained as

$$\frac{\partial p_d}{\partial r} = C \frac{(T(r))^{0.5} \phi(r_B) R_w}{\phi(r) r c_k(r_B)} \quad (4.34)$$

Using equations 4.32 and 4.34 the velocity of the evaporation front and the fluid flow into the borehole are calculated.

#### 4.5.4 Two Phase Flow code TOUGH2

TOUGH2 is a multi-dimensional numerical model for simulating the coupled movement of water, vapour, gas, and heat as well as the transport of radionuclides and black oil in porous and fractured media (Pruess et al., 1999). It offers a flexible handling of different fluid mixtures, and provides options for specifying injection or withdrawal of heat and fluids. Although primarily designed for studies of high-level nuclear waste

isolation in partly saturated geological media, it is also useful for a wide range of problems in heat and moisture transfer involving heat driven flow. A multi-phase approach to fluid and heat flow is used, which fully accounts for the movement of gaseous and liquid phases.

### ***Modeling capabilities***

The governing equations used in TOUGH2, and their numerical implementation, are applicable to one-, two- or three-dimensional anisotropic porous or fractured media. TOUGH2 does not perform stress calculations for the solid skeleton, but it allows for porosity changes in response to changes in pore pressure (compressibility) and temperature (expansivity).

The TOUGH2 simulator takes account of the following physical processes:

- Fluid flow in both liquid and gaseous phases occurs under pressure, viscous, and gravity forces according to Darcy's law.
- Interference between the phases are represented by means of relative permeability functions. Capillary pressures and relative permeability's will usually depend on phase saturation, but more general relationships are possible (e.g. temperature dependence; however, TOUGH2 does not allow for hysteresis). A library of the most commonly used functional forms is provided in the TOUGH2 code, and can be selected by means of input data. Additional capillary pressure and relative permeability functions may be used by adding FORTRAN code to the appropriate subroutines.
- Binary diffusion is considered in the gas phase. However, no account is presently made of Knudsen diffusion, which will effectively enhance gas phase permeability under conditions when the mean free path of gas molecules becomes comparable to or larger than typical pore sizes. This effect will become important for media with very small pores and/or at small gas pressures.
- Capillary and phase adsorption effects are taken into account for the liquid phase, but no allowance is made for vapour pressure lowering, which will become significant for very strong suction pressures (for example, a suction pressure of -14.5 MPa will cause approximately 10 % reduction in vapour pressure).

- Also, no allowance is made for hysteresis in either capillary pressure or relative permeability.
- All thermophysical properties of liquid water and vapour are obtained within experimental accuracy from steam table equations.
- Air is treated as an ideal gas, and additivity of partial pressures is assumed for air/vapour mixtures.
- Air dissolution in water is represented by Henry's law neglecting the temperature dependence of Henry's constant.
- Heat transport occurs by means of conduction, with thermal conductivity dependent on water saturation, and convection and binary diffusion, which includes both sensible and latent heat.

TOUGH2 includes a number of fluid property modules, referred to as „equation-of-state” or „EOS” modules, which make the code applicable to a variety of subsurface flow systems, including groundwater aquifers, unsaturated zones and geothermal reservoirs. The five basic „EOS” modules included in the original version of the code are summarized and described in the table below.

***Fluid property modules of TOUGH2***

Module	Capabilities
EOS1	water, water with tracer*
EOS2	water, CO <sub>2</sub>
EOS3	water, air*
EOS4	water, air, with vapor pressure lowering
EOS5	water, hydrogen
EOS7	Fluid property module for mixtures of water, brine, and air
EOS7R	Fluid property module for water, brine, air, plus volatile tracers with optional parent - daughter chain decay
EOS8	Fluid property module for three-phase flow of water, non-condensable gas, and black oil
EOS9	Fluid property module for saturated/unsaturated flow according to Richards' equation (gas phase a passive bystander)
EWASG	Fluid property module for three-component two-phase mixtures of water, water-soluble salt, and non-condensable gas; includes salt dissolution and precipitation, and associated porosity and permeability change
T2DM	Strongly coupled flow and transport, with full hydrodynamic dispersion

The thermophysical properties of fluid mixtures needed in assembling the governing mass and energy-balance equations are provided by EOS modules. There is nothing in the formulation to restrict the number of fluid components and phases that may be present. The flow modules of TOUGH2 are coded in general fashion for calculating mass balances of an arbitrary number of NK components that are distributed among NPH phases.

#### **4.5.5 Thermo-hydro-mechanical simulation code FLAC**

*FLAC* and *FLAC*<sup>3D</sup> are explicit finite difference programs for engineering mechanics computation (Itasca Consulting Group, 2000). This program simulates the behavior of structures built of soil, rock or other materials that may undergo plastic flow when their yield limits are reached. Materials are represented by elements, or zones, which form a grid that is adjusted by the user to fit the shape of the object to be modeled. Each element behaves according to a prescribed linear or nonlinear stress/strain law in response to the applied forces or boundary restraints. The material can yield and flow, and the grid can deform (in large-strain mode) and move with the material that is represented. The explicit, Lagrangian calculation scheme and the mixed-discretization zoning technique used in *FLAC* ensure that plastic collapse and flow are modeled very accurately. Because no matrices are formed, large two-dimensional calculations can be made without excessive memory requirements. The drawbacks of the explicit formulation (i.e., small timestep limitation and the question of required damping) are overcome to some extent by automatic inertia scaling and automatic damping that do not influence the mode of failure.

Though *FLAC* was originally developed for geotechnical and mining engineers, the program offers a wide range of capabilities to solve complex problems in mechanics. Several built-in constitutive models are available that permit the simulation of highly nonlinear, irreversible response representative of geologic, or similar, materials. In addition, *FLAC* contains many special features including:

- interface elements to simulate distinct planes along which slip and/or separation can occur
- plane-strain, plane-stress and axisymmetric geometry modes
- groundwater and consolidation (fully coupled) models with automatic phreatic surface calculation

- optional swelling model to simulate the swelling of a clay (bentonite) material due to the saturation process
- structural element models to simulate structural support (e.g., tunnel liners, rock bolts, or foundation piles)
- optional dynamic analysis capability
- optional viscoelastic and viscoplastic (creep) models
- optional thermal (and thermal coupling to mechanical stress and pore pressure) modeling capability
- optional two-phase flow model to simulate the flow of two immiscible fluids (e.g., water and gas) through a porous medium; and
- optional facility to add new, user-defined, constitutive models written in C++ and compiled as dynamic linked libraries (DLLs) that can be loaded when needed.

The two-phase flow option in *FLAC* allows numerical modelling of the flow of two immiscible fluids through porous media. The formulation applies to problems, such as those encountered in reservoir simulation, in which a fluid displaces another and simultaneous flow of the two fluids takes place in the porous medium with no mass transfer between them. The formulation is not suitable for describing piston-like processes in which a sharp interface between the two fluids moves at the average speed of fluid flow.

In two-phase flow, the void space is completely filled by the two fluids. One of the fluids (the wetting fluid, identified by the subscript *w*) wets the porous medium more than the other (the non-wetting fluid, identified below by either subscript *g* or *nw*). As a result, the pressure in the non-wetting fluid will be higher than the pressure in the wetting fluid. The pressure difference  $P_g - P_w$  is the capillary pressure  $P_c$ , which is a function of saturation  $S_w$ . Darcy's law is used to describe the flow of each fluid. The effective intrinsic permeability in the law is given as a fraction of the single-fluid (or saturated) intrinsic permeability. The fractions (or relative permeabilities) are functions of saturation,  $S_w$ . In the *FLAC* implementation, the curves for capillary pressure and relative permeabilities are built-in empirical laws of the van Genuchten form.

The flow modeling with *FLAC* may be done by itself or in parallel with the mechanical modeling. In the latter case, the solid grains forming the matrix are assumed to be

incompressible (equivalent to the Biot coefficient equal to one for single phase flow). The following features of the fluids/solid interaction is captured using the built-in logic:

- Changes in effective stress cause volumetric strain to occur (the effective stress increment for two-phase flow is the Terzaghi effective stress increment, with pore pressure increment replaced by mean, saturation weighted, fluid pressure increments).
- Volumetric deformation causes changes in fluid pressures.
- Bishop effective stress is used in the detection of yield in constitutive models involving plasticity.

Volumetric deformations induce changes in porosity, which in turn impact permeability and the capillary pressure curve parameters. These dependencies are not accounted for automatically in the code. However, the user can implement them using appropriate *FISH* functions. (*FISH* access is provided to most of the two-phase flow parameters and fluid properties.)

In the *FLAC* formulation, changes in effective stress induce deformation. Any of the built-in constitutive models can be used in conjunction with a two-phase fluid flow calculation to model this effect. In transient fluid-mechanical calculations, volumetric deformations generate pore pressures and saturation changes taken into consideration by incorporation of the corresponding mathematical terms in the numerical scheme.

#### **4.5.6 Code EQ3/6**

EQ3/6 is a set of computer codes and associated databases for use in modeling the complex geochemical processes that occur when aqueous solutions (e.g., groundwaters, saline waters, effluent streams) react with soil, rock, or solid waste materials. The processes of interest that can be modeled using EQ3/6 include mineral dissolution, mineral precipitation, wasteform leaching, and incorporation of heavy metals and other inorganic toxic components into secondary minerals. The software allows the user to create and evaluate models that include the effects of chemical equilibrium, disequilibrium, and kinetics. The software can handle both dilute waters and high-ionic-strength brines. The database is the most comprehensive of its kind, and includes data for both inorganic and organic species of interest.

EQ3/6 was originally developed to model rock/water interactions in hydrothermal and geothermal systems over the temperature range of 0 to 300 degrees Celsius. The software later underwent extensive development under the sponsorship of the Department of Energy for use in modeling geochemical processes pertinent to the geologic disposal of high-level nuclear waste. The software package has been used in this application to model the leaching of radionuclides from spent fuel and glass wasteforms, and the rock/water interactions that could take place in the local hydrothermal environment that might be created in the vicinity of an underground waste repository. Many of the refinements that have been incorporated into the code for use in nuclear waste applications are readily adaptable to applications in other environmental areas, such as the evaluation of acid mine waters, low-level radioactive waste, and chemical waste. It can be applied to waste treatment, assessment of contaminated sites, assessment of the effects of natural remediation processes, and the design and assessment of engineered remediation processes.

#### **4.5.7 Code CemApp**

ChemApp is a programmer's library consisting of a comprehensive set of subroutines, based on the thermodynamic phase equilibrium calculation module of ChemSage. It permits the calculation of complex, multicomponent, multiphase chemical equilibria and their associated extensive property balances. ChemApp is available as object code for a wide range of platforms and as a Dynamic Link Library (DLL). ChemApp has been developed in 1996 in Germany. It is being used increasingly for geochemical reaction path calculations in the field of waste disposal for applications which before were performed by EQ3/6. It is easier to integrate ChemApp into fluid-transport codes than EQ3/6. GRS has developed an interface between ChemApp and the performance assessment code EMOS.

Potential applications for the use of ChemApp are almost limitless and can cover an extremely diverse range of applications. Two distinctly different groups of applications of ChemApp are possible:

- using it for the development of application-specific programs; for example, for handling repetitive complex equilibrium calculations, for analysis, and for process control in well-defined technological areas,

- linking it to third-party process simulation package for modelling new or optimising existing processes; for example, commercial CFD programs such as Phoenics, CFX®, etc., general simulation programs, including Aspen Plus®, and also a company's own process simulation program.

By embedding it in an appropriate code, ChemApp can be employed to investigate time-dependent and kinetic effects using the concept of „local equilibria”.

#### 4.5.8 Code LINSOURPREPOST

The LINSOURPREPOST computer code (Müller-Hoeppe et al., 1994) relies on the analytical solution of the heat transfer differential equation for a finite, line shaped, instationary heat source emplaced in an infinite, homogenous and isotropic medium with constant material data. With respect to the linearity of the differential equation LINSOURPREPOST uses the superposition to model the temperature field of more than one source. The analytical solution is a complicated integral; the integration is achieved using the trapezoidal rule with increasing step size. The trapezoidal rule denotes an A-stable 2. order method.

To perform pre- and post processing, which yields a correct impression of the results, a special problem related smoothing algorithm is included. Note that real containers or drifts are modeled by a line source. Therefore all sampling points, which are very close to the line source, overestimate the temperatures. To overcome this problem a radius can be specified which defines a region around the source, where the temperatures are smoothed. The radius of the container is recommended as a good choice for the smoothing region.

A source with the length 2h, which extends symmetrically from the origin of coordinates in direction of axis z and which has a time dependent heat output  $\phi(t)$

$$T(t,R,z) = \frac{1}{8\rho c_p (\pi\lambda)^{\frac{3}{2}}} \int_0^t \frac{e'(t')}{(t-t')^{\frac{3}{2}}} \int_{-h}^h \exp\left[-\frac{R^2(z')}{4\lambda(t-t')}\right] dz' dt' \quad (4.35)$$

where

$$R^2(z') = x^2 + y^2 + (z-z')^2 = r^2 + (z-z')^2 \quad (4.36)$$

and

- $\rho$  = density of heat conducting material
- $c_p$  = heat capacity
- $\lambda$  = thermal conductivity
- $e'(t)$  = heat generation rate per unit length
- $R$  = radial distance from the intersection of line source and source median plane
- $z$  = axial distance from the source median plane
- $h$  = half of the length of the line source

$$T(t, r, z)_j = \frac{e'_{j,0} \exp(-\eta_j t)}{4\rho c_p \pi \lambda} \int_{\frac{1}{\sqrt{t}}}^{\infty} \exp\left[\frac{\eta_j}{\tau^2} - \frac{r^2 \tau^2}{4\lambda}\right] \left[ \operatorname{erf}\left(\tau \frac{z+h}{2\sqrt{\lambda}}\right) - \operatorname{erf}\left(\tau \frac{z-h}{2\sqrt{\lambda}}\right) \right] \frac{d\tau}{\tau} \quad (4.37)$$

- $e'_{j,0}$  = initial heat output per unit length for the nuclide j
- $\eta_j$  = decay coefficient of the nuclide j
- $\operatorname{erf}$  = error function

$$\operatorname{erf}(\sigma) = \frac{2}{\sqrt{\pi}} \int_0^{\sigma} \exp(-\xi^2) d\xi \quad (4.38)$$

In order to determine the temperature at a certain time and a field point in the surrounding of a line shaped heat source with n radioactive nuclides it has to be summed up on all nuclides and the initial temperature must be added. The contribution of each source has to be considered, because there exist m heat sources at a certain point of time.

Finally the temperature at a certain field point (R, z) at a certain point of time t results from the following equation:

$$T(t, R, z) = \sum_{i=1}^m \sum_{j=1}^n T(t, r_i, z_i)_{ij} + T_0 \quad (4.39)$$

$T(t, r_i, z_i)_{ij}$  = contribution of the nuclide j at the source i to the temperature increase at the interesting field point

With the help of equation (4.37) to (4.39) the DBE computer code LINSOURPREPOST calculates temperatures at specified, discrete field- and time points in a random repository configuration. Equation (4.37) will be integrated for a certain number of significant nuclides. The error function will be evaluated according to equation (4.38) using a variable polynomial approximation.

#### **4.6 Modelling of chemical processes in the EBS**

In order to describe the complex chemical reactions which can occur in the EBS several independent reactions must be understood from a qualitative and qualitative point of view:

- reactions of intruding water or brines with the salt formation
- reactions of brines with cementitious materials
- reactions of brines with silicates
- reactions of brines with iron

The reactions of intruding water or brines within the salt formation influence the total amount of resulting solutions, their chemical composition and the total volume of open spaces in the repository. The resulting brines are high saline solutions of the multi-component sea water system (Na-K-Mg-Ca-Cl-SO<sub>4</sub>-HCO<sub>3</sub>-H<sub>2</sub>O). For the modelling of this system a set of Pitzer parameters and solubility constants at 25 °C has been developed by Harvie et al. (1984). The Harvie-Møller-Weare database is internally consistent and the geochemical modelling renders results which are in good agreement with experimental data (see Herbert, 2000). An important limitation of this database consists in the fact, that it is limited to the temperature of 25 °C.

For the interpretation of the corrosion of cementitious materials in the EBS the seawater system of Harvie, Møller and Weare must be extended by Pitzer coefficients for Al and Si. However, such data are not available. They were estimated by Reardon (1990). Solubility data needed for cement phases were published by Revertegat et al. (1997), Berner (1990) and NEA data listed in Glasser et al. (2001). With a new database compiled in the above described way it was possible to describe accurately experimental data from laboratory experiments (Herbert and Meyer, 2001) as well as from long-term in-situ experiments in the Asse salt mine (Kienzler et al. 2000).

An accurate geochemical modelling of brines with silicates is not possible yet. Therefore, the dissolution/precipitation processes of clay materials such as bentonites in repositories in salt formations is not possible. The need for a database including Pitzer parameters for Si and Al in a wide pH range is evident. Since 2001, GRS is conducting an R&D program for the determination of the solubility of these parameters in high saline solutions at different pH.

Steel canisters are part of the EBS as they are used as waste containments. Nuclides will not be released to the near-field as long as the steel canister does not fail. Failure is caused due to the corrosion in contact with brines. Corrosion is a complex reaction. „Corrosion” in general means the ongoing destruction of a metallic matrix by the continuous release of metal cations into solution. It is an electrochemical process where electrons are transferred from the metal across its boundary to acceptors in solution. Though corrosion in most cases is possible thermodynamically, the kinetics of corrosion is highly dependant on conditions such as temperature, pH and the presence of further solution constituents. Corrosion time may be prolonged by the partial passivation of the surface or may be limited to the extent of available solution. The time elapsing to the complete failure of a steel canister is further influenced by construction details such as welding seams or fittings. The time for the steel canister to fail is of primary interest for the performance assessment. Up to know, the corrosion is not modelled by the codes for release of radionuclides from underground storage facilities. On the basis of experiments it is rather assumed that the canisters maintain their integrity during a certain time before it completely fails. However, for a better understanding of corrosion it is important to be able to calculate iron activities in solutions of the sea water system up to saturation. Thus, GRS has set up experimental and theoretical work. A report will be available by the end of September 2002.

## **5 Work Package 3.2: Application of conceptual & mathematical models for predicting THMBC performance**

In the German in-situ research programme on radioactive waste disposal in geological salt formations main emphasis was put on the analyses of the integrity of the host rock (sealing function) as the most important barrier and on potential backfill materials for the sealing of underground disposal rooms. Two important experiments were performed in the Asse mine to assess the thermo-mechanical processes related to the interaction between simulated heat generating waste canisters, the crushed salt backfill in the disposal rooms and the surrounding host rock. These were the „Thermal Simulation of Drift Emplacement (TSDE)” and the „Development of Borehole Seals for Radioactive Waste (DEBORA)” experiments. Further tests were performed to investigate the importance of hydraulic processes like brine migration or fluid flow, respectively, through host rock and backfill materials. Experiments in this regard were the Temperature Test 5 (TV 5) and the joint American-German Brine Migration Test (BMT).

The objectives of in-situ experiments are manifold. The most important ones are the:

- observation and measurement of thermal, hydraulic and mechanical (THM) processes in the host rock and EBS under complex in-situ conditions in order to check the validity of laboratory results under in-situ conditions
- observation of the dynamics of different processes and their importance for the long-term safety of repositories
- validation of models used to predict THM processes in the host rock and EBS by comparing predicted and measured data
- application, appraisal and improvement of instruments used to measure crucial quantities and to survey repositories
- demonstration of the feasibility and safety of disposal techniques.

In order to enable an adequate long-term simulation of the above-mentioned processes, several codes were developed. A distinction is to be made between the codes developed for integrated safety analyses (e. g., EMOS) and those developed for a detailed analyses of individual processes (rock stability, chemical evolution...).

Coupling of processes was only considered for thermo-mechanical analyses. The code SUPERMAUS (Breidenich, 1994) or FLAC<sup>3D</sup>, for instance, allows the fully coupled calculation of the temperature evolution as well as the mechanical stress and strain processes in a high-level waste (HLW) repository. With a view towards the migration of radionuclides in the host rock, other codes like MUFTE and TRAVAL were developed for the analyses of fluid flow in (fractured) porous media.

In this report, specific examples will be given for the application of the codes which have been used to design and predict full-scale experiments in the Asse mine. A comparison of predicted and measured data is presented in order to demonstrate the prediction capability of the codes.

## **5.1 Backfill compaction in HLW disposal drifts**

The drift disposal concept represents an option which has been developed in Germany for the direct disposal of spent fuel (Hartje et al., 1989). Large self-shielding Pollux casks will be emplaced in 200 m long drifts. Following the emplacement of a Pollux cask, the remaining voids in the drift will be backfilled with crushed salt for final sealing of the drift.

### **5.1.1 Models and data used for modelling**

#### **5.1.1.1 Conceptual model**

The conceptual model considered in this concept consists of disposal drifts of 4.5 m width and 3.7 m height to store waste canisters (POLLUX type) of 1.54 m diameter and 5.46 m length with a minimum distance of 1 m from each other. The minimum pillar width is 9.6 m. The drifts including the seal area at the drift entrance and the free space surrounding and separating the canisters are backfilled with crushed salt. The drifts are surrounded by an excavation disturbed zone (EDZ) with increased porosity and permeability.

A situation of drift emplacement was simulated in the TSDE experiment (Figure 5.1). The experiment was performed in two parallel drifts at the 800-m level of the Asse

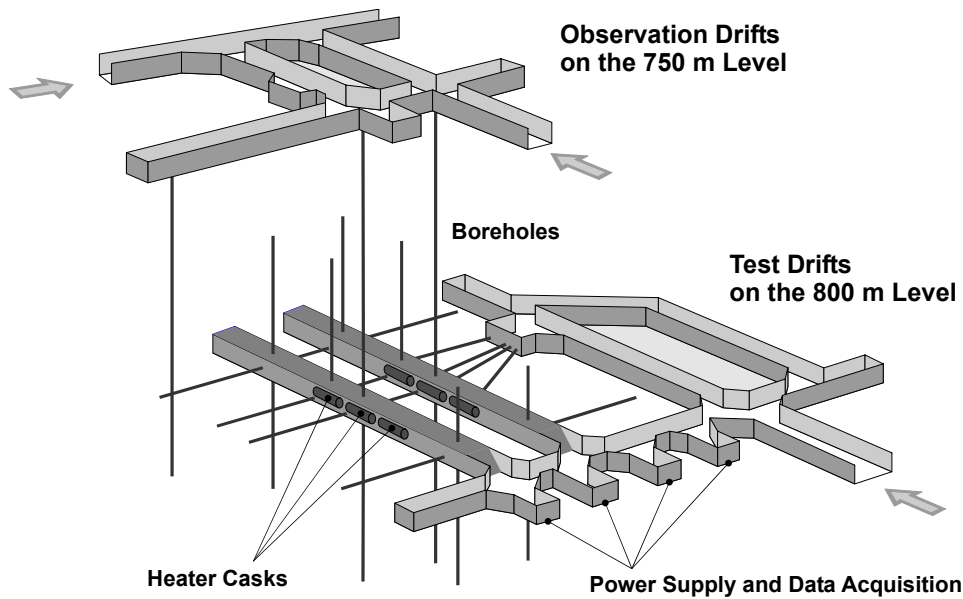


**Figure 5.1** Layout of the TSDE experiment-according to the drift emplacement concept (Bechthold et al., 1999)

mine. The drifts were 70 m long each, 3.5 m high, and 4.5 m wide and separated by a pillar of 10 m width. Three electrically heated casks with a nominal power of 6.4 kW were deposited in each drift. Crushed salt with an initial porosity of 0.35 was used as backfill material. Backfill and host rock temperature, drift closure, and resulting backfill pressure were measured in different cross sections. Additional points of interest were gas release and metal corrosion. The initial salt temperature was about 36 °C and the initial stress at the test field level was assumed to 12 MPa. The heating phase started on 25 September 1990 and was terminated on 1 February 1999.

#### 5.1.1.2 Theoretical models

The empirical models used for describing the creep behaviour of the elasto-viscoplastic rock salt and the crushed salt were published within the BAMBUS (**B**ackfill **a**nd **M**aterial **B**ehaviour in **U**nderground **R**epositories in **S**alt) project by Bechthold et al. (1999) (for details see section 4). The data and parameter values of the models used in the numerical calculations were determined by laboratory investigations mainly performed by Forschungszentrum Karlsruhe (FZK) (Korthaus, 1996) and Groupement pour l'Etude des Structures Souterraines de Stockage (G.3S) (Bechthold et al., 1999).

### **Processes studied and modelled**

The processes studied and modelled in the TSDE experiment were mainly the temperature evolution in the rock and the backfill and the thermally modified stresses and resulting creep deformations in the rock and the backfill (compaction). An overview of the main processes is given in the following Table 5.1. Among others, one of the objectives of BAMBUS I (1995-1998) was to verify the results of different modellers in case of 2D-calculations, and of BAMBUS II (2000-2004) to give a more realistic approximation of the TSDE experiment by 3D-calculations.

**Table 5.1** Processes studied in the TSDE experiment (■ yes; □ no)

<b>Repository System Component</b>	<b>Process</b>	<b>Measured in Experiment</b>	<b>Modelled numerically in Experiment</b>
Near-field rock	Temperature Evolution	■	■
	Stress Field Evolution	■	■
	Displacement Evolution	■	■
Backfill	Temperature Evolution	■	■
	Stress Field Evolution	■	■
	Displacement Evolution	■	■
	Porosity	□	■
	Hydraulic Evolution	■	□

### **Data used**

The data used in the numerical simulations of the TSDE experiment in the phase I of the BAMBUS project are given in Table 5.2. Changes were made in phase II of the BAMBUS project with respect to thermal properties, cf. Table 5.4.

## **5.1.2 Modelling**

### **5.1.2.1 Codes used**

The codes MAUS/TAUS (see section 4.5) were used by DBE in the numerical simulation of the TSDE experiment in BAMBUS I. The code FLAC<sup>3D</sup> was applied in BAMBUS II. MAUS and TAUS are two-dimensional finite element codes where MAUS is for mechanical and TAUS for thermal analysis. A weak coupling between thermal

**Table 5.2** Data used in BAMBUS I for the numerical simulation of the TSDE experiment

Parameter	Value
<p><b>A) Rock</b></p> <ul style="list-style-type: none"> <li>• <i>Mechanical properties</i> (Bechthold et al., 1999) <ul style="list-style-type: none"> <li>– Young's modulus E [MPa]</li> <li>– Poisson's ratio <math>\nu</math> [ - ]</li> </ul> </li> <li>• <i>Thermal properties</i> (Bechthold et al., 1999) <ul style="list-style-type: none"> <li>– heat capacity <math>c_{v,rs}</math> [J/(kg · K)]  <math>c_{v,rs}(T) = b_0 + b_1 T</math></li> <li>– thermal conductivity <math>\lambda</math> [W/(m ·K)]  <math>\lambda_{rs}(T) = a_0 + a_1 T + a_2 T^2 + a_3 T^3</math></li> <li>– coefficient of thermal expansion <math>\beta_T</math> [K<sup>-1</sup>]</li> </ul> </li> <li>• <i>Density</i> <math>\rho</math> [kg/m<sup>3</sup>]</li> </ul>	<p>E = 25,000</p> <p><math>\nu = 0.27</math></p> <p><math>b_0 = 806.86 \text{ J/(kg}\cdot\text{K)}, b_1=0.1773 \text{ J/(kg} \cdot \text{K}^2)</math></p> <p><math>a_0 = 13.196 \text{ W/(m} \cdot \text{K)}</math>  <math>a_1 = -3.738 \cdot 10^{-2} \text{ W/(m} \cdot \text{K}^2)</math>  <math>a_2 = 4.097 \cdot 10^{-5} \text{ W/(m} \cdot \text{K}^3)</math>  <math>a_3 = -1.510 \cdot 10^{-8} \text{ W/(m} \cdot \text{K}^4)</math></p> <p><math>\beta_T = 4.2 \cdot 10^{-5} \text{ K}^{-1}</math></p> <p><math>\rho = 2,187 \text{ kg/m}^3</math></p>
<p><b>B) Crushed Salt</b></p> <ul style="list-style-type: none"> <li>• <i>Mechanical properties</i> (Bechthold et al., 1999) <ul style="list-style-type: none"> <li>– Young's modulus E [MPa]  <math>E = E_0 \exp(-cE \cdot \phi (1-\phi_0)/(1-\phi))</math></li> <li>– initial porosity <math>\phi_0</math> [ - ]</li> <li>– Poisson's ratio <math>\nu</math> [ - ]</li> </ul> </li> <li>• <i>Thermal properties</i> (Bechthold et al., 1999) <ul style="list-style-type: none"> <li>– heat capacity <math>c_{v,cs}</math> [J/(kg · K)]</li> <li>– thermal conductivity <math>\lambda</math> [W/(m ·K)]  <math>\lambda_{cs}(T) = \lambda_{rs}(T) \cdot (1 - c \cdot \phi)</math></li> <li>– coefficient of thermal expansion <math>\beta_T</math> [K<sup>-1</sup>]</li> </ul> </li> </ul>	<p><math>E_0 = 25,000, c_E = 9.07</math></p> <p><math>\phi_0 = 0.35</math></p> <p><math>\nu = 0.27</math></p> <p><math>c_{v,cs}(T) = c_{v,rs}(T)</math></p> <p><math>c = 2.91</math></p> <p><math>\beta_T = 4.2 \cdot 10^{-5} \text{ K}^{-1}</math></p>

and mechanical calculation is used within the time history. FLAC<sup>3D</sup> is a three-dimensional finite difference code which includes a mechanical and a thermal module. So, FLAC<sup>3D</sup> provides a weak thermo-mechanical coupling within a time increment.

### 5.1.2.2 Features of analysis

In the calculations of BAMBUS I, a plane strain model consisting of 1,511 8-node elements with 4,644 nodes was adopted (Figure 5.2). The heaters were modelled with uniform thermal power. In the modelling, the actual history of the test field was taken into account. Hence, the assumed reduced initial stress was 12 MPa at the drift level with a vertical gradient corresponding to the rock-salt density. Heating started 1.5 years after drift excavation and lasted for 2,503 days, with a thermal power of 433 W/m<sup>3</sup>, which is the average power of the three casks in a drift with regard to the length of the heated area, and an initial backfill porosity of 31 %. In BAMBUS II, the model was extended in the third dimension. Therefore, the thermal power of 643 W/m<sup>3</sup>, used in the model is the nominal heater power. The initial porosity was increased to the measured value of 0.35.

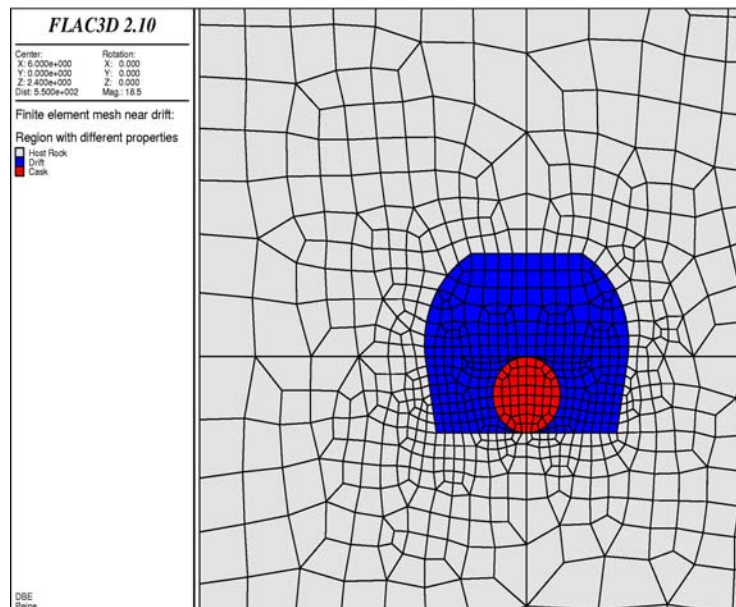


**Figure 5.2** Finite element mesh used in the DBE calculations of the TSDE experiment

### 5.1.2.3 Comparison of predicted and measured results and conclusions

Results of measured and predicted data are shown in Figures 5.3 and 5.4 for the convergence and the temperature evolution. The convergence calculated in BAMBUS I is significantly higher than the measured data due to overestimated temperatures caused by the restriction to only two dimensions. Nevertheless, there is a preponderantly good agreement between the results from different modellers. A 3D-calculation performed during BAMBUS II shows a better agreement between measured data and calculated convergence values. This improvement can be seen in the temperature plot (Figure 5.4) as well.

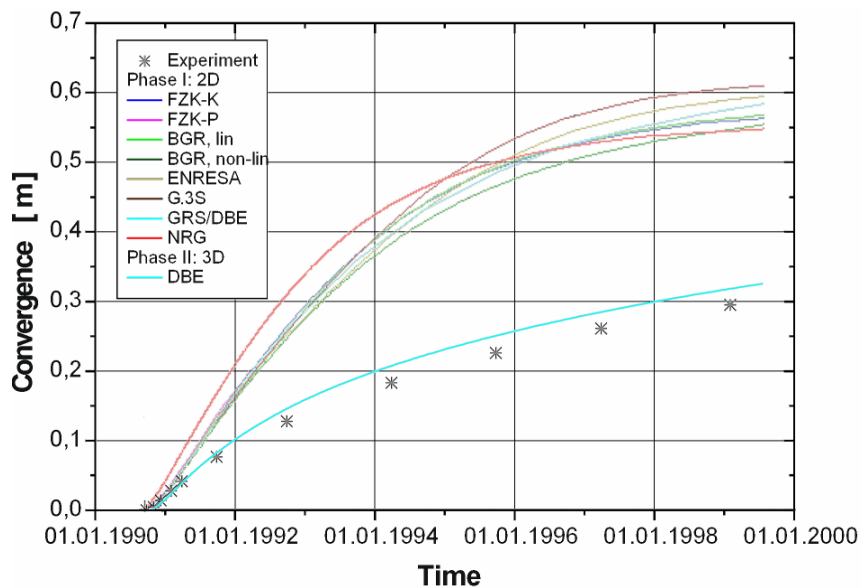


**Figure 5.3** Convergence in the middle cross section of TSDE from 2D- (Phase I) and 3D-calculations (Phase II)

However, some discrepancies appeared in the temperature of the drift near field (Figure 5.4) and in quantities like stresses and porosity, which are derived from the primary calculated quantities. The reason could be seen in the constitutive law of heat conductivity of crushed salt as well as in the parameter values used for the mechanical part of crushed salt. The backfill in the simulations responds softer to heating than the real material. The discrepancies between measurements and calculation might also be caused by discretization of the geometrical model. But a very fine mesh requires an extremely high computational effort.

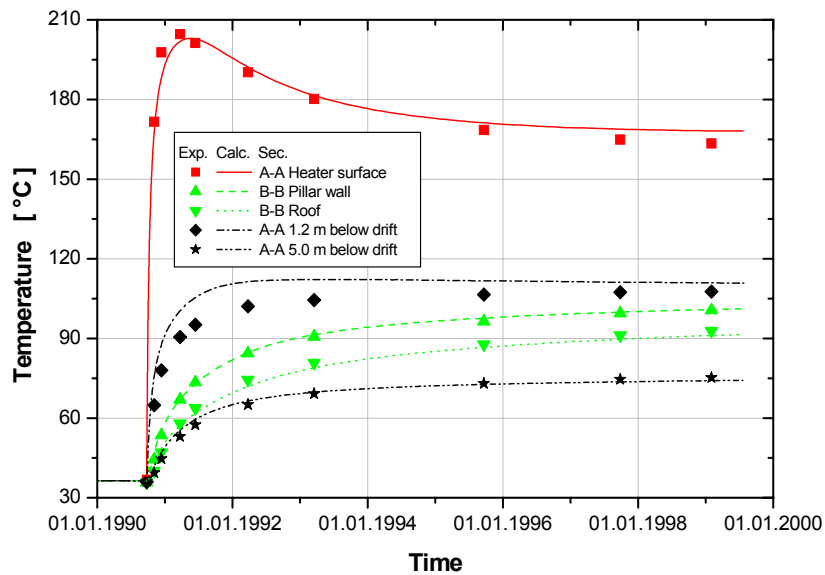


**Figure 5.4** Temperature at selected points of two cross sections from 3D-calculation

In conclusion it can be stated that at least the temperature prediction must be 3D to estimate the thermo-mechanical behaviour at the mid-plane. The 3D-model seems to be suited to predict the compaction behaviour of crushed salt qualitatively. However, the observed quantitative deviations and the inconsistencies regarding the prediction of deformations and stresses indicate shortcomings in the material models that need to be clarified.

## 5.2 Backfill compaction in disposal boreholes

The borehole disposal concept represents a further option in addition to the drift disposal concept for spent fuel. High-level waste remaining from reprocessing of spent fuel will be vitrified in steel canisters. The steel canisters will be disposed of in about 300 m to 600 m deep and 0.6 m wide boreholes (BfS 1990) reaching vertically down from a disposal level at a depth of about 880 meters below ground. About 200 canisters will be lowered into a borehole. In order to transfer the weight load of the canister stack to the surrounding rock mass, the annulus between the canisters and the borehole wall is foreseen to be backfilled with crushed salt. The canisters will be completely encapsulated by the creeping salt. At top of the borehole, a seal consisting of crushed salt will be placed.

## **5.2.1 Models and data used for modelling**

### **5.2.1.1 Conceptual model**

The conceptual model considered in this concept is shown in Figure 5.5. The model includes the disposal drift of 6 m width and height, a disposal borehole of 0.6 m diameter and 300 m or 600 m depth and a waste canister stack (Cogéma type 7/86) of 0.43 m diameter. The drift, the seal area at the top of the borehole and the 0.085 m wide annulus between the canister stack and the host rock are backfilled with crushed salt. The maximum grain size of the material is 30 mm in the drift and the seal and 10 mm in the annulus. The whole drift and borehole system is surrounded by an excavation disturbed zone (EDZ) with increased porosity and permeability compared to the undisturbed salt rock.

In the DEBORA-2 experiment (Figure 5.6), the situation of the borehole seal at the top of the canister stack was simulated. The experiment was performed in a 15 m deep non-lined borehole with a diameter of 0.6 m located at the 800-m level of the Asse mine. The heat production of the waste canisters was simulated by four peripheral heaters surrounding the borehole at a radius of 1.1 m. The lower third of the borehole representing the borehole seal section was backfilled with crushed salt. Backfill temperature, borehole closure, and resulting backfill pressure were measured at three levels in the backfilled section. The initial salt temperature was about 32 °C and the initial stress at the test field level was assumed to 12.5 MPa. DEBORA 2 was heated from 22 September 1997 until 4 December 1998.

### **5.2.1.2 Theoretical models**

The empirical models used for describing the creep behaviour of the elasto-viscoplastic rock salt and the crushed salt were published by Wallner (1979), Hunsche and Hampel (1999) and Hein (1991) (for details see section 3). The data and parameter values of the models used in the numerical calculations were determined by laboratory investigations mainly performed by the Bundesanstalt für Geowissenschaften und Rohstoffe (BGR) (Hunsche and Hampel, 1999) and by GRS (Feddersen, 1999).

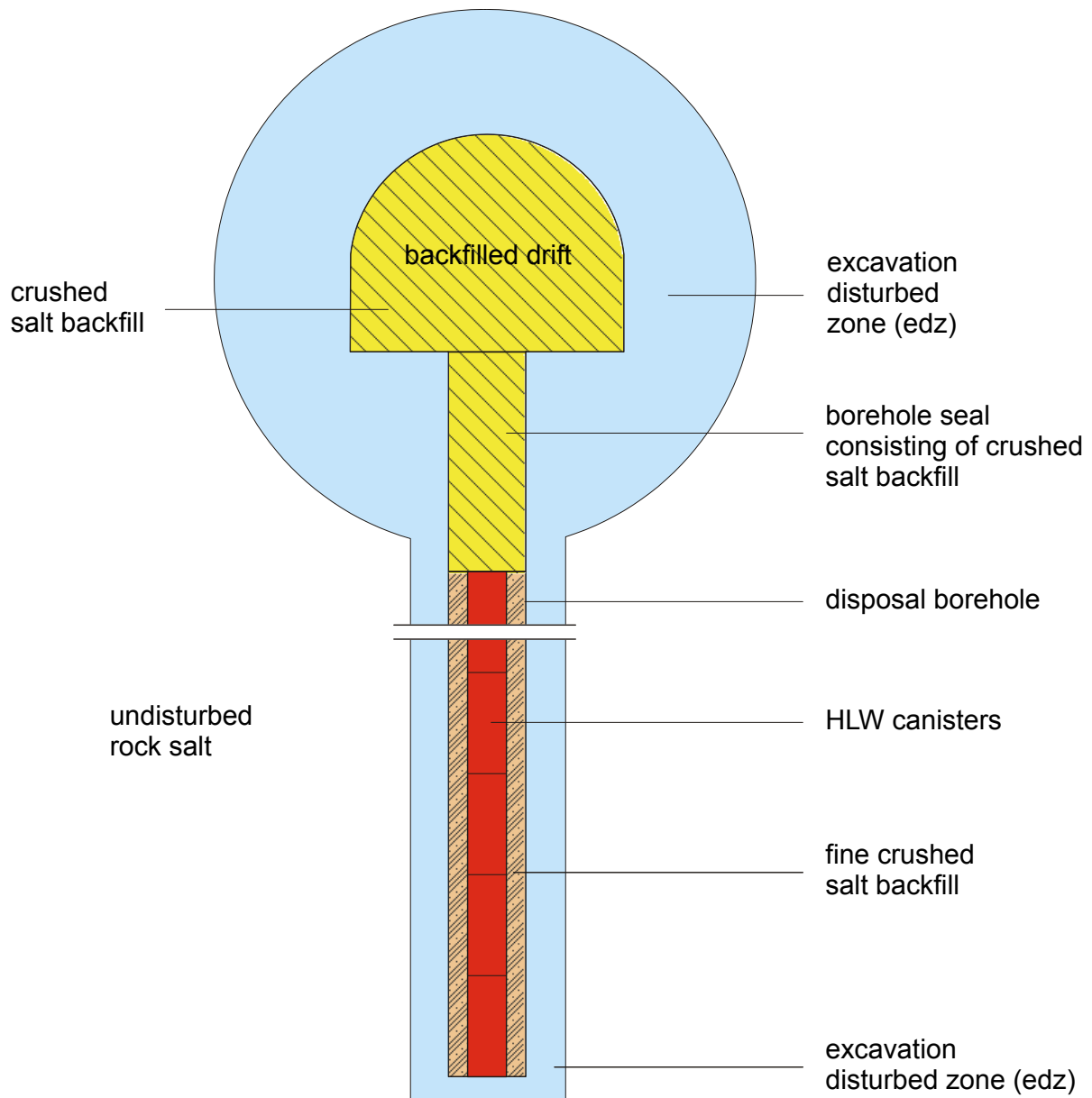


**Figure 5.5** Situation of a HLW disposal borehole in a German repository in a geological salt formation

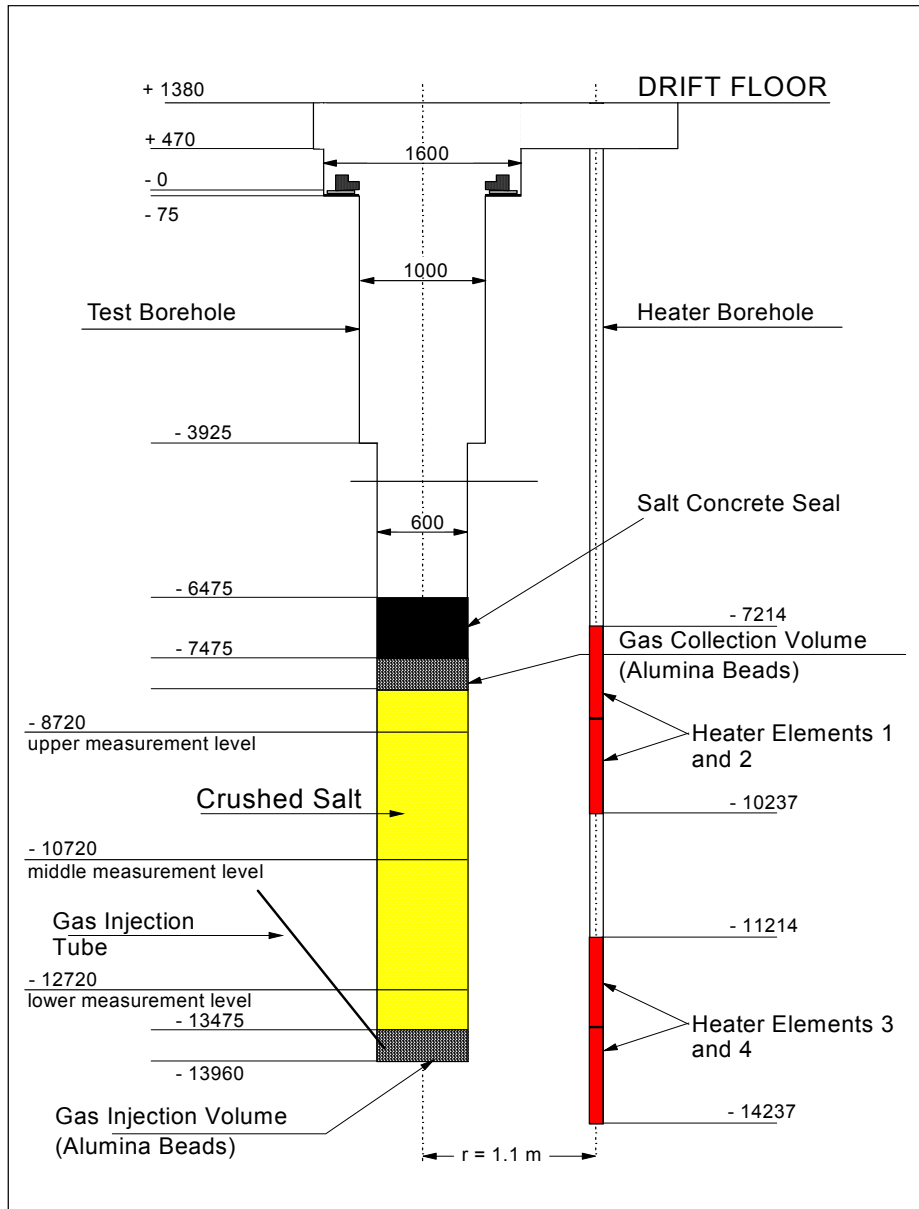


Figure 5.6 Layout of the DEBORA-2 experiment

**Processes studied and modelled**

The processes studied and modelled in the DEBORA experiment were mainly the temperature evolution in the rock and the backfill and the thermally induced stresses as well as resulting creep deformations in the rock and in the backfill (compaction). In addition to this, the scenario of a brine inflow into the sealed borehole and the resulting two-phase flow of gas and brine in the backfill was analysed by numerical simulation. An overview of the main processes is given in the following Table 5.3.

**Table 5.3** Processes studied in the DEBORA experiment (■ yes; □ no)

Repository System Component	Process	Measured in Experiment	Modelled numerically in Experiment
Near-field rock	Temperature Evolution	■	■
	Stress Field Evolution	■	■
	Displacement	■	■
	Thermal/Mechanical Coupled Evolution	□	■
Backfill	Temperature Evolution	■	■
	Stress Field Evolution	■	■
	Displacement	■	■
	Hydraulic Evolution	■	□
	Thermal/Mechanical Coupled Evolution		■

**Data used**

The data used in the numerical simulations of the DEBORA experiment are comprised in Table 5.4.

**Table 5.4** Data used in the numerical simulations of the DEBORA experiments

Parameter	Value
<b>A) Rock</b>	
• <i>Mechanical properties (Bechthold et al., 1999)</i>	
– Young's modulus E [MPa]	E = 24000
– Poisson's ratio $\nu$ [ - ]	$\nu = 0.27$
• <i>Thermal properties (Bechthold et al., 1999)</i>	
– specific heat capacity $\rho c_p$ [J/(m <sup>3</sup> · K)]	$\rho c_p(T)$ : 0.607 at 25 °C 0.610 at 50 °C 0.617 at 100 °C 0.627 at 180 °C 0.642 at 200 °C
– thermal conductivity $\lambda$ [W/(m · K)]	$\lambda (T)$ : 5.51 at 25 °C 5.1 at 50 °C 4.26 at 100 °C 3.33 at 180 °C 2.51 at 200 °C
– coefficient of thermal expansion $\beta_T$ [K <sup>-1</sup> ]	$\beta_T = 4.2 \cdot 10^{-5}$
• <i>Hydraulic properties</i>	
– Permeability k [m <sup>2</sup> ] (Wieczorek and Zimmer 1998)	$k < 10^{-20}$
– initial porosity $\phi$ [-] (Jockwer et al., 1995)	$\phi = 0.001$
• <i>Mineralogy</i>	
	Rock salt consisting of halite (NaCl) and accessory minerals like polyhalite (K <sub>2</sub> MgCa <sub>2</sub> (SO <sub>4</sub> ) <sub>4</sub> ·2H <sub>2</sub> O and anhydrite (CaSO <sub>4</sub> )
<b>B) Crushed Salt</b>	
• <i>Mechanical properties (Bechthold et al., 1999)</i>	
– Young's modulus E [MPa]	$E = E_r \exp(-c_k \phi / ((1 - \phi_o) / (1 - \phi)))$ $c_k = 12.27$
– Poisson's ratio $\nu$ [ - ]	$\phi_o = 0.35$ $\nu = 0.27$
• <i>Thermal properties (Bechthold et al., 1999)</i>	
– heat capacity $\rho c_p$ [J/(m <sup>3</sup> · K)]	$\rho c_p(T, \phi) = \rho c_p(T) \cdot (1 - \phi)$

<ul style="list-style-type: none"> <li>– thermal conductivity <math>\lambda</math> [W/(m ·K)]</li> <li>• <i>Hydraulic properties (Müller-Lyda et al., 1999)</i> <ul style="list-style-type: none"> <li>– Permeability <math>k</math> [m<sup>2</sup>]</li> <li>– initial porosity <math>\phi</math> [-]</li> </ul> </li> <li>• <i>Mineralogy</i></li> </ul>	$\lambda(T, \phi) = \frac{\lambda(T)(1 - \phi)}{(h_o(1 - (1 - \phi)^b) + (1 - \phi)^b)}$ $h_o = 4.56 \quad b = \ln(2/3)/\ln(-\phi_o)$ $k = 2.54 \cdot 10^{-10} \cdot \phi^{4.175} \text{ m}^2$ $\phi = 0.35$ <p>Rock salt consisting of halite (NaCl) and accessory minerals like polyhalite (K<sub>2</sub>MgCa<sub>2</sub>(SO<sub>4</sub>)<sub>4</sub>·2H<sub>2</sub>O and anhydrite (CaSO<sub>4</sub>)</p>
--	--

## 5.2.2 Modelling

### 5.2.2.1 Codes used

The code used by GRS in the numerical simulation of the DEBORA experiment was the code SUPERMAUS. This code was developed at the Technical University of Aachen (Breidenich, 1994). It is a two-dimensional finite element code based on the modules TAUS (for thermal analysis) and MAUS (for mechanical analysis). It provides coupling between thermal and mechanical calculation in the sense that not only the thermal influence on the mechanical parameters and quantities, but also the influence of mechanics on the thermal behaviour is taken into account. This is of special importance for the „soft” backfill which was subjected to great changes in its thermal parameters during mechanical compaction. Further details are reported in section 3.

### 5.2.2.2 Features of analysis

In the calculations, an axisymmetric finite element model consisting of 752 8-node elements with 2345 nodes was used (Figure 5.7). The peripheral heaters were modelled as heater rings consisting of rock salt with uniform thermal power distribution. In the modelling, the actual history of the test field was taken into account (i. e., excavation and drilling of the boreholes). The initial stress was assumed to be 12.5 MPa at the heater mid-height with a vertical gradient corresponding to the rock-salt density of 2180 kg/m<sup>3</sup>. Heating started 12.42 years after test field excavation and

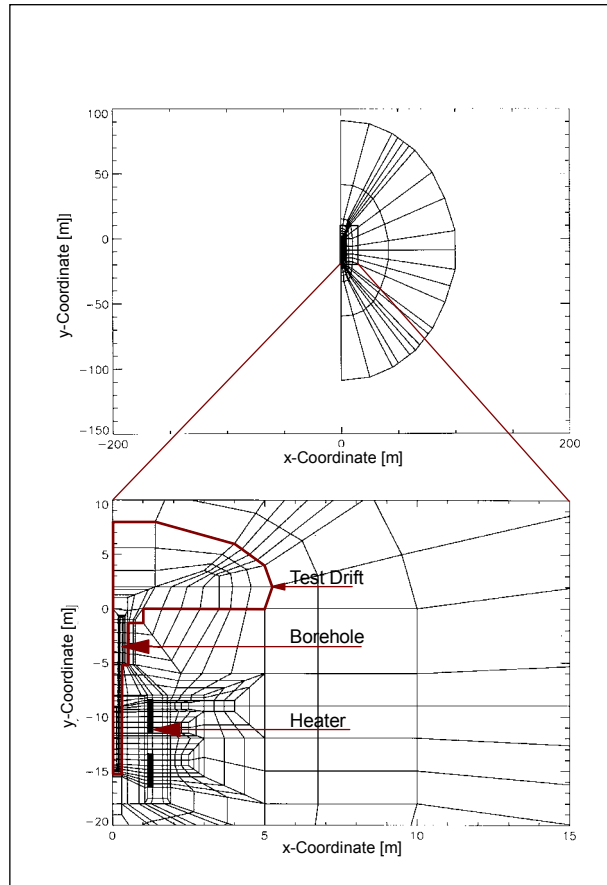


**Figure 5.7** Schematic representation of the finite element mesh used by GRS calculations of the DEBORA-2 experiment

lasted for 547 days, with a thermal power of 14 kW and an initial backfill porosity of 36.6 %.

### 5.2.2.3 Comparison of predicted and measured results and conclusions

Results of predicted and measured data are shown in Figures 5.8 and 5.9 for the temperature evolution and the porosity decrease in the backfill. The porosity was determined on basis of borehole convergence data. The development of the porosity in the DEBORA experiment is somewhat different in comparison to the results of the numerical predictions. Also, a softer material behaviour is predicted in the DEBORA experiments than observed in situ. This is especially true for porosities above 0.2. A

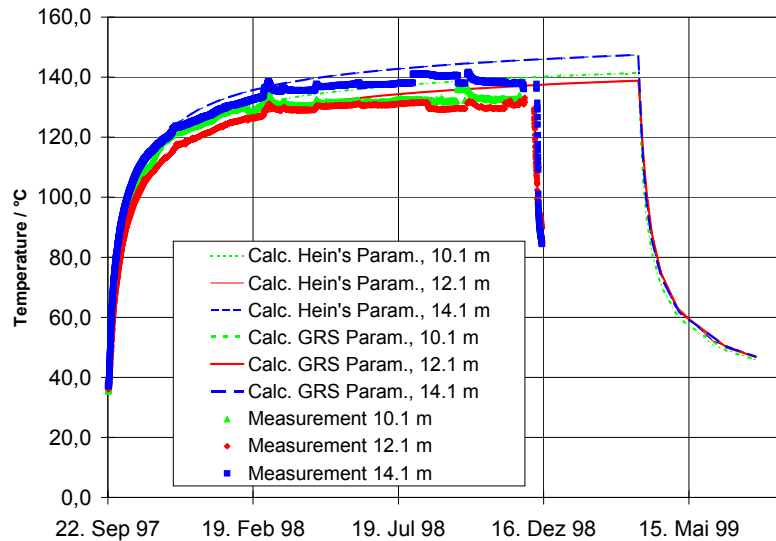


**Figure 5.8** Temperature development in the backfilled borehole of DEBORA 2

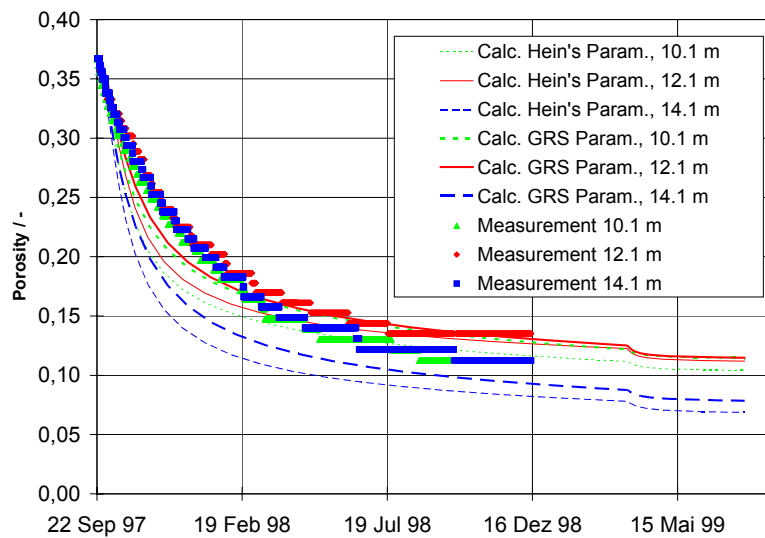


**Figure 5.9** Porosity development in the backfilled borehole of DEBORA 2

possible explanation might be that the material parameter values used in the calculations are not valid for this porosity range because they were always derived from laboratory experiments on samples with porosities below 0.2. The compaction rates observed in the late stage of the experiments at porosities below 0.2 agree much better, thereby confirming the aforementioned assumption. The discrepancies between measurements and calculations might also be caused by restraints of the assumed

model of rotational symmetry. These models neglect the true extension of the test drift above the test boreholes which leads, especially in the early phase of the heating period, to an overestimation of thermally induced stresses and thus of deformations in the rock salt around the test boreholes.

In summary it is concluded that the used material model and the SUPERMAUS code are adequate for predicting the compaction behaviour of crushed salt backfill.

### 5.3 Two-phase flow in the backfill of HLW disposal boreholes

#### 5.3.1 Models and data used for modelling

Two-phase flow in the backfill is of interest for the investigation of altered evolution scenarios. Because of its importance for the long-term performance of a repository, the concerning modelling exercise is described here even if no related in-situ experiment has been performed yet.

##### 5.3.1.1 Conceptual model

The considered system consists of a short horizontal drift and a vertical borehole which contains the waste canister stack and a seal (see Figure 5.10). Each of the three parts

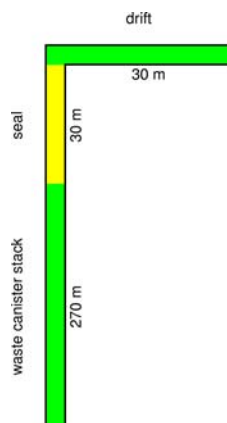


**Figure 5.10** Sketch of the disposal borehole and connected drift

is assumed to be filled with crushed salt in a different state of compaction. The cross-section areas were 10.50 m<sup>2</sup> for the drift, 0.2827 m<sup>2</sup> for the seal and 0.1385 m<sup>2</sup> for the annulus around the canister stack.

Three altered evolution scenarios were investigated:

- brine inflow into the drift from an instantaneously flooded 500-m-high shaft,
- hydrogen production in a flooded borehole due to corrosion of the HLW steel canisters and
- spontaneous connection of an unexplored brine pocket with the bottom of the borehole.

#### **5.3.1.2 Theoretical model**

The theoretical concept underlying the model calculations is that of the flow of two immiscible fluids in a porous medium. One of the fluids is a compressible gas, the density of which is calculated using the ideal gas law.

#### **5.3.1.3 Processes studied**

The main objective of this work was to investigate the two-phase flow processes in view of the high material parameter contrasts at discontinuities like, for instance, shaft-drift interface or the seal-drift-interface. In order to improve the understanding of the principal mechanisms and the significance of the two-phase flow in a sealed disposal borehole, the dynamics of the processes were to be analysed. Specific problems with the numerical models for a realistic repository in rock salt were anticipated. The behaviour of the code and the reliability of the results were therefore to be identified and analysed as well.

#### **5.3.1.4 Data used**

The material data used are based on laboratory investigations of two-phase flow in compacted crushed salt samples (Cinar et al., 1998). Homogeneity and isothermal conditions as well as constant porosity in the crushed salt were assumed in the model

for the sake of simplicity. In a refined investigation, these properties should be treated as time-dependent. The data are summarized in Table 5.5.

### 5.3.2 Modelling

#### 5.3.2.1 Codes used

The calculations were done with the finite element code MUFTE (Helmig et al., 1994). It is designed to simulate two-phase flow - especially gas-water flow - in porous fractured media (see also section 4).

**Table 5.5** Material data, initial and boundary conditions for the two-phase flow models

	Annulus	Seal	Drift
permeability [m <sup>2</sup> ]	10 <sup>-15</sup>	10 <sup>-14</sup>	10 <sup>-13</sup>
porosity [-]	0.02	0.06	0.10
relative permeability after Brooks-Corey	$\lambda = 1.8095$ $S_{wr} = 0.12$ $S_{nwr} = 0.03$	$\lambda = 1.8095$ $S_{wr} = 0.10/0.14^*$ $S_{nwr} = 0.03$	$\lambda = 1.8095$ $S_{wr} = 0.10$ $S_{nwr} = 0.03$
capillary pressure after Van-Genuchten	$\alpha = 4.0$ $n = 0.0005$ $S_{wr} = 0.08$ $S_{nwr} = 0.02$	$\alpha = 4.0$ $n = 0.000158$ $S_{wr} = 0.08$ $S_{nwr} = 0.02$	$\alpha = 4.0$ $n = 0.0005$ $S_{wr} = 0.08$ $S_{nwr} = 0.02$
initial brine pressure	scenario 1: 0.085 MPa scenario 2: 5 MPa in the drift and a hydrostatically increasing pressure in the borehole scenario 3: 0.085 MPa		
initial brine saturation	scenario 1: 0.14 with an exponential increase up to 1 at the inflow boundary in the drift scenario 2: 0.97 everywhere scenario 3: as in scenario 1 with the exponential increase at the bottom of the borehole		
boundary conditions (scenario 1)	no flow		$p_w = 5 \text{ MPa}$ $S_w = 100 \%$
boundary conditions (scenario 2)	$\dot{m}_{nw} = 9.8 \cdot 10^{-10} \text{ kg/(s}\cdot\text{m)}$ for 830 years		$p_w = 5 \text{ MPa}$ $S_w = 100 \%$
boundary conditions (scenario 3)	$p_w = 8 \text{ MPa}$ $S_w = 98 \%$	$p_w = 0.85 \text{ MPa}$ $S_w = 14 \%$	(not included in the model)

\*) in the third model for numerical reasons

### 5.3.2.2 Features of analysis

In MUFTE, one-, two- and three-dimensional elements can be combined to reproduce fractures explicitly in a porous medium. For this purpose, the one- and two-dimensional elements can be arbitrarily oriented in space. Advantage was taken of this option and drift, seal, and annulus around the canister stack were discretised using one-dimensional elements. The initial and boundary conditions for the two-phase flow models are comprised in Table 5.5 as well.

### 5.3.2.3 Model results

In the first scenario the drift is flooded within one day. But it takes about a year for the brine front to cross the seal and reach the canister stack. Gas and brine pressure are almost constant throughout the entire model at that time so that gravity and capillary pressure are the only remaining driving forces. The brine saturation in the borehole is significantly lower than in the drift allowing the gas to move upward. This is the beginning of a counter flow system in which brine moves downward and pushes the gas upward and out of the system.

Brine reaches the bottom of the borehole after 40 years and afterwards the borehole becomes completely saturated from bottom to top. The velocity of this process depends on the gas mobility. The further the pores are filled with brine, the slower the gas flows in the remaining pore space. Most of the pore space is filled with brine within about another 20 years. The time-dependent distribution of brine saturation and gas pressure are shown in Figure 5.11.

Hydrogen generation builds up the gas pressure in the second scenario. The gas production rate considered in the model relates to the corrosion of pollux canisters with a maximum corrosion rate of 60  $\mu\text{m/a}$  (Smailos et al., 1992). Just before the gas enters the seal, the gas pressure exceeds the hydrostatic pressure by almost 3 MPa at the bottom of the borehole (see Figure 5.12). Subsequently, the pressurised gas phase pushes brine out of the annulus for the first few months while the corresponding gas flow into the seal remains insignificant due to the low mobility.

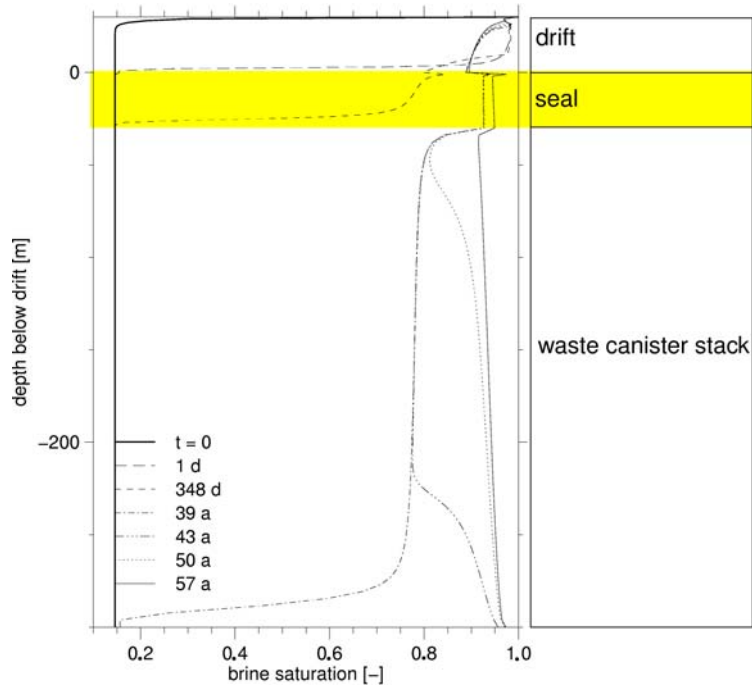


**Figure 5.11a** Time-dependent brine saturation distribution for scenario 1

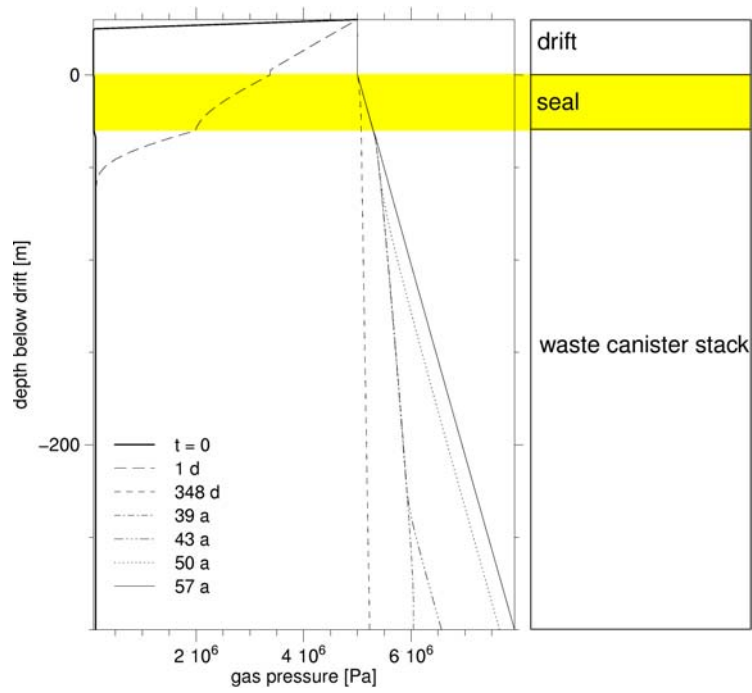


**Figure 5.11b** Time-dependent pressure distribution for scenario 1

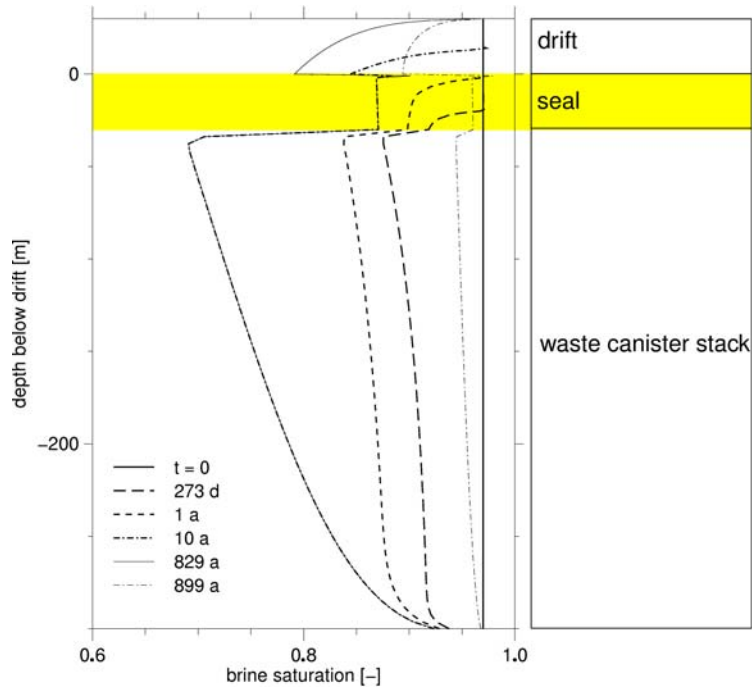


**Figure 5.12a** Time-dependent brine saturation distribution for scenario 2

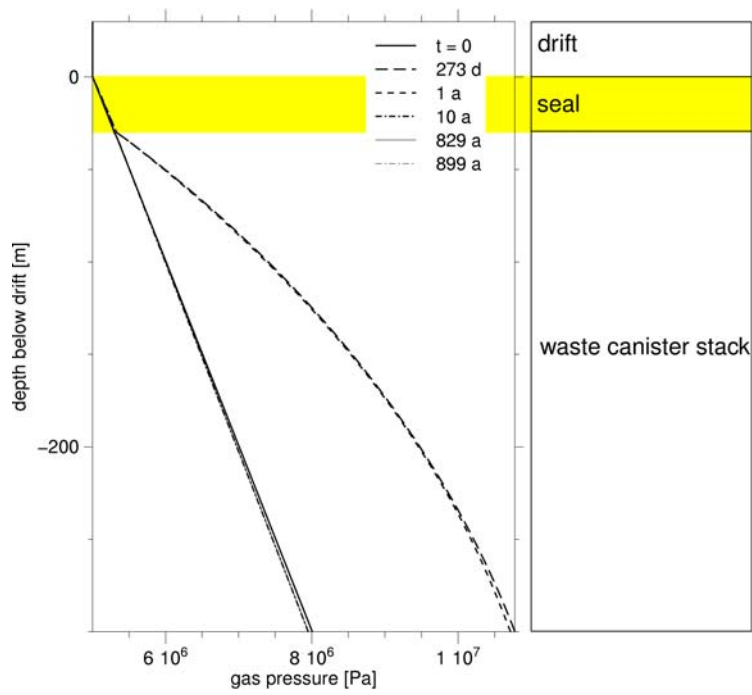


**Figure 5.12b** Time-dependent pressure distribution for scenario 2

Hydrogen reaches the drift after little more than one year. When this happens, the gas pressure begins to decrease again because the resistance to flow is much lower in the drift (higher permeability, porosity, and cross-section area values) than in the seal.

Flow reaches a state similar to a dynamic equilibrium after 10 years. Any gas produced after that time leaves the system without changing saturation or gas pressure in the backfilled borehole and in the seal. Only a little fraction of it is stored in the drift. When the hydrogen production stops after 830 years, brine returns replacing the gas again. It takes about 70 years to fill most of the system.

The brine pocket considered in the third scenario is assumed to be large enough to keep the brine pressure and the corresponding inflow rate constant. These conditions can be provided by a pocket volume of at least 200 m<sup>3</sup> since the free pore volume in the model amounts to little more than one cubic meter. In this case, a sharp saturation front simply moves upwards and leaves the system. The front moves so slowly that the gas pressure does not rise significantly.

Despite the physically simple results, the modelling is a demanding task for numerical reasons. Flow in the upward direction means that gravity opposes the capillary forces and thereby sharpens the saturation front. The big jump in the saturation, which is always difficult to handle for a numerical two-phase flow simulator, is therefore maintained during the whole simulation.

#### **5.3.2.4 Conclusions**

The analyses show that complex displacement processes of one phase by the other are to be expected in the boreholes. These processes are controlled by the principal mechanisms of the two-phase flow and cannot be captured by single-phase flow models.

Predictive two-phase flow calculations for repositories in rock salt are different from modelling conventional soil systems mainly due to the hydrologic parameters of the porous media involved. The crushed salt is typically rather tight and shows comparatively high capillary pressures and low permeabilities. The contrast of the material properties between different sections in the repository - like borehole seal and drift - can easily exceed the contrast between layers of natural soil formations.

Modelling of altered evolution scenarios implies therefore demanding conditions for the numerical simulator and the results are sensitive to almost all model parameters: the material parameters especially the equations of state, the model geometry, and the initial and boundary conditions for the considered scenarios.

Due to the strong non-linearity of the differential equations it is not possible to anticipate the reaction of a two-phase flow system to changes of the input parameters. This implies that it is very important to know the uncertainties of the quantities mentioned above as well as the data themselves. Actual predictions need therefore a profound understanding of the material laws of compacting crushed salt and an adequate description of the repository layout.

#### 5.4 Brine migration in the host rock

The migration of traces of brine contained in the rock salt towards heat sources like HLW canisters in disposal boreholes was especially measured and modelled in the Temperature Test 5 (Figure 5.13) at the Asse mine (Rothfuchs, 1986), see also section 4.2.3).

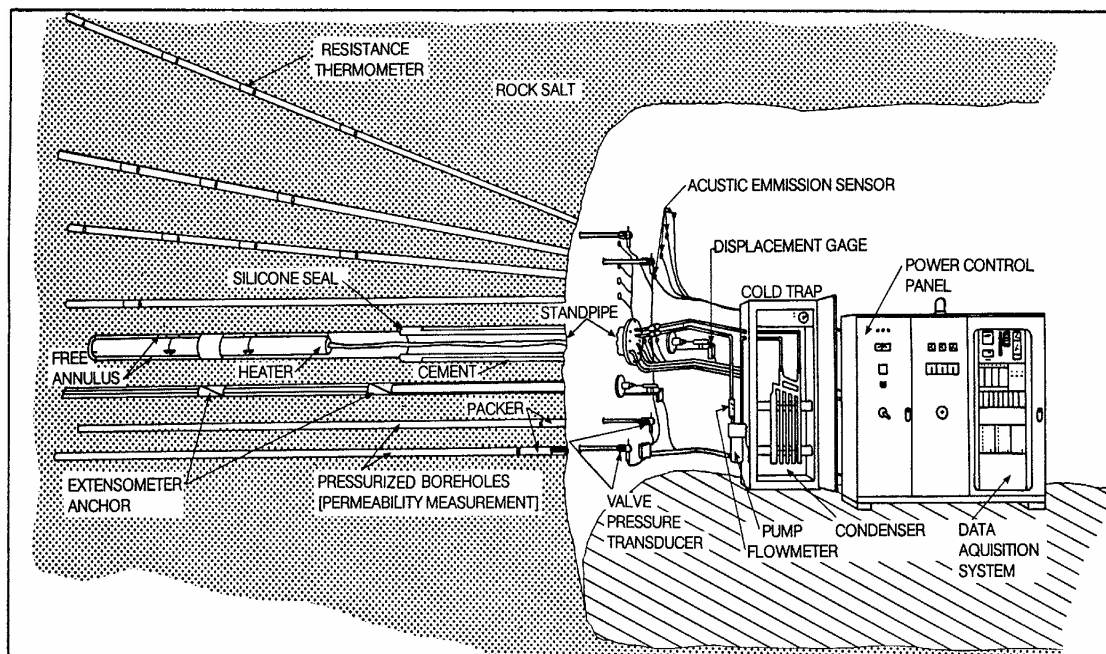


**Figure 5.13** Layout of Temperature Test 5

## 5.4.1 Models and data used for modelling

### 5.4.1.1 Conceptual model

The evaporation front model (Figure 5.14) used by GRS for predicting the amount of brine released into a HLW disposal borehole was published by Schlich (1986). In this model it is assumed that initially the complete intergranular pore space (IP) is filled with brine. In the borehole, the concentration and the pressure of water vapour is low in contrast to the area of the IP filled with brine. In the evaporation front model, brine starts to vaporise at the borehole wall. The released vapour is then transported in the direction of the borehole because of the high gradient of partial pressure. Accordingly, the transition zone between vapour and brine moves from the heated borehole into the rock salt.

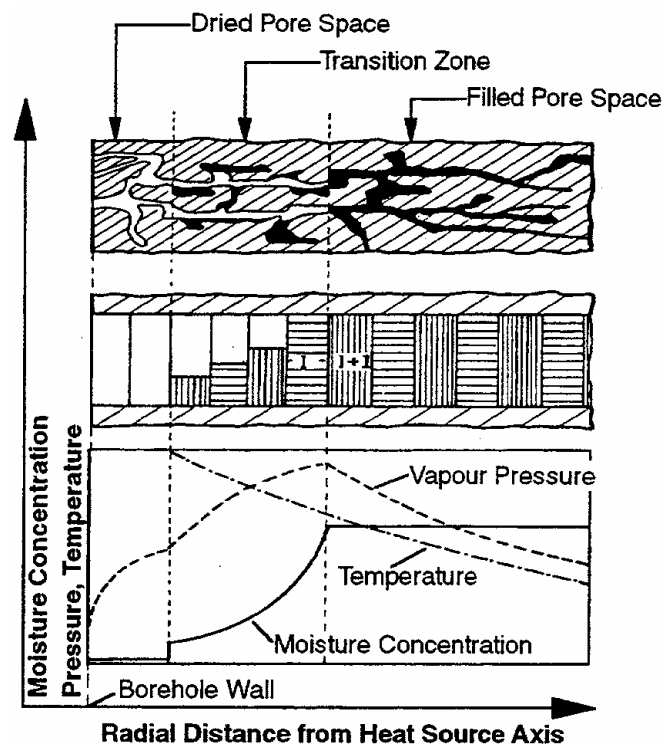


**Figure 5.14** Evaporation front model

In the Temperature Test 5, the situation of a HLW disposal borehole was simulated in a 7 m deep unlined horizontal borehole at the 775-m level. The heater was installed concentrically in the borehole between 4 and 7 m depth. The width of the annulus between the heater surface and the borehole wall was 4 cm. The water release to the

borehole was measured by continuous condensation of the water in a cold trap, thereby keeping the water vapour partial pressure in the borehole at a low level.

#### 5.4.2 Theoretical model

The equations describing the water vapour/brine migration in the solid rock salt are those presented in section 4.1.2.3, namely the equation giving the velocity of the evaporation front, the continuity equation and the equation of the state of gases.

For the vapour flow the laws of Darcy and Knudsen come into question. Whether the Darcy flow or the Knudsen diffusion prevails depends on the relationship of the radius of the salt pores to the average free path length of the water molecules. If the radius of the salt pores is smaller than the average free path length of the water molecules, Darcy flow becomes zero and the Knudsen diffusion becomes dominant.

Further details on the theory considered for modelling migration of water/brine in rock salt in the temperature field around HLW disposal boreholes can be taken from sections 4.1.2.3 and 4.3.3.

##### 5.4.2.1 Processes studied and data used

The only process studied in this modelling exercise was the vapour migration in the form of Darcy and Knudsen flow. The used data are given in Table 5.6.

**Table 5.6** Data used for modelling brine migration in the Temperature Test 5 at Asse (Schlich, 1986)

density of rock salt [ $\text{kg} \cdot \text{m}^{-3}$ ]	$\rho_s = 2163$
water content of rock salt [ $\text{kg} \cdot \text{m}^{-3}$ ]	$W_c = 0.865$
permeability of rock salt [ $\text{m}^2$ ]	$k = 6 \cdot 10^{-21}$
Knudsen factor [ $\text{m}^2 \cdot \text{s}^{-1} \cdot \text{K}^{0.5}$ ]	$C_k = 7.3 \cdot 10^{-12}$
porosity of rock salt [-]	$\phi = 0.000865$
special gas constant for water vapour [ $\text{J} \cdot \text{kg}^{-1} \cdot \text{K}^{-1}$ ]	$R_w = 461.7$

### **5.4.3 Modelling**

#### **5.4.3.1 Code used and features of analysis**

The finite difference 1D-code TRAVAL has been used for modelling the brine migration and water release in the Temperature Test 5. After specification of boundary and initial conditions, the continuity equation is solved to obtain the distribution of partial pressure in the IP. First, the mass flux density of the vapour phase at the borehole wall is calculated. In order to take 3D effects into account, the total flux into the borehole is calculated considering 2/3 of the borehole length only. As a result, the accumulated amount of vapour in the borehole as well as the pressure increase in the sealed borehole are derived.

The temperature distribution  $T(r)$  in TRAVAL is being approximated by a parabola which is determined by three separately calculated temperature values at the borehole wall, the location of the evaporation front and the middle between these both points, respectively.

#### **5.4.3.2 Comparison of predicted and measured results and conclusions**

In order to identify the adequate flow law calculations were performed with both types of migration models.

Figure 5.15 shows the measured data of accumulated water released into the heated borehole in comparison to the calculated data.

The parameter values for the permeability  $k$  and the Knudsen factor  $c_k$  were selected by parameter variation so that the calculated total amount of water in both cases meets the measured value of the total amount of water released into the borehole. That means that the dynamics of the release rate can be used to estimate the adequacy of the used model. From the shape of the curves it is concluded that the Knudsen diffusion model represents the measured data better than the Darcy flow model, but a significant difference between both results can not be seen. Hence, Darcy flow seems also to be adequate to model water migration processes in the solid rock salt (especially in case of higher permeability).

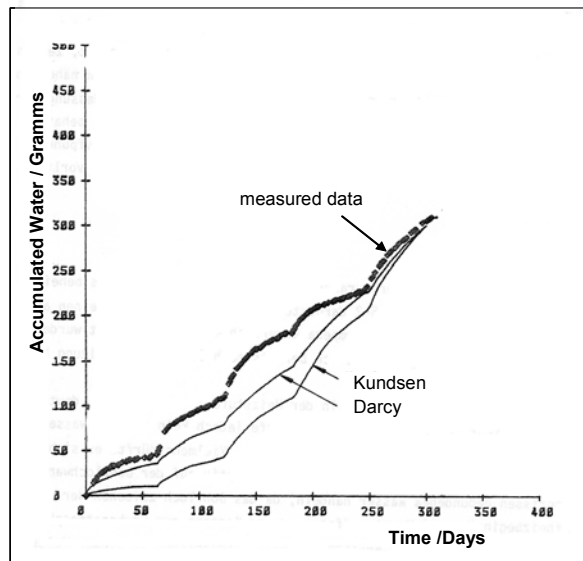


**Figure 5.15** Comparison of measured and predicted data of water release in the Temperature Test 5

### 5.5 Volume changes due to dissolution-precipitation reactions in a flooded repository in salt formations

For safety considerations of a repository for radioactive and chemical wastes in salt formations, the potential inflow of water and brines and the resulting chemical processes must be considered quantitatively. Three processes are important during the reactions of salt minerals with water:

1. Dissolution of minerals
2. Precipitation and transformation of minerals
3. Disintegration of the rock structure

In order to assess the impact of these processes on the effectiveness of EBS systems, the involved volume changes must be quantified, i.e., the volume of the dissolved salts, of the precipitated minerals, of the influenced rock mass, and of the initial and the resulting solution.

The volume changes depend upon the chemical composition of the inflowing brines as well as upon the mineralogical composition of the salt formations.

Water contact with the three most abundant salt formations, rock salt, carnallite and Hartsalz results in the formation of the brine compositions known as IP9, IP19 and IP21 solutions. For a constant temperature, i.e., 25 °C, these compositions are invariant solutions of the six component seawater system (Na-K-Ca-Mg-Cl-SO<sub>4</sub>).

Along the reaction path, minerals will be dissolved, new minerals will be formed which again can become unstable and disappear, other minerals precipitate until the final thermodynamical equilibrium is reached. The reaction path of the above-mentioned reactions with rock salt, and the potash seams Carnallite and Hartsalz have been modelled with the computer code EQ3/6 using the Harvie-Møller-Weare (1984) database. The mineral and volume changes are presented in Figure 5.16. The reliability of the modelling results has been demonstrated in laboratory experiments (Herbert, 2000) as well as in large-scale in-situ experiments (Herbert, 2000).

The long-term behaviour of a cemented coal fly ash in high saline brines was investigated by means of a time accelerating leaching experiment and by geochemical modelling of the observed reactions. The investigated material was a mixture of hard coal fly ash, Portland cement and saturated NaCl-solution. The leaching fluid was a high saline salt solution in equilibrium with the salt minerals halite, carnallite, sylvite, kainite and polyhalite (IP21 solution). This solution is likely to occur in salt and potash mines which are used in Germany as repositories for radioactive and hazardous chemical wastes. The leaching experiment was developed by GRS specifically for the boundary conditions of underground repositories in salt formations. The experiment was conducted in several steps towards the thermodynamic equilibrium between the leaching fluid and the involved solid phases. In each step, the resulting chemical composition of the leaching solution was determined as well as the dissolved and newly formed minerals. The experimentally observed reaction path was modelled using the code EQ3/6 and compared with results of a full-scale experiment in the Asse salt mine (see Table 5.7).

A good agreement between experimental data and the modelling results was obtained (Figures 5.17 and 5.18). The employed experimental and modelling tools have thus proved to be suitable for the assessment of the long-term stability of cementitious materials in repositories in salt formations.

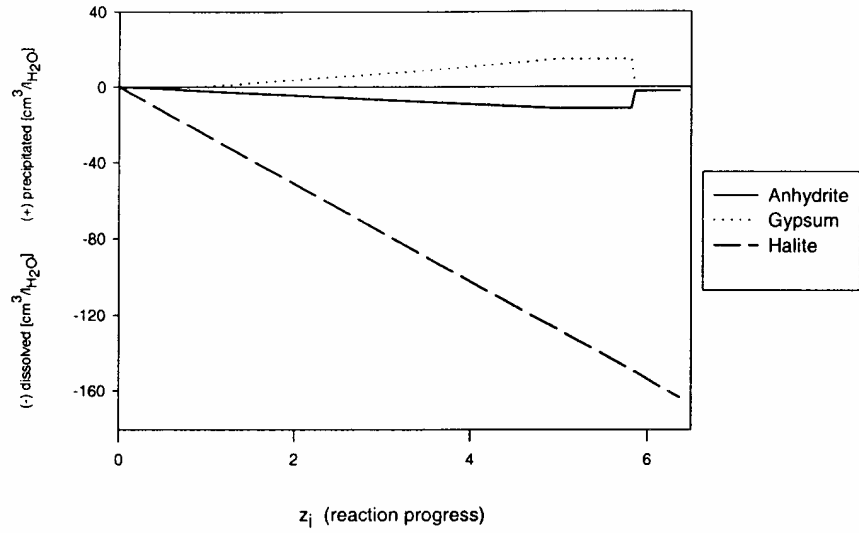


Figure 5.16a Dissolution of rock salt – volume changes

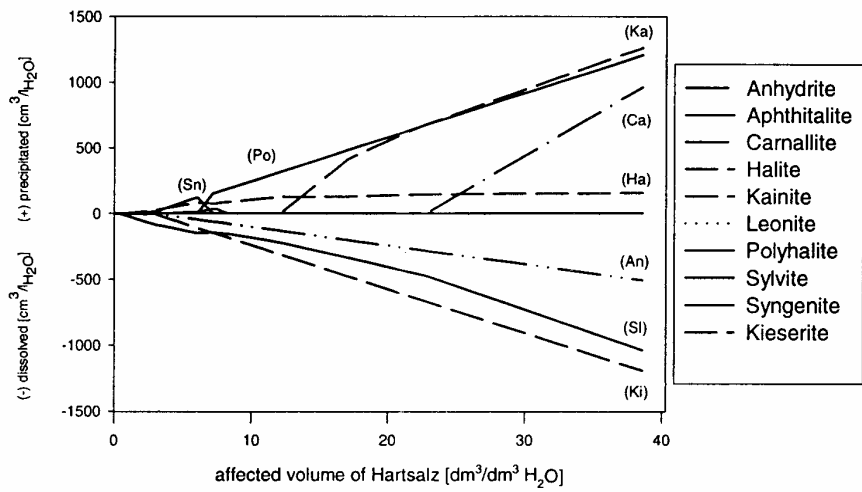


Figure 5.16b Dissolution of carnallite – volume changes

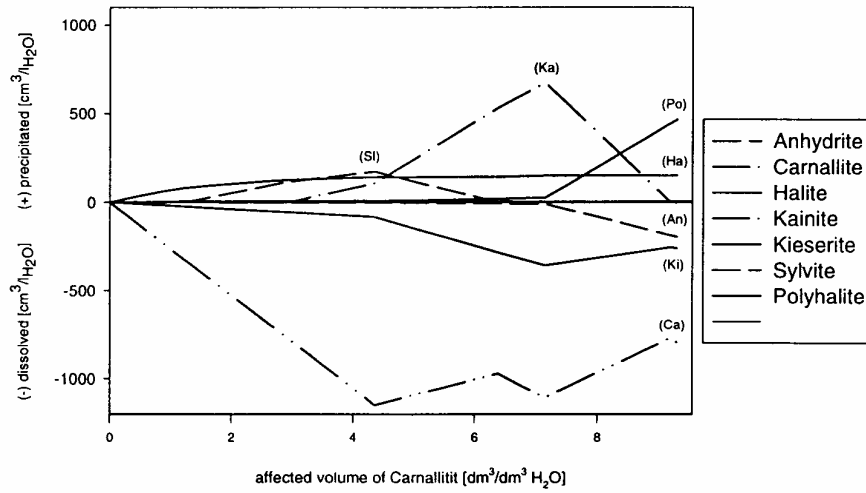


Figure 5.16c Dissolution of Hartsalz - volume changes

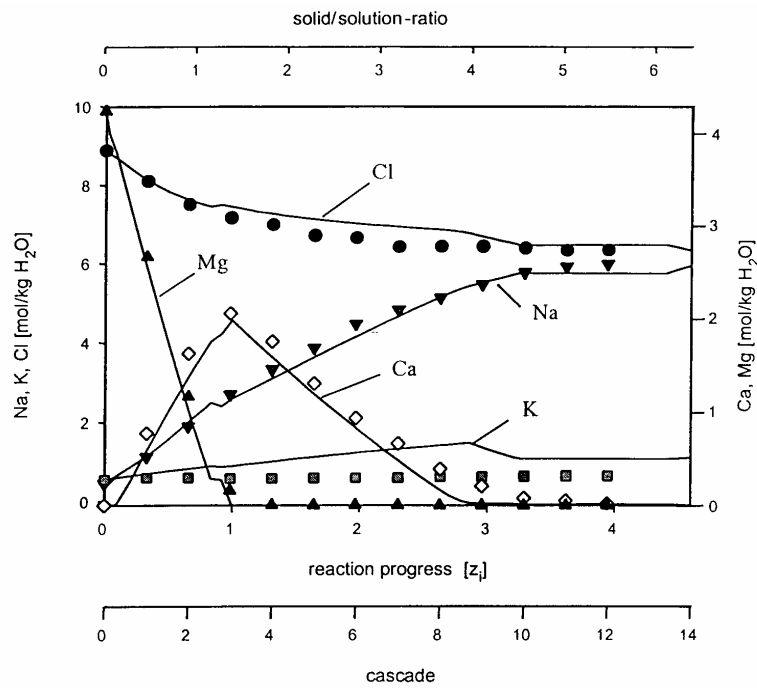
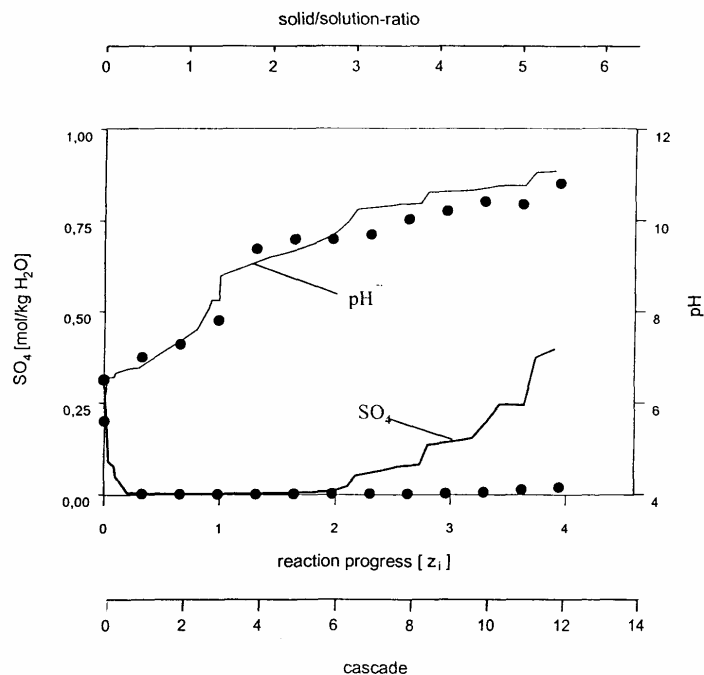


Figure 5.17 Experimentally observed and calculated evolution of the ( $\text{Na}^+$ ), ( $\text{K}^+$ ), ( $\text{Ca}^{2+}$ ), ( $\text{Mg}^{2+}$ ) and ( $\text{Cl}^-$ ) in solution during dissolution of cemented fly ash in IP21 brine



**Figure 5.18** Experimentally observed and calculated evolution of ( $\text{SO}_4^{2-}$ ) and pH in solution during SFA dissolution in IP21 brine

**Table 5.7** Comparison of the ( $\text{Ca}^{2+}$ ), ( $\text{Mg}^{2+}$ ) and ( $\text{SO}_4^{2-}$ ) and the pH in solution in the corrosion experiments in the Asse salt mine and the laboratory cascade experiment

Parameter/element	Asse mine experiment	Cascade experiment Solution composition of cascade 2.25
pH	7,2	7,3
	(mol/kg $\text{H}_2\text{O}$ )	(mol/kg $\text{H}_2\text{O}$ )
$\text{Ca}^{2+}$	1,45 – 260	1,74
$\text{Mg}^{2+}$	0,90	0,92
$\text{SO}_4^{2-}$	$10^{-4}$	$< 10^{-4}$

## 5.6 Discussion and conclusions

Due to heat accelerated room convergence HLW canisters disposed of in backfilled boreholes and drifts in a repository in salt rock will be completely encapsulated within a relatively short period of time. This was shown by in-situ experiments and by model calculations. According to Prij et al. (1995), the backfill porosity in a disposal borehole reduces to about 1 % within 10 years. Experimental evidence is given by the DEBORA-2 experiment where a porosity of 12 % was already reached after ten months. To

further reduce this porosity, an unrealistic experiment duration would have been required. Thus, calculations and models aimed to predict backfill compaction to low porosities of 1 % or less could not be validated by these experiments, but require special laboratory tests.

However, the short-term in-situ data are representative for the repository operation phase and thus useful for model validation. The confidence in long-term assessments of repository evolution is increased if a sufficient agreement between measured and calculated data can be demonstrated.

The comparison of measuring and modelling results indicates shortcomings in the existing material models used to predict the compaction behaviour of crushed salt backfill in a HLW repository. Most of the predictive calculations overestimated the creep deformation of rock salt and the compaction of crushed salt with a corresponding underestimation of stresses. Apparently, the upscaling of material parameters to in-situ conditions results in a softer material behaviour than in reality. Additionally, in test set-up like in the TSDE experiment 2D- instead of 3D-modelling is insufficient and causes considerable deviations between predictions and measuring results. Actual 3D-calculations as described in section 2 lead to much better results. In addition, further laboratory testing seems to be required to confirm the parameter values in the models especially for the upper and the very low porosity range.

Hydraulic modelling has so far only be performed with rather simple models or poorly validated material data. One reason to limit this effort was that the experiments conducted at Asse yielded brine release data which were considered acceptable with regard to repository safety issues. Regarding altered repository conditions, however, the importance of fluid flow in a backfilled repository is of high importance and require the determination of two-phase flow parameters for natural crushed rock salt. Also, the coupling of hydraulic and mechanical models is considered extremely important, but has not yet been realised for the salt option.

## **6 Lessons Learned and potential areas for improvements**

### **6.1 Disposal concepts**

The borehole and the drift disposal concepts developed in Germany for HLW disposal in deep geological salt formations (see section 2) were tested in several full-scale in-situ experiments in the Asse mine and also partly in surface demonstration facilities. Besides the development of the technical systems needed to emplace Cogéma canisters into deep disposal boreholes (Müller and Rothfuchs, 1995) and Pollux casks in disposal drifts (Engelmann, 1996) the investigation of the long-term compaction behaviour of crushed rock salt used as backfill in the disposal rooms was in the foreground of most experiments. No indications were found in the full-scale experiments that would call the considered concepts into question. Consequently, detailed plans of a HLW repository basing on the borehole and drift disposal concepts were developed and presented by DBE (1998).

However, possibilities to improve disposal concepts for heat generating waste were and are being discussed in Germany (GNB, 1998). One possibility would be to dispose of vitrified HLW canisters in Pollux casks, too, and to store these casks also in drifts (in the same way as it is foreseen for Spent Fuel assemblies). This concept has the advantage that the gamma dose rate at the outer cask surface would be reduced remarkably making any consideration of radiation damage in salt (Den Hartog et al., 1992) obsolete.

The possibility to dispose of Spent Fuel in 300-m-deep vertical boreholes was also addressed (DBE, 1998). This concept would be advantageous if the lateral extension of the salt formation is limited. Also the advantage of a soon and complete encapsulation of the waste canister can be regarded as considerably high and a reduction of emplacement costs is possible.

### **6.2 Design and construction of URLs**

A portion of the abandoned Asse salt mine has served as the only German repository-sciences URL for salt rock since 1967. The Asse salt mine was operated from 1908 until 1964 and about 130 excavations were left from the mining of rock salt in the southern flank of the salt anticline when the Gesellschaft für Strahlenforschung (GSF)

on behalf of the German government took over the mine in 1965. At the beginning of the underground research work, the experiments were conducted in the old existing excavations in the Leine Halite Na3 salt formation located in the southern flank of the Asse anticline between the 490-m and the 750-m levels (Figures 3.1).

Similar to any other underground opening, with time, the surrounding „undisturbed” stress field and hydrologic regime become disturbed and the data obtained in the „disturbed” rock may not be representative of ambient conditions with regard to THM processes. Hence, to minimise the impact of the old mine workings, all experimental locations/areas in the Asse mine/URL were selected as far as possible based on the transferability of the results to other potential salt rock repository sites with particular attention to the conditions and requirements expected at the Gorleben site.

Thus, from the late seventies onwards, most of the experiments were conducted at a representative depth of between 750 m and 900 m below the ground surface in the centre of the salt anticline where, similar to the conditions at the Gorleben site, the formation of the Staßfurth Halite Na2 exists.

This and the

- detailed characterisation of the CHMT properties of the host rock in and around the test locations/areas, including the determination of initial and boundary conditions, allowed the adequate verification of surface-laboratory-based material and advanced computer models by the comparison of predicted and measured data.

However, on-site confirmation of the Asse results would be useful in an undisturbed salt rock formation, preferably at the candidate Gorleben site.

Furthermore, the experiments at Asse were designed, as far as possible, at full-scale to avoid scale effects and to test handling and disposal systems for HLW in a representative way.

Hence, testing of the following technical components was successfully accomplished:

- Components used to operate a repository, e.g., systems for handling waste containers (Figure 6.1), borehole drilling equipment, and dust protection and ventilation equipment; and



**Figure 6.1** Testing of a HLW disposal system/concept in the Asse mine/URL.

- Appropriate techniques for the construction of shafts, tunnels, and other openings.

Areas with judged significant potential for improvement are summarised in section 6.5.

### **6.3 Instruments and experimental procedures**

Full-scale in-situ experiments are indispensable to the understanding of the complex processes that will occur in a final repository and for providing valuable experience for repository design, construction, and operation. During the experiments, most data need to be obtained remotely because inspection and maintenance are impossible during the test period. Furthermore, instrument accuracy and reliability cannot be checked after installation. Therefore, calibration of the instruments before and after testing is an indispensable requirement with regard to QA. However, in most in-situ experiments, the instrumentation is installed in a non-retrievable manner. In such cases, post-test uncovering of parts of the test area and representative retrieving of the used measuring equipment is necessary to enable performance studies regarding sensor drift, measurement errors, and failure reasons.

Based on the experience gained in connection with the in-situ experiments conducted in the Asse mine/URL, it can generally be stated that the chosen measuring equipment performed well throughout the duration of the tests. Only a limited number of gauge

failed during the tests, proving that the gauge design of the different instruments was successful. Actually, the most frequent failures occurred in the measuring systems and most of these failures were due to damage at the measuring lines. Especially, multicore cables were affected by squeezing due to convergence of cable slots and boreholes or by electrolyte intrusion into the multicores, which lead to the following conclusions/recommendations:

- A multicore cable design should not be used for in-situ measurements in heated areas. A single cable design is more appropriate/robust.
- Measuring-line protection and cable-duct design are very important features.

#### **6.4 EBS testing and process understanding**

Full-scale in-situ testing of EBS systems and confirmation of models of important processes are needed to enable reasonable long-term safety analyses. Various functions of crushed salt backfill and various processes were investigated in the Asse experiments in the past thirty years.

##### **6.4.1 EBS testing**

As outlined above, investigation of the long-term behaviour of crushed salt backfill is of high interest for the actual disposal concepts.

The backfill is needed

- to stabilize the salt formation by generating a counter pressure in the backfill in consequence of its compaction due to room convergence, the latter being accelerated especially at higher temperature.

The coupled behaviour of backfill compaction and drift convergence was investigated in the BAMBUS project in the Asse mine. Although the results show reasonable agreement between predictions and measurements it was concluded that modelling improvements may be achievable by both ongoing material parameter value determination and application of 3D-models. Also the modelling of the thermal behaviour of backfill and rock shows some shortcomings which are to be overcome by further research on the material models.

- to distribute the waste canister weight into the surrounding host rock in case of the borehole disposal concept because of the limited mechanical strength of the waste canisters (high stacking loads in 300-m-deep boreholes!).

Feuser et al. (2000) showed that this weight distribution is always existing (several cases were studied and experimentally tested) and that the maximum stacking load in 300-m-deep backfilled boreholes is always 2.5 orders of magnitude below the stacking load without backfill and thus far below the maximum allowable one.

- to seal the borehole against brine intrusion and the biosphere against radionuclides possibly released from corroded and leached waste packages.

The compaction behaviour in consequence of disposal room convergence was investigated in detail in many laboratory investigations (see Bechthold et al., 1999, Stührenberg and Zhang 1995) and also in the full-scale experiments at the Asse mine (see section 3.2.3). The agreement between predictions and measurements was found reasonable and thus confirmed results of earlier analyses (Prij et al. 1995).

The laboratory investigations of several investigators yielded a high number of data on the porosity/permeability relation that is used in safety analyses (Müller-Lyda et al. 1999). The laboratory data were confirmed excellently by in-situ data generated and measured in the full-scale field tests at Asse (Rothfuchs et al. 1999).

- to enable high specific heat generation in the disposal fields by accelerating heat dissipation from the waste into the host rock in consequence of increasing thermal conductivity of the compacting backfill.

The increase of the thermal conductivity of crushed salt backfill was investigated in the BAMBUS project (Ghoreychi, 1999). The relation between thermal conductivity and backfill porosity  $\phi$  shows an increase of the thermal conductivity from 1 W/m·K to 5.1 W/m·K in the range of  $\phi = 30$  to 0 %.

#### **6.4.2 Process understanding**

The short-term in-situ data obtained from the German URL research are only representative for the repository operation phase and, thus, of limited use for long-term

model validation. The confidence in long-term assessments of repository evolution, however, is increased if a sufficient agreement between measured and calculated data can be demonstrated in URL experiments. Following is a summary of the main code- and model-related lessons learned at the Asse mine/URL involving important processes such as backfill compaction, heat conduction, and fluid flow in a HLW repository in domal salt:

- Drift convergence and backfill compaction

The results of advanced 3-D models show reasonable agreement between predictions and measurements of host rock and backfill behaviour. Most of the predictive calculations, however, overestimate the creep deformation of rock salt and the compaction of crushed salt with a corresponding underestimation of stresses. Apparently, the upscaling of material parameters to in-situ conditions results in a softer material behaviour than in reality. To overcome these shortcomings in the existing material models some further research in this area is recommended.

- Heat conduction in salt rock, crushed salt rock, canisters, and other materials in a repository in salt rock

Several temperature experiments were conducted during the past 30 years at the Asse mine. In most of them, the development of the temperature fields was predicted with sufficient accuracy in time and space. In recent years, 3-D modelling yielded a further increase in prediction accuracy so that the current modelling capabilities can be considered sufficient. Special computer programmes were developed for modelling the temperature evolution in a HLW repository under consideration of very complex geological conditions in salt formations (Stührenberg, D., e.g., 1999). Thus, there is no need for significant improvements in this field of research.

- Fluid flow (Darcy and Knudsen) in porous backfill and low porous rock salt

The release of volatile components such as water vapour and other gases from the host rock was studied in some of the in-situ experiments conducted in the Asse mine/URL. The major finding is that the application of the Darcy flow model seems to be adequate in most considered cases, including flow in both crushed and intact salt rocks. Some experiments, however, showed better agreement between predictions and measurements if the Knudsen diffusion model was applied, but only with minor improvement of the results. Thus, Darcy flow seems to be adequate for most

applications. Hence, the development or consideration of further flow models is not deemed necessary.

Areas with judged significant potential for improvement are summarised in the following section 6.5.

#### **6.4.3 Future research needs**

Further to the areas described, discussed, and listed above, following are topical areas deemed to embody significant potential for improvement based on the lessons learned in connection with the R&D programme performed in the Asse mine/URL during the past 35 years:

- Compaction behaviour of crushed salt backfill in case of brine intrusion

In the safety analyses, an intrusion of limited amounts of brine into backfilled disposal boreholes and drifts is being considered possible. Laboratory investigations have shown that adding of 1wt.% of brine leads to a reduction of the compaction resistance by one order of magnitude (DBE, 2001). Further investigations have been conducted in this area but the results have been not yet published. The data published by BGR have been used by the DBE to analyse compaction of moist backfill in large disposal rooms. In (DBE, 2001) it is stated that the BGR data are the only ones available, so far. Further investigation is, therefore, considered necessary to confirm the BGR data and could be accomplished by using Asse reference backfill material.

- EDZ generation and healing

Detailed research on EDZ evolution in salt formations started about a decade ago in order to enable the assessment of its importance for the long-term safety analysis of radioactive waste repositories. Constitutive models to predict damage, dilatancy and permeability distribution around excavated drifts have been developed recently. The results of the first numerical simulations of underground experiments/analogues are very promising. However, the extent and degree of healing of the EDZ around the backfilled and over nine years heated TSDE experiment at Asse were significantly underestimated in model calculations. To enable satisfactory simulation of the long-term reduction/healing of the EDZ, adequate model improvement is considered indispensable.

- Hydraulic modelling

Hydraulic modelling has so far only been performed with rather simple models or poorly validated material/parameter data. One reason limiting this effort was that the experiments conducted in the Asse mine/URL yielded brine-release data that were considered acceptable with regard to the repository safety issues then at hand. However, if very unlikely altered repository conditions were to be considered, fluid flow in a backfilled repository would be of high, possibly critical, importance and would require the determination of two-phase flow parameters for both the EDZ and the crushed salt rock backfill. First modelling results for altered evolution scenarios show a very complicated flow behaviour, even if only the basic two-phase flow effects are considered. Additional effects like a non-isothermal temperature distribution or a time-dependent porosity are therefore to be included for more realistic predictions. This leaves a vast open field for the investigation of material behaviour as well as for code-developing even if it is not clear if a fully coupled THM approach is necessary.

The issue of fracturing of the host rock in case of gas generation in disposal rooms has not yet been addressed in the German research programme to a satisfactory degree. Respective R&D-work is thus recommended since high gas pressure may evolve due to corrosion and microbial degradation of waste forms if the disposal rooms are sealed gas tight. The corresponding improvement of existing coupled H and M models is considered very important, too.

## 7 Summary and conclusions

Sections 2 through 5 of this report correspond to the country annexes on the salt option provided by GRS and DBE during the past three years to the CROP project. The report summarizes experiences gained during about 20 years of successful design, construction, and operation of the Asse mine/URL. The Asse mine/URL is situated in a Permian salt anticline (dome) with complicated internal structure due to the salt movements and deformations caused by the increasing overburden during Mesozoic and Cenozoic times and the regional stress regime. The experiences and lessons learned at Asse include the design, development, and operation of:

- A test repository for LLW and ILW between 1967 and 1978.
- A URL, primarily located 750 m to 800-m below the ground surface.

The major part of the research programme conducted in the Asse mine/URL focused on the disposal of HLW and related issues.

The following two main different disposal concepts have been considered in Germany:

- Disposal of Cogéma-type stainless steel canisters containing vitrified fission products remaining from reprocessing of SNF in deep vertical boreholes and
- Disposal of SNF in heavy self-shielding Pollux casks in horizontal repository drifts.

In both concepts, the geological barrier is considered the main barrier against radionuclide releases to the biosphere but, in addition to that, backfill and EBSs are required to ensure repository stabilization and sealing of repository areas against any potential brine inflow from undetected brine reservoirs in the early post-closure phase. To meet these EBS objectives, crushed salt is used in both concepts to fill the voids in the disposal boreholes and the drifts. With time, stress and creep-induced room closure (convergence) lead to consolidation of the crushed-salt backfill and, ultimately, the complete encapsulation of waste containers, thereby sealing the repository and permanently isolating the emplaced waste from the biosphere. No other near-field buffer material than crushed salt is considered necessary in the aforementioned two domal salt repository concepts. However, a special, multi-component seal will be installed in the access drifts to seal off repository areas after the completion of waste emplacement. Finally, upon completion of the disposal operations, a seal system will

be installed in the shaft to safeguard the repository on the long-term against any inflow from water bearing strata overlying the repository formation.

Summarised below in random order of importance are the major observations and conclusions provided by the GRS and DBE in support of CROP.

- In the initial phase of the Asse research programme, the in-situ investigations focused on host rock characterisation in terms of T and M properties. Later on, the main emphasis was on the assessment of the short and long-term evolution of the host rock sealing capability or H properties, respectively, in interaction with the backfill material under the impact of the HLW-induced heat load. During the last decade, the development of coupled THM models has been a major focus area. Good progress has been achieved so far in modelling the excavation induced effects, e.g., EDZ generation and accelerated backfill compaction after heat source emplacement, whereas, adequate prediction of EDZ healing needs further R&D.
- The THM behaviour of crushed salt backfill is largely understood. Adding of geochemical additives to increase sorption of special radionuclides in the near-field is under discussion and has not yet been tested adequately.
- In section 2 information is presented on drift seals (plugs) between the shaft area and the disposal fields that will be installed after the repository-operations period. However, the possible drift seal design presented by Stockmann et al., (1994) was never tested in situ under representative conditions and is still pending.
- The host rock integrity in case of high gas pressures in disposal rooms has not yet been addressed in the German research programme to a satisfactory degree. Respective R&D-work is thus recommended in combination with the necessary improvement of existing coupled H and M models.
- Between 1984 and 1993, preparations were undertaken to conduct a full-scale experiment simulating the disposal of HLW in boreholes at the Asse mine (Rothfuchs et al., 1995). This experiment would have involved the retrievable emplacement of 30 highly-radioactive radiation sources in six 15-m-deep disposal boreholes on the 800-m level of the Asse mine. During the preparation phase, a complete transport and emplacement system was developed, successfully tested, and technically approved by the responsible mining authority. In 1993, the project was prematurely terminated because direct disposal of SNF became an alternative disposal option in Germany. Thus, the emplacement system was never tested with

highly radioactive material. Hence, final confirmation of the technical emplacement system for Cogéma canisters, as well as the testing of the feasibility of the emplacement of alternative canisters for SNF into 300-m-deep boreholes, is still pending.

As explained in section 2 in the year 2000, a national expert group (named AkEnd) was asked by the German government to develop new, formation-independent, site-selection criteria for the identification of repository sites with favourable geological settings. The final report of this group was published in December 2002 (AkEnd, 2002). According to this report, the geological formation the repository is built in must meet the following requirements:

- The thickness of the host rock must be at least 100 m;
- The disposal level shall not be closer than 300 m to and not deeper than 1500 m below the ground surface;
- The potential disposal area at the disposal level must be at least 3 km<sup>2</sup>
- The hydraulic conductivity of the host rock must be smaller than 1E-10 m/s; and
- The aforementioned properties must be assured for 1 million years.

In the light of these requirements, it is necessary to reconsider the conclusions drawn from the research work done to date. For instance, the importance of slow migration processes, such as diffusion of carrier fluids like brines and gases in the whole repository system, including the EBSs, the EDZ in the early as well as in the late (healed) repository stages, in the undisturbed host rock, and in the overburden rock strata, increases significantly.

Since 1995, the Asse mine, which contains 130,000 200-l drums with LLW and about 1,300 200-l drums with ILW, is being backfilled at the request of the government of Federal State of Lower Saxony. Backfilling of most of the underground openings will be completed within the next five years. The research in the Asse mine/URL has thus been significantly reduced during the past nine years and will come to an end in the very near future. Because of the current moratorium of the salt option in Germany, an alternative German URL will not be available in the next years. Hence, URL research addressing the aforementioned open issues will shortly only be possible on a case to case basis in Germany.

## **Acknowledgements**

The work described in this report was funded by the European Commission under contract No. FIRI-CT-2000-20023. The authors would like to thank for this support. Special thanks also to all project partners for their continuous support and the fruitful discussions in the many project meetings.

## References

- AkEnd, 2002: Auswahlverfahren für Endlagerstandorte - Empfehlungen des AkEnd - Arbeitskreis Auswahlverfahren Endlagerstandorte, W&S Druck GmbH, Köln
- Bastian, P., K. Birkens, S. Lang, K. Johannsen, N. Neuss, H. Rentz-Reichert, 1996: Ug - a flexible software toolbox for solving partial differential equations. Technical report, Computing and Visualization in Science, 1, Springer Verlag
- Bechthold, W., Closs, K. D., Knapp, U., Papp, R., 1993: System analysis for a dual-purpose repository, Nuclear Science and Technology, European Commission, EUR 14595 EN
- Bechthold, W., Rothfuchs, T., Poley, A., Ghoreychi, M., Heusermann, S., Gens, A., Olivella, S., 1999: „Backfilling and Sealing of Underground Repositories for Radioactive Waste in Salt (BAMBUS Project)”, Final Report, European Commission, EUR19124 EN
- Berner, U., 1990: PSI report No. 62
- BfS, 1990: „Fortschreibung des zusammenfassenden Zwischenberichtes über bisherige Ergebnisse der Standortuntersuchungen Gorleben vom Mai 1983“, Bundesamt für Strahlenschutz, Bericht ET-2/90, Salzgitter
- BMI, 1983: Sicherheitskriterien für die Endlagerung radioaktiver Abfälle in einem Bergwerk, Bundesgesetzblatt 35, 45 - 46
- Breidenich, G., 1994: Gekoppelte Berechnung der thermo-mechanischen Feldgrößen in einer Steinsalzformation infolge der Einlagerung radioaktiver wärmefreisetzender Abfälle, These, Aachener Beiträge zur Energieversorgung Band 16

- Breidung, K.-P., 2001: Schachtverschlüsse für untertägige Deponien in Salzbergwerken, Fünftes Statusgespräch Untertägige Entsorgung, Forschungszentrum Karlsruhe - Projektträger des BMWi und BMBF für Entsorgung, Wissenschaftliche Berichte FZKA-PTE Nr. 7.
- Brinkmann, R., 1977: Abriß der Geologie, Bd. II: Historische Geologie.- 400 S., Stuttgart (Enke).
- Brown, E.T. (Ed.), 1981: „Rock Characterization - Testing and Monitoring - ISRM Suggested Methods”, International Society for Rock Mechanics, Pergamon Press
- Brüggemann, R., Hossain, S., Kasachanian, B., Kühle, Th., Nies, A., Ohme, G., Pattloch, F., Podtschaske, R., Rimkus, D., Stelte, N. Storck, R., 1985: Modellansätze und Ergebnisse zur Radionuklidfreisetzung aus einem Modellsalzstock. PSE-Abschlußbericht, Fachband 16, Berlin.
- Cinar, Y., Müller, W., Pusch, G., Reitenbach, V., (1998): „Gas Migration in Salt, Part II: Experimental Work”. In European Commission Report: Projects on the Effect of Gas in Underground Storage Facilities for Radioactive Waste (Pegasus Project), Proceedings of a progress meeting in Naantali, Finland, DOC XII/276/98-EN.
- DBE 1998: Aktualisierung des Konzepts „Endlager Gorleben”, Deutsche Gesellschaft zum Bau und Betrieb von Endlagern für Abfallstoffe (DBE), Peine, unpublished
- DBE, 2001: Numerische Untersuchungen zum Konvergenzverhalten eines Einzelhohlraums, Deutsche Gesellschaft zum Bau und Betrieb von Endlagern für Abfallstoffe (DBE), Peine, unpublished
- Den Hartog, H.W., Seinen, J., Datema, H., Jacobs, J., Pol, H., 1992: Radiation Damage in NaCl, Effects of High Irradiation Doses, State University of Groningen, Report SEO 93-07

- Droste, J., Feddersen, H.-K., Rothfuchs, T., 2001: Experimental Investigations on the Backfill Behaviour in Disposal Drifts in Rock Salt (VVS-Project), Final Report, GRS-173
- Droste, J., Feddersen, H.-K., Rothfuchs, T., Zimmer, U., 1996: „The TSS-Project: Thermal Simulation of Drift Emplacement, Final Report Phase 2”, Gesellschaft für Anlagen- und Reaktorsicherheit (GRS) mbH, GRS-127
- Engelmann, H. J., 1996: Endlagerkonzepte und Einlagerungstechniken für abgebrannte Brennelemente, Proceedings: Abschlussveranstaltung Direkte Endlagerung, Forschungszentrum Karlsruhe - Technik und Umwelt, Wissenschaftliche Berichte, FZKA-PTE Nr.2
- Engelhardt, W., 1960: Der Porenraum der Sedimente, Springer Verlag
- EUR 11778, 1988: PAGIS-Performance Assessment of Geological Isolation Systems for Radioactive Waste, Disposal in Salt Formations, Commission of the European Communities, Nuclear Science and Technology
- EUR 8179, 1982: Zulässige thermische Belastung in geologischen Formationen - Konsequenzen für die Methoden der Endlagerung radioaktiver Abfälle, Band 3, Kommission der Europäischen Gemeinschaften, Kernforschung und Technologie, Bericht EUR 8179 DE
- Feddersen, H.-K., 1983: Section 4.3.1 „Absolutspannungsmessungen” in: „Simulationsversuch im Älteren Steinsalz Na2ß im Salzbergwerk Asse - Temperaturversuchsfeld 4 (TVF4)”, Gesellschaft für Strahlen- und Umweltforschung mbH München,
- Feddersen, H.-K., 1999: Section 3.3.1.3.1 and 3.4.1.8 in: „Backfilling and Sealing of Underground Repositories for Radioactive Waste in Salt (BAMBUS Project)”, Final Report, European Commission, EUR19124 EN
- Feuser, W., Vijgen, H., Barnert, E., 2000: Validierung der Modelle zur Lastabtragung durch Einbettung in Salzgrus - LEISA, Abschlussbericht für die Projektphase 1997 - 1999, Forschungszentrum Jülich GmbH, Institut für Sicherheitsforschung und Reaktortechnik

- Fischle, W.R., Schwieger, K., Olfers, M., 1988: „Spannungsermittlung im Salz mit der Methode der hydraulischen Aufreißversuche“, GSF 12/88, Gesellschaft für Strahlen- und Umweltforschung mbH München
- FZK-PtWT+E, 1998: Schwerpunkte zukünftiger FuE-Arbeiten bei der Endlagerung radioaktiver Abfälle (2202 - 2006), Förderkonzept des Bundesministeriums für Wirtschaft und Technologie, Forschungszentrum Karlsruhe - Projekt-trägerschaft Entsorgung
- Gies, H., Jockwer, N., Mönig, J., 1989: Geochemistry of the HAW Test Field and Occurrence of Primary and Secondary Gases, Proc. Waste Management '89. Tucson , USA
- Glasser, F.P., Paul, M., Dickinson, C.L., Reed, D., 2001 : Report EUR 19780 EN
- GNB 1998: Status of the development of final disposal casks and prospectives in Germany, DisTec-Conference 1998, Hamburg
- GNS, 1991: Gesellschaft für Nuklear-Service (GNS): Datenblatt GNS- TES/WK/91017/01, Rev. 0, 10.1.91.
- Ghoreychi, M., 1999: Thermal Properties of Crushed Salt in: Backfilling and Sealing of Underground Repositories for Radioactive Waste in Salt (BAMBUS Project), Final Report, European Commission, EUR19124 EN
- GSF, 1990: Endlagersicherheit in der Nachbetriebsphase - Rahmenplan für notwendige FE-Arbeiten, Stand Oktober 1989, Gesellschaft für Strahlen- und Umweltforschung - Institut für Tieflagerung, GSF-Bericht 6/90
- GSF, 1997: Forschungsbergwerk Asse - Salz wird in ein Bergwerk geblasen, Auszug aus dem GSF-Jahresbericht 1996, GSF-Forschungszentrum für Umwelt und Gesundheit, München
- GSF-ECN, 1992: The DEBORA-Project, Progress Report July - December 1991, Joint Report of GSF-Institut für Tieflagerung and Energy Research Foundation Netherlands - ECN, Abteilungsbericht IFT 2/92

- H.- J. Herbert and H. C. Moog, 2000: Experimental Results and Modeling of the Swelling of Compacted Bentonites Under Different Saline Conditions - ICEM 2000, Bruegge, Belgium, Session 18, Radioactive Waste Management and Environmental Research, 8p.
- H.-J. Herbert and Th. Meyer, 2001: Corrosion of cementitious materials under geological disposal conditions with resulting effects on the geochemical stability of clay minerals - Proceedings of the EUROSAFE conference, 5-6 November 2001, Paris, Seminar 3, 39 - 54.
- Hartje, B., Engelmann, H.-J., Schrimpf, C., 1989: „Repository Design for the Systems Analysis Dual-Purpose Repository”, Proc. Waste Management '89, Tucson, USA
- Harvie, C. E., Møller, N. and Weare, J. H. 1984: The prediction of mineral solubilities in natural waters: the Na-K-MGCa-H-Cl-SO<sub>4</sub>-OH-HCO<sub>3</sub>-CO<sub>3</sub>-CO<sub>2</sub>-H<sub>2</sub>O system to high ionic strengths at 25 °C. - Geochim. et Cosmochim. Acta, 48, 723 - 751
- Hein, H. J., 1991: „Ein Stoffgesetz zur Beschreibung des thermomechanischen Verhaltens von Salzgranulat”, doctoral thesis RWTH Aachen
- Helmig, R., C. Braun, M. Emmert, 1994: MUFTE - A numerical model for simulation of multiphase flow processes in porous and fractured-porous media. Programmdokumentation (HG 208), technical report 94/3, Institut für Wasserbau, Universität Stuttgart
- Helmig, R., Bastian, P., Class, H., Ewing, J., Hinkelmann, R., Huber, R., Jakobs, H., Sheta, H., 1998: Architecture of the modular program system MUFTE\_UG for simulating multiphase flow and transport processes in heterogeneous porous media. Mathematische Geologie, 2, Dresden
- Hente, B., 1992: „Seismicity”, in: „The HAW Project: Demonstration Facility for the Disposal of High-Level Waste in Salt - Synthesis Report 1988-89”, GSF-Bericht 14/90, Gesellschaft für Strahlen- und Umweltforschung mbH, München

- Herbert, H.J., 2000: „Zur Geochemie und geochemischen Modellierung hochsalinärer Lösungen mineralischer Rohstoffe“, Geologisches Jahrbuch, Sonderheft, Reihe D, Mineralogie, Petrographie, Geochemie, Lagerstättenkunde, Heft SD 1, Hannover
- Heusermann, S., 1987: „Evaluation of Stress Measurements in the Asse Salt Mine“, in: Working Papers from the US/FRG Workshop on Geotechnical Instrumentation and Measurement Techniques, Asse Salt Mine near Braunschweig, FRG, May 4-8, 1987“, Gesellschaft für Strahlen- und Umweltforschung mbH, München
- Heusermann, S., 1995: Analysis of Initial Rock Stress Measurements in salt. Proc. 5<sup>th</sup> Int. Symp. on Numerical Models in Geomechanics, 669 - 674, Balkema, Rotterdam
- Hirse Korn, R.-P., Nies, A., Rausch, H., Storck, R., 1991: Performance Assessment of Confinements for Medium-Level and Alpha-Contaminated Waste - PACOMA Project, Rock Salt Option, GSF-Report 12/91, TL 7/91
- Hunsche, U. and Hampel, A., 1999: „Rock salt - the mechanical properties of the host rock material for a radioactive waste repository“, Engineering Geology, 52, 271-291
- Hunsche, U. and Schulze, O., 1996: Effect of humidity and confining pressure on creep of rock salt. The Mechanical Behavior of Salt. Proc. 3rd Conf., Eds. M. Ghoreychi, P. Berest, H.R. Hardy, Jr., and M. Langer. Trans Tech Publ. Clausthal-Zellerfeld, 237-248
- Hunsche, U., 1993: Failure Behaviour of Rock Salt Around Underground Cavities. Proc. 7th Symp. On Salt, Kyoto. Eds. H. Kakihana, H.R. Hardy Jr., T. Hoshi and T. Toyokura. Elsevier, Amsterdam, Vol. 1, 59-65.
- IAEA, 1987: In situ experiments for disposal of radioactive waste in deep geological formations, Report prepared by a group of consultants organized by the International Atomic Energy Agency, IAEA-TECDOC-446, Vienna, 1987

- IAEA, 1991: Earthquakes and associated topics in relation to nuclear power plant siting. A safety guide, Safety series No. 50-SG-S1 (Rev. 1), International Atomic Energy Agency, Vienna
- IFC, International Formulation Committee, 1967: A Formulation of Thermodynamic Properties of Ordinary Water Substance. IFC secretariat, Düsseldorf, Germany
- Itasca Consulting Group, 2000: FLAC User's Guide, Minneapolis, Minnesota, USA
- Jockwer, N., 1980: Die thermische Kristallwasserfreisetzung des Carnallits in Abhängigkeit von der absoluten Luftfeuchtigkeit, Kali und Steinsalz 8, S. 55/58
- Jockwer, N., 1981: Laboratory investigation of water content within rock salt and its behaviour in a temperature field of disposed high-level waste, Proc.: Scientific basis for nuclear waste management, Vol. 3, Plenum publishing corporation
- Jockwer, N., Rothfuchs, T., 1995: „Investigations and modelling of fluid release from rock salt at elevated temperature“, Proc. Workshop Testing and Modelling of Thermal, Mechanical and Hydrogeological Properties of Host Rocks for Deep Geological Disposal of Radioactive Waste, EUR 16219 EN, CEC, Brussels
- Kamlot, P. et al., 1999: Untersuchungen der Barrierewirksamkeit des Gesteinsverbandes Steinsalz/Anhydrit/Salzton (Bariton), Abschlussbericht zum BMBF-Vorhaben FB 02E8755
- Kamlot, P., Flach, D., 2001: Untersuchung des Barriereverhaltens von Anhydrit bei großräumigen Spannungsumlagerungen, Proceedings 5. Projektstatusgespräch zu FuE-Vorhaben auf dem Gebiet der Entsorgung gefährlicher Abfälle in tiefen geologischen Formationen, PtWT+E, Forschungszentrum Karlsruhe, to be printed
- Kern, H. and Franke, J.-H., 1980: Thermische Stabilität von Carnallit unter Lagerstättenbedingungen. Sonderabdruck aus Glückauf-Forschungshefte, 41. Jahrg., Vol.. 6, S. 252/55

- Kernforschungszentrum Karlsruhe, 1993: Testplan zum Demonstrationsversuch „Thermische Simulation der Streckenlagerung“ im Salzbergwerk Asse - Hauptband, Februar 1993
- Kessels, W., 1984: „Testing of an Absolute Measuring Flat Jack According to the Compensation Method (AWID)“, in: „CEC/NEA Workshop on Design and Instrumentation of In-Situ Experiments in Underground Laboratories Associated with Geological Disposal of Radioactive Waste, 15 - 17 May 1984“, Brussels
- Kiehl, J.R., Pahl, A., 1990: „Empfehlung Nr. 14 des Arbeitskreises 19 - Versuchstechnik Fels - der Deutschen Gesellschaft für Erd- und Grundbau e.V.: Überbohr-Entlastungsversuche zur Bestimmung von Gebirgsspannungen“, Bautechnik 67, H. 9.
- Kienzler, B., Vejmelka, P., Herbert, H.-J., Meyer, H., Altenhein-Haes, C., 2000: Long-Term Leaching Experiments of Full-Scale Cemented Waste Forms: Experiments and Modeling - Nuclear Technology, Radioactive Waste Management, vol. 129, 101-118
- Knapp, U. and Closs, K. D., 1990: Direkte Endlagerung, Kernforschungszentrum Karlsruhe
- Kolditz, H., 1993: Herstellung tiefer Großbohrlöcher zur Endlagerung umweltgefährdender Abfallstoffe im Salz, Glückauf 129, Nr. 2, Verlag Glückauf GmbH, Essen
- Korthaus, E., 1996: „Consolidation and deviatoric deformation behaviour of dry crushed salt at temperatures up to 150°C“, Proc. 4th Conference on the Mechanical Behaviour of Salt, Montreal
- KTA 2201, 1990: Sicherheitstechnische Regel des KTA. Auslegung von Kernkraftwerken gegen seismische Einwirkungen, Fassung 6/90, Kerntechnischer Ausschuss (KTA), Carl Hauptmanns Verlag, Köln, Berlin

- Leydecker, G., Kopera, J. R., Rudolff, A., 1999: Abschätzung der Erdbebengefährdung in Gebieten geringer Seismizität am Beispiel eines Standortes in Norddeutschland. DGEB-Publikationen Nr. 10, Seite 89 - 97, Vortragsband der Dreiländertagung D-A-CH 1999 der deutschen Gesellschaft für Erdbebeningenieurwesen und Baudynamik e.V. (DGEB), 24. - 25. November 1999, Technische Universität Berlin, Savidis, S.A., 1999, ISBN 3-930108-06-2
- Manthei, G., Eisenblätter, J., Kamlot, P., Heusermann, S., 1998: Acoustic Emission Measurements During Hydraulic Fracturing Tests in a Salt Mine Using a Special Borehole probe, Proc. 14<sup>th</sup> International Acoustic Emission Symposium & 5<sup>th</sup> Acoustic Emission World Meeting, August 9-14, 1998, Big Island, Hawaii, USA
- Müller-Hoeppe, N., Engelmann, H.-J., and Biurrun, E., 1994: „On the reliability of the temperature calculation code LINSOURPREPOST suitable to design a HLW-repository”, Proceedings from the Waste Management 1994 (WM94) Conference, Tucson, Arizona, USA, 1994
- Müller-Lyda, I., Birthler, H., Fein, E., 1999: „Ableitung von Permeabilitäts-Porositätsrelationen für Salzgrus”, Gesellschaft für Anlagen- und Reaktorsicherheit (GRS) mbH, GRS-148, Köln
- Müller, K., Rothfuchs, T., 1995: The HAW-Project: Test disposal of highly radioactive radiation sources in the Asse salt mine. Documentation and appraisal of the disposal system, Commission of the European Communities. Nuclear science and technology. EUR 16554 EN.
- Pahl, A., Heusermann, S., 1989: „Der Einfluss des zeitabhängigen Stoffverhaltens auf die Bestimmung gebirgsmechanischer Parameter”, Felsbau 7, Nr. 2
- Papp, R., 1997: GEISHA - Gegenüberstellung von Endlagerkonzepten in Salz und Hartgestein. - Forschungszentrum Karlsruhe, Technik und Umwelt, Wissenschaftliche Berichte, FZKA-PTE Nr. 3

- Paul, A., Gartung, E., 1991: „Empfehlung Nr. 15 des Arbeitskreises 19 - Versuchstechnik Fels - der Deutschen Gesellschaft für Erd- und Grundbau e.V.: Verschiebungsmessungen längs der Bohrlochachse-Extensometermessungen“, Deutsche Gesellschaft für Erd- und Grundbau e.V., Wilhelm Ernst & Sohn Verlag, Berlin
- Prij, J., B. van den Horn, A., 1993: Thermomechanical calculations. In: The DEBORA-project, progress report January - June 1993, Joint report of GSF-Institut für Tief Lagerung and Stichting Energieonderzoek Centrum Nederland (ECN), IfT-Abteilungsbericht 4/93
- Prij, J., Graefe, V., Rothfuchs, T., Vons, L.H., 1995: Modelling of the thermomechanical behaviour of solid rock salt and crushed salt. In: Proc. of Workshop „Testing and Modelling of thermal, mechanical and hydrogeological properties of host rocks for deep geological disposal of radioactive waste“, Brüssel, 12. - 13. 01.1995, CEC, EUR 16219 EN, 213 - 229
- Pruess, K., Oldenburg, C., Moridis, G., 1999: TOPUGH2 User's Guide Version 2.0 , LBNL-43134, Berkeley, California, USA
- Reardon, E. J., 1990 Cement and Concrete Research, 20, 175-192
- Revertegat, E., Adenot, F. Richet, C., L. Wu, L. Glasser, F.P., Damidot, D., Stronach, S.A., 1997: Report EUR 17642 EN
- Richter-Bernburg, G., 1987: Exkursionen in den deutschen Zechstein. - Int. Symp. Zechstein 87, Exkf., I, 15 - 24, Wiesbaden
- Rothfuchs, T., 1986: Untersuchung der thermisch induzierten Wasserfreisetzung aus polyhalitischem Steinsalz unter In-situ-Bedingungen, Temperaturversuch 5 im Salzbergwerk Asse, Kommission der Europäischen Gemeinschaften, Kernforschung und -technologie, EUR 10392 DE
- Rothfuchs, T., Wieczorek, K., Feddersen, H.-K., Staupendahl, G., Coyle, A. J., Kalia, H., Eckert, J., 1988: Brine Migration Test - A joint project of Office of Nuclear Waste Isolation (ONWI) and Gesellschaft für Strahlen- und Umweltforschung (GSF), GSF-Bericht 6/88

- Rothfuchs, T. et al., 1995: The HAW-Project: Test disposal of highly radioactive radiation sources in the Asse salt mine. Final report, Commission of the European Communities, Nuclear science and technology, EUR 16688 EN
- Rothfuchs, T., Prij, J., Kröhn, K.-P., Van den Horn, B.A., Wieczorek, K., 1996: The DEBORA-Project Phase 1: Development of borehole seals for high-level radioactive waste repositories in salt formations, Final Report, Nuclear Science and Technology, European Commission, EUR 16928 EN
- Rothfuchs, T., Feddersen, H.-K., Kröhn, K.-P., Miehe, R., Wieczorek, K., 1999: The DEBORA-Project: Development of Borehole Seals for High-Level Radioactive Waste - Phase II, Final Report, Gesellschaft für Anlagen- und Reaktorsicherheit (GRS) mbH, Köln, GRS - 161
- Rothfuchs, T., Bollingerfehr, W., Heusermann, S., Kamlot, P., 2001: Abschließende Auswertung des Projekts „Thermische Simulation der Streckenlagerung/Experimentelle Untersuchungen zum Verhalten von Versatz in Endlagerstrecken im Salinar“, Proceedings 5. Projektstatusgespräch zu FuE-Vorhaben auf dem Gebiet der Entsorgung gefährlicher Abfälle in tiefen geologischen Formationen, PtWT+E, Forschungszentrum Karlsruhe, to be printed
- SAM, 1989: Systemanalyse Mischkonzept, Hauptband zusammengestellt von der Projektgruppe Andere Entsorgungstechniken, Kernforschungszentrum Karlsruhe
- Sander, W., Herbert, H. J., 2000: A new Hydraulic Barrier-Performance of a Self-Healing Salt Backfill Material, Proc. DISTEC 2000, International Conference on Radioactive waste Disposal, Berlin, 4-6 Sept. 2000
- Scheibel, G. et al., 1990: Voruntersuchung zum weiteren Vorgehen auf dem Gebiet Gebindeabsturz und Aerosolfreisetzung im Endlager, Batelle-Institut e. V., Abschlußbericht BF R 67.347-01 (Förderkennzeichen KWA 5902.7 des BMFT), Frankfurt/M.

- Schlich, M., 1986: Simulation der Bewegung von im natürlichen Steinsalz enthaltener Feuchte im Temperaturfeld, Gesellschaft für Strahlen- und Umweltforschung mbH München, GSF-Bericht 2/86
- Schmidt, M.W., Fruth, R., Stockmann, N., Birthler, H., Boese, B., Storck, R., Sitz, P., Krauß, A., Eulenberger, K.-H., Schleinig, J.-P., Duddeck, H., Ahrens, H., Menzel, W., Salzer, K., Minkley, W., Busche, H., Lindhoff, U., Gierenz, S., 1995: Schachtverschlüsse für untertägige Deponien in Salzbergwerken - Vorprojekt, GSF-Forschungszentrum für Umwelt und Gesundheit, GSF-Bericht 32/95
- SEK, 1993: Direkte Endlagerung, Sammlung der Vorträge anlässlich der Abschlußveranstaltung Systemanalyse Endlagerkonzepte am 9. und 10. November 1993, Kernforschungszentrum Karlsruhe GmbH, AE Nr. 29
- Sitz, P., Koch, G., 1999: Langzeitstabile Streckenverschlussbauwerke im Salinar: in Proc. 4. Statusgespräch Untertägige Entsorgung; Projektträger des BMWi und BMBF für Entsorgung, Forschungszentrum Karlsruhe, Wissenschaftliche Berichte FZKA-PTE Nr. 6, pp 169 - 207
- Smailos, E., Schwarzkopf, W., Kienzler, B., Köster, R., (1992): „Corrosion of Carbon-Steel Containers for Heat-Generating Nuclear Waste in Brine Environments Relevant for a Rock-Salt Repository”, Mat. Res. Soc. Symp. Vol. 257
- Spilker, H., 1998. Status of the Development of Final Disposal Casks and Prospects in Germany. Proceedings of DisTec 98, International Conference on Radioactive Waste Disposal, Hamburg, 1998
- Sponheuer, W., 1965: Bericht über die Weiterentwicklung der seismischen Skala (MSK 1964), Deutsche Akademie d. Wiss., Veröff. Inst. Geodynamik, Jena, Heft 8, Akademie Verlag, Berlin
- Stephan K. and F. Mayinger, 1990: Thermodynamic: Grundlagen und technische Anwendungen. Band 1: Einstoffsysteme. Springer Verlag
- Stockmann, N. et al., 1994: Dammbau im Salzgebirge, Abschlussbericht Projektphase II, GSF-Forschungszentrum für Umwelt und Gesundheit mbH München, GSF-Bericht 18/94

- Storck, R., Aschenbach, J., Hirsekorn, R. P., Nies, A., Stelle, N., 1988: „Disposal in Salt formations”. Commission of the European Communities, Nuclear Science and Technology, EUR 11 778 EN
- Stührenberg, D., Zhang, C., 1995: Untersuchungen zum Kompaktionsverhalten von Salzgrus als Versatzmaterial für Endlagerbergwerke im Salz. Abschlussbericht zum Vorhaben 02E8552 8, Bundesanstalt für Geowissenschaften und Rohstoffe, Hannover
- Stürenberg, D. 1999: Triaxiale Kompaktionsversuche, Permeabilitätsversuche und Langzeitprognosen, in: „Eigenschaften von Salzgrus als Versatzmaterial im Wirtsgestein Salz”, Gesellschaft für Anlagen- und Reaktorsicherheit (GRS) mbH, GRS-143
- TSS-Testplan, 1993: Testplan zum Demonstrationsversuch „Thermische Simulation der Streckenlagerung” im Salzbergwerk Asse (Revidierte Fassung). Hauptband Direkte Endlagerung, Kernforschungszentrum Karlsruhe
- Wallner, M., Caninenberg, C., Gonther, H., 1979: Ermittlung zeit- und temperaturabhängiger mechanischer Kennwerte von Steinsalz, Proc. 4<sup>th</sup> Int. Congress Rock Mechanics, Vol 1, Montreux
- Wallner, M., Stührenberg, D., 1989: Fernfeldanalysen, TA 6 zum Abschlussbericht Systemanalyse Mischkonzept, KWA-3603 A3, Bundesanstalt für Geowissenschaften und Rohstoffe (BGR), Hannover
- Wieczorek, K., Zimmer U., 1999: Hydraulic behavior of the excavation disturbed zone around openings in rock salt, ICEM' 99 - 7th International conference on radioactive waste management and environmental remediation, Nagoya, Japan, September 26-30,1999, JSME/ASME International
- Wieczorek, K., Zimmer, U., 1998: Untersuchungen zur Auflockerungszone um Hohlräume im Steinsalzgebirge, Abschlußbericht, Gesellschaft für Anlagen- und Reaktorsicherheit (GRS) mbH, GRS-A-2651, Köln

Yaramanci, U., Flach, D., 1989. Entwicklung einer vollautomatischen Gleichstrom-  
Geoelektrikanlage für den Einsatz im Vorhaben „Dammbau im Salz-  
gebirge“. Gesellschaft für Strahlen- und Umweltforschung, GSF-Bericht  
1/89

## List of Tables

Table 2.1	Specification of the HLW-canister Cogéma 7/86 (see GNS 1991).....	5
Table 2.2	Expected number of HLW-Containers until year 2040 .....	5
Table 2.3	Heat power of Cogéma HLW-canisters calculated with data presented by Scheibel et al. (1990).....	14
Table 2.4	Heat power of a Pollux-8-DWR cask (Source: DBE 1998).....	14
Table 2.5	Possible geometrical data of the Gorleben repository concept (DBE 1998).....	17
Table 3.1	Overview of in-situ tests at Asse mine on HLW disposal .....	29
Table 3.2	Instrumentation Used of Asse Underground Research Laboratory.....	60
Table 5.1	Processes studied in the TSDE experiment (■ yes; □ no).....	114
Table 5.2	Data used in BAMBUS I for the numerical simulation of the TSDE experiment .....	115
Table 5.3	Processes studied in the DEBORA experiment (■ yes; □ no) .....	122
Table 5.4	Data used in the numerical simulations of the DEBORA experiments .....	123
Table 5.5	Material data, initial and boundary conditions for the two-phase flow models.....	129
Table 5.6	Data used for modelling brine migration in the Temperature Test 5 at Asse (Schlich, 1986).....	136
Table 5.7	Comparison of the ( $\text{Ca}^{2+}$ ), ( $\text{Mg}^{2+}$ ) and ( $\text{SO}_4^{2-}$ ) and the pH in solution in the corrosion experiments in the Asse salt mine and the laboratory cascade experiment .....	142

## List of Figures

Figure 2.1	Disposal drift with HLW boreholes.....	6
Figure 2.2	Drift disposal of Pollux casks (source DBE) .....	6
Figure 2.3	Typical layout of a high-level waste repository in a salt formation in Germany (source DBE) .....	16
Figure 2.4	Cross section of the Asse research mine .....	21
Figure 2.5	Principle seals in a salt repository .....	24
Figure 2.6	Principle design of a drift seal (dam) .....	25
Figure 2.7	Principle design of a shaft seal.....	25
Figure 3.1	Cross section of Asse salt mine .....	28
Figure 3.2	Temperature Test 5.....	32
Figure 3.3	Brine Migration Test .....	33
Figure 3.4	Layout of the Debora experiments .....	35
Figure 3.5	General view of the TSDE test field.....	37
Figure 3.6	Longitudinal section of a TSDE heater cask.....	38
Figure 3.7	TSDE-test drifts on the 800-m level with monitoring cross sections.....	40
Figure 3.8	Temperatures at the heater surface in the TSDE experiment .....	43
Figure 3.9	Opening of a heater cask .....	44
Figure 3.10	Bent convergence measuring device .....	44

Figure 3.11a	Completely closed cable slot in the drift wall at cross section D1 of the TSDE test field.....	59
Figure 3.11b	Squeezed cable in a cable slot in the drift wall at cross section D1 of the TSDE test field .....	59
Figure 3.12	Cable duct (upper left) at cross section D1 in the TSDE test field.....	59
Figure 4.1a	Typical layout of a high-level waste repository in a salt formation (source DBE).....	71
Figure 4.1b	Borehole disposal concept .....	71
Figure 4.1c	Drift disposal concept .....	71
Figure 4.2	Principle of the self healing process due to the brine-backfill interaction .....	74
Figure 4.3	Development of brine and crystallisation pressures during the brine-backfill interaction in the laboratory experiment .....	74
Figure 4.4	Evaporation front model .....	78
Figure 4.5	Asse anticline .....	91
Figure 5.1	Layout of the TSDE experiment-according to the drift emplacement concept (Bechthold et al., 1999).....	113
Figure 5.2	Finite element mesh used in the DBE calculations of the TSDE experiment .....	116
Figure 5.3	Convergence in the middle cross section of TSDE from 2D-(Phase I) and 3D-calculations (Phase II).....	117
Figure 5.4	Temperature at selected points of two cross sections from 3D-calculation.....	118

Figure 5.5	Situation of a HLW disposal borehole in a German repository in a geological salt formation .....	120
Figure 5.6	Layout of the DEBORA-2 experiment.....	121
Figure 5.7	Schematic representation of the finite element mesh used by GRS calculations of the DEBORA-2 experiment .....	125
Figure 5.8	Temperature development in the backfilled borehole of DEBORA 2 .....	126
Figure 5.9	Porosity development in the backfilled borehole of DEBORA 2 .....	126
Figure 5.10	Sketch of the disposal borehole and connected drift.....	127
Figure 5.11a	Time-dependent brine saturation distribution for scenario 1 .....	131
Figure 5.11b	Time-dependent pressure distribution for scenario 1 .....	131
Figure 5.12a	Time-dependent brine saturation distribution for scenario 2 .....	132
Figure 5.12b	Time-dependent pressure distribution for scenario 2 .....	132
Figure 5.13	Layout of Temperature Test 5 .....	134
Figure 5.14	Evaporation front model .....	135
Figure 5.15	Comparison of measured and predicted data of water release in the Temperature Test 5 .....	138
Figure 5.16a	Dissolution of rock salt – volume changes .....	140
Figure 5.16b	Dissolution of carnallite – volume changes.....	140
Figure 5.16c	Dissolution of Hartsalz - volume changes .....	141

Figure 5.17	Experimentally observed and calculated evolution of the ( $\text{Na}^+$ ), ( $\text{K}^+$ ), ( $\text{Ca}^{2+}$ ), ( $\text{Mg}^{+2}$ ) and ( $\text{Cl}^-$ ) in solution during dissolution of cemented fly ash in IP21 brine .....	141
Figure 5.18	Experimentally observed and calculated evolution of ( $\text{SO}_4^{2-}$ ) and pH in solution during SFA dissolution in IP21 brine.....	142
Figure 6.1	Testing of a HLW disposal system/concept in the Asse mine/URL.....	147

**Gesellschaft für Anlagen-  
und Reaktorsicherheit  
(GRS) mbH**

Schwertnergasse 1  
**50667 Köln**  
Telefon +49 221 2068-0  
Telefax +49 221 2068-888

Forschungsinstitute  
**85748 Garching b. München**  
Telefon +49 89 32004-0  
Telefax +49 89 32004-300

Kurfürstendamm 200  
**10719 Berlin**  
Telefon +49 30 88589-0  
Telefax +49 30 88589-111

Theodor-Heuss-Straße 4  
**38122 Braunschweig**  
Telefon +49 531 8012-0  
Telefax +49 531 8012-200

**[www.grs.de](http://www.grs.de)**